

TABLE OF CONTENTS

Chapter	Topic	Page No.
Chapter 1	Introduction	1
Chapter 2	Literary Review	4
Chapter 3	Data Collection	46
Chapter 4	Image Transformation	80
Chapter 5	Image Enhancements	84
Chapter 6	Image Segmentation	89
Chapter 7	Results And Discussion	97
Chapter 8	Conclusion	144
Appendix	References	145

List of Tables

Table No.	Caption	Page No.
1	Data Collection	43
2	Gender Distribution	97
3	Ethnicity Distribution	98
4	Age Distribution	100
5	Results & Discussion	108

List of Figures

Figure No.	Caption	Page No.
1	Proposed System Flowchart	3
2	Sample image	87
3	Grey Level Histogram	87
4	Input image for median filtering	88
5	Median Filtering of image effected by salt and pepper noise	88
6	Gender-Frequency Bar Graph	97
7	Gender Statistics	98
8	Ethnicity-Frequency Bar Graph	99
9	Ethnicity Statistics	99
10	Age Statistics	102
11	Age-Frequency Bar Graph	102
12	Fast Fourier Transformation of image	103
13	Inverse Fast Fourier Transformation	103
14	Value Distribution of LoG Edge Detection	105
15	Value Distribution of Roberts Edge Detection	105
16	Value Distribution of Sobel Edge Detection	106
17	Value Distribution of Prewitt Edge Detection	106
18	Value Distribution of Canny Edge Detection	107

INTRODUCTION

1. Introduction

1.1 Abstract

One of most important application of image processing is face recognition; face recognition is used in diverse areas such as network security systems, access control systems and other multimedia information systems. This project presents the pre-processing steps to a face detection system. The pre-processing steps form the basis for a face detection system.

The steps discussed here are

1. Image Transformation
2. Image Segmentation
3. Image Enhancement
4. Image Segmentation.

Each pre-processing step involves a correction mechanism to improve the input face given to system. These pre-processing stages are provided to face detection system to avoid the problems faced by the face detection systems. In specific these set of process avoidance problems due to picture quality and lighting.

1.2 Problem Definition

Face recognition systems face the following categories of problems:

1. Picture Quality: Due to wear out of the system, picture captured maybe distorted or technically noise is added to the system, due to which the exact edge of the system cannot be detected. This particular problem is analyzed the most in this project. To be specific the image filtering techniques are used for correction of this problem

2. Lighting: Due to differences in the lighting conditions when the face is been captured, the system doesn't recognize the face as a trained face. So matching of face doesn't happen leading to the failure of the face recognition system. The issue is corrected by image enhancement technique, with which the face's contrast is increased or sharpens the face or even equalized for the clarity of the face.
3. Pose: The problem occurs when face recognition is used when the input image is not posed, for example the recognition system is used by a surveillance camera. This problem is not addressed here, only posed facial images are considered by this system.

1.3 Objectives

This project is aimed to build a pre-processing of a facial recognition system which can recognize static images. This system is mainly applied for posed images.

The objectives of the project are as follows:

1. To recognize a sample image from the given facial database
2. To applying the image preprocessing functions in the sample image
 - a. Make it easier to process the data and increase the chances of getting correct matches.
 - b. Better chances of success with changes in illumination, pose, picture quality.
 - c. Decrease processing time.
3. To take correct combination of image processing algorithms such that face detected from input image can be detected without many ambiguity.

1.4 Proposed System – Flowchart

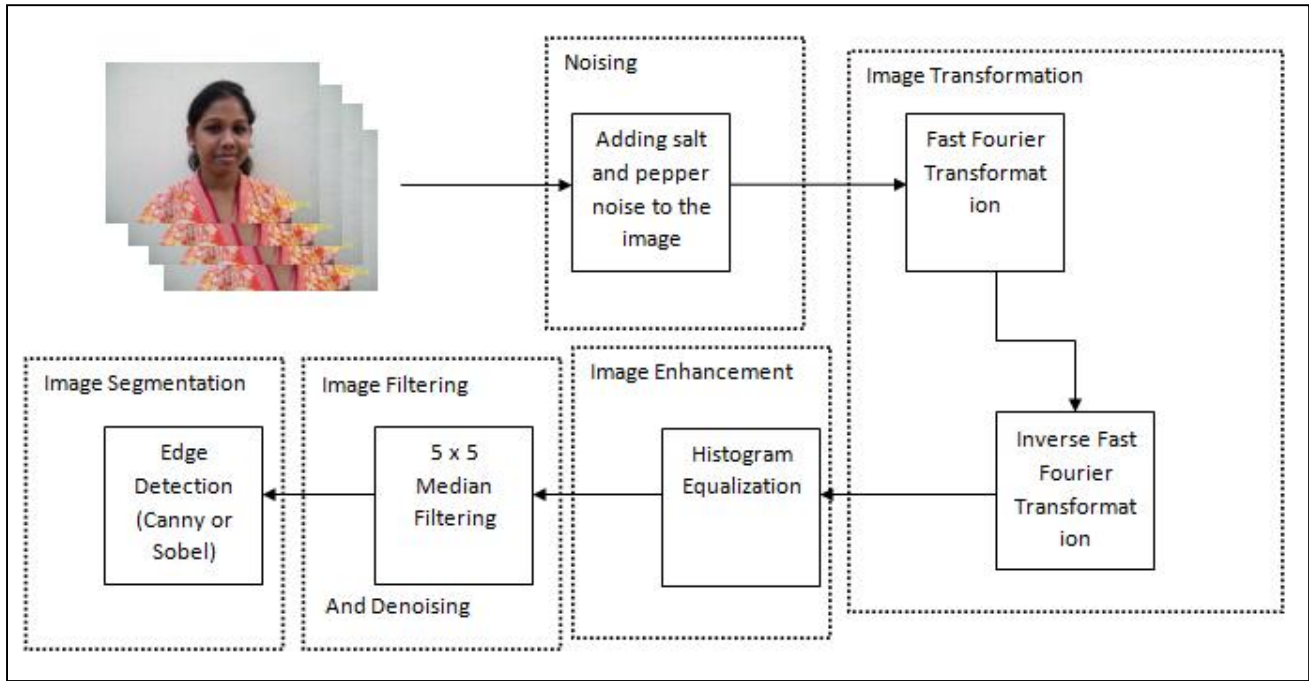


Figure 1: Proposed System Flowchart

LITERATURE REVIEW

2. Literature Review

A probabilistic model for recognizing human faces present in a video sequence which derived important features such as the temporal fusion for tracking and recognition, the computational efficiency of the Sequential Importance Sampling (SIS) Algorithm in solving the model and the sophisticated appearance models. (Rama & Shaohua, 2011)

The computational approach taken in the system can locate and track subject's head and then recognize the person by comparing characteristics of the face to those of known individuals. The system functions by projecting face images onto a feature space that spans the significant variations among known face images, this is known as 'Eigen faces'. (Mathew & Alex, 1991)

The face recognition is implemented using Principal Component Analysis (PCA) by projecting the face image from the original vector space and Linear Discriminant Analysis (LDA) using a linear classifier. (Wenyi, Arvindh, Rama, Daniel, & John)

Two modified Hausdroff distances namely, "spatially eigen-weighted Hausdroff distance" (SEWHD) and "spatially eigen-weighted 'doubly' Hausdroff distance" (SEW2HD) are proposed, which incorporate the information about the location of important facial features such as eyes, mouth, and face contour so that distances at those regions will be emphasized. (Kwan-Ho, Kin-Man, & Wan-Chi, 2002)

An optimization approach is proposed that creates and successively improves such a model by means of genetic algorithms which performs robust and high-speed face localization based on the Hausdroff distance. (Klaus, Oliver, & Robert, 2002)

A similarity measure based on hausdroff distance for face recognition is proposed which is different from the conventional hausdroff distance based on measures. The proposed system not only provides the dissimilar information but also similar information of two objects. This added similarity information can increase the discriminating capabilities of object recognition system for similar objects such as faces with variant lighting condition and facial expression. (Yunakui & Zengfu, 2006)

An efficient algorithm for human face detection and facial feature extraction is used to detect the face locations using genetic algorithm and Eigen face technique. The genetic algorithm is used to search for possible face regions in an image, while Eigen face technique is used to determine the fitness of the regions. Here due to the complicate nature of genetic algorithm, only the eye location is being considered. (Kwok-Wai, Kin-man, & Wan-Chi, 2001)

An efficient algorithm computing the Hausdroff distance between all possible relative positions of a binary image and a model. It focuses primarily on the case in which the model is only allowed to translate with respect to the image. (Daniel, Gregory, & Willian, 1993)

The novel approach for robust face detection based on enhanced Hausdroff Distance(HD) which using the technique to automatically determine an appropriate size of elliptical model and also achieves he detection in much less computational time than the conventional HD. (Sanun & Werasak, 2001)

A new powerful distance measure called Normalized Unmatched Points (NUP) can be used in face recognition system to discriminate facial images by counting the number of unmatched pixels between query and database images. It is observed that NUP distance measure performs better than other existing similar variants. (Aditya & Phalguni, 2009)

A new face detection approach is implemented which is capable of detecting human faces from complex backgrounds and a new skin color modeling process is done which is applied to the face segmentation process. (Khalid, Wei, & John, 2011)

The different face regions have different degrees for importance for face recognition. In previous Hausdroff distance (HD) measures, points are treated as same importance, or weight different points that calculated from gray domain. A new weighting function of HD on the Eigen face from edge domain, which reflects the discriminative properties of face edge images effectively, is proposed for face recognition. (Huachun, Yu-Jin, Wuhong, Guandong, & Hui, 2011)

The use of computer vision techniques is implemented to analyze students' moods during one-to-one teaching institution. The eventual goal was to create an automated tutoring system that are sensitive to the student's mood and affective state but the problem of accurately determining a child's mood from a single video frame is difficult so a video of 10-30 seconds is considered. (Nicholas, Georgios, Matthai, & Javier, 2011)

A classification technique is implemented for face expression recognition using Adaboost that learns by selecting the relevant global and local appearance features with the most discriminating information. A comparative study is done with another leading margin-based classifier, the Support Vector Machines (SVM)

and identifies the advantages of using Adaboost over SVM in this context. (Piyanch, Deepak, & Hanson, 2005)

The Automated Facial Expression Recognition System (AFERS) automates the manual practice of Facial Action Coding System (FACS), leveraging the research and technology. This portable, near real-time system will detect the seven universal expressions of emotion (disgust, fear, anger, contempt, sadness, surprise, happiness), providing the investigators with indicators of the presence deception during the interview process. (Andrew, Jeffery, Jason, Patrick, Fernando, & Adam, 2009)

A novel validation of an automated tracking tool is implemented on a naturalist tutoring dataset, comparing Computer Expression Recognition Toolbox (CERT) results with manual annotations across a prior video corpus. (Joseph, Joseph, Kristy, Eric, & James, 2013)

The influence of facial production training on the perception of facial expression by employing a novel production training intervention built on feedback from automated facial expression recognition is explored and is aimed that production training using the automated feedback system would improve an individual's ability to identify dynamic emotional faces. (David, et al., 2012)

Systematic Comparison of machine learning methods applied to the problem of fully automatic recognition of facial expressions, including Adaboost, support vector machines, and linear discriminant analysis. Each video-frame is first scanned in real-time to detect approximately upright-frontal faces. (Gwen, Marian, Ian, Joshua, & Javier, 2006)

The localization of human faces in digital images is a fundamental step in the process of face recognition. A shape comparison approach is used to achieve fast and accurate face detection that is robust to the changes in illumination and background. The Hausdroff measure is used as a similarity measure between a general face model and possible instances of the object within the image. (Oliver, Klaus, & Robert, 2001)

A computer vision system for human gesture recognition and tracking based on a new nonlinear dimensionality reduction method is presented in this paper. Due to the variation of posture appearance, the recognition and tracking of human hand gestures from one single camera remain a difficult problem. An unsupervised learning algorithm, distributed locally linear embedding (DLLE), to discover the intrinsic structure of the data, such as neighborhood relationships information is presented. After the embedding of input images are represented in a lower dimensional space, probabilistic neural network (PNN) is employed and a database is set up for static gesture classification. For dynamic gesture tracking, the similarity among the images sequence are utilized. Hand gesture motion can be tracked and dynamically reconstructed according to the image's relative position in the corresponding motion database. The method is robust against the input sequence frames and bad image qualities. Experimental results show that the approach is able to successfully separate different hand postures and track the dynamic gesture. (Ge, Yang & Lee, 2008)

As part of the Face Recognition Technology (FERET) program, the U.S. Army Research Laboratory (ARL) conducted supervised government tests and evaluations of automatic face recognition algorithms. The goal of the tests was to provide an independent method of evaluating algorithms and assessing the state of

the art in automatic face recognition. This report describes the design and presents the results of the August 1994 and March 1995 FERET tests. Results for FERET tests administered by ARL between August 1994 and August 1996 are reported. (Phillips, 1996)

An algorithm to automatically detect facial features from color images has been developed. First, face region is located using skin-color information. Then, the iris candidates are extracted from the intensity valleys created from the detected face. Next, the costs for each pair of iris candidates are computed to determine the real pair of irises. Mouth region and corners are detected using color space method, image processing and corners detection techniques. This algorithm has been tested to specifically reduce the effects of beard, moustache, hairstyle and facial expression in automated facial features detection. (Yuen , Rizon ,San & Sugisaka , 2008)

An auto adaptive neuro-fuzzy segmentation and edge detection architecture is presented. The system consists of a multilayer perceptron (MLP)-like network that performs image segmentation by adaptive thresholding of the input image using labels automatically pre-selected by a fuzzy clustering technique. The proposed architecture is feed forward, but unlike the conventional MLP the learning is unsupervised. The output status of the network is described as a fuzzy set. Fuzzy entropy is used as a measure of the error of the segmentation system as well as a criterion for determining potential edge pixels. The proposed system is capable to perform automatic multilevel segmentation of images, based solely on information contained by the image itself. No a priori assumptions whatsoever are made about the image (type, features, contents, stochastic model, etc.). Such a universal algorithm is most useful for applications that are supposed to work with

different (and possibly initially unknown) types of images. The proposed system can be readily employed, “as is,” or as a basic building block by a more sophisticated and/or application-specific image segmentation algorithm. By monitoring the fuzzy entropy relaxation process, the system is able to detect edge pixels. (Boskovitz & Guterman,2002)

Contrast enhancement is an important factor in the image preprocessing step. One of the widely accepted contrast enhancement method is the histogram equalization. Although histogram equalization achieves comparatively better performance on almost all types of image, global histogram equalization sometimes produces excessive visual deterioration. A new extension of bi histogram equalization called Bi-Histogram Equalization with Neighborhood Metric (BHENM). First, large histogram bins that cause washout artifacts are divided into sub-bins using neighborhood metrics, the same intensities of the original image are arranged by neighboring information. Then the histogram of the original image is separated into two sub-histogram based on the mean of the histogram of the original image; the sub-histogram are equalized independently using refined histogram equalization, which produces flatter histogram. BHENM simultaneously preserved the brightness and enhanced the local contrast of the original image. Simulation result shows better brightness preservation. (Rani, Rajagopal & Jagadeeswaran, 2013)

The center weighted median (CWM) filter, which is a weighted median filter giving more weight only to the central value of each window, is studied. This filter can preserve image details while suppressing additive white and/or impulsive-type noise. The statistical properties of the CWM filter are analyzed. It is shown that the

CWM filter can outperform the median filter. Some relationships between CWM and other median-type filters, such as the Winsor zing smother and the multistage median filter, are derived. In an attempt to improve the performance of CWM filters, an adaptive CWM (ACWM). We show the ACWM filter is an excellent detail preserving that can suppress signal dependent noise as well as the signal independent noise. (Ko & Lee, 1991)

In this paper, classified and comparative study of edge detection algorithms are presented. Experimental results prove that Boie-Cox, Shen-Castan and Canny operators are better than Laplacian of Gaussian (LOG), while LOG is better than Prewitt and Sobel in case of noisy image. Subjective and objective methods are used to evaluate the different edge operators. The morphological filter is more important as an initial process in the edge detection for noisy image and used opening-closing operation as preprocessing to filter noise. Also, smooth the image by first closing and then dilation to enhance the image before the edge operators affect. (Roushdy, 2006)

Many face recognition algorithms have been developed over the past few years but the problem remains challenging, especially for images taken under uncontrolled lighting conditions. We show that the robustness of several popular linear subspace methods and of Local Binary Patterns (LBP) can be substantially improved by including a very simple image preprocessing stage based on gamma correction, Difference of Gaussian filtering and robust variance normalization. LBP proves to be the best of these features, and we improve on its performance in two ways: by introducing a 3-level generalization of LBP, Local Ternary Patterns (LTP), and by using an image similarity metric based on distance transforms of LBP image slices. We give experimental results on two face recognition sets

chosen for their difficult lighting conditions: version 1 of the Face Recognition Grand Challenge experiment 4, and the full Yale-B dataset. (Tan & Triggs, 2007)

This paper attempts to undertake the study of three types of noise such as Salt and Pepper (SPN), Random variation Impulse Noise (RVIN), Speckle (SPKN). Different noise densities have been removed between 10% to 60% by using five types of filters as Mean Filter (MF), Adaptive Wiener Filter (AWF), Gaussian Filter (GF), Standard Median Filter (SMF) and Adaptive Median Filter (AMF). The same is applied to the Saturn remote sensing image and they are compared with one another. The comparative study is conducted with the help of Mean Square Errors (MSE) and Peak Signal to Noise Ratio (PSNR), to choose the base method for removal of noise from remote sensing image. (Al-amri, Kalyankar & Khamitkar, 2010)

Data representation is an important pre-processing step in many machine learning algorithms. There are a number of methods used for this task such as Deep Belief Networks (DBNs) and Discrete Fourier Transforms (DFTs). Since some of the features extracted using automated feature extraction methods may not always be related to a specific machine learning task, in this paper we propose two methods in order to make a distinction between extracted features based on their relevancy to the task. We applied these two methods to a Deep Belief Network trained for a face recognition task. (Pezeski, Gholami & Nickabadi, 2013)

As one of the most successful applications of image analysis, face recognition has received significant attention, especially during past few years. Automatic human face recognition has received substantial attention from researchers in biometrics, pattern recognition and computer vision communities. The machine learning and computer graphics communities are also increasingly

involved in face recognition. The localization of human faces in digital images is a fundamental step in the process of face recognition. Although the existing automated machine recognition systems have certain level of maturity, but their accomplishments are limited due to real time challenges. For example, face recognition for the images which are acquired in high contrast with different levels of illumination is a critical problem. It is known that image variation due to lighting changes is larger than that, due to different personal identity, because lighting direction alters the relative gray scale distribution of a face image. In handling these types of practical scenarios, the system must be robust enough to deal with dynamic changes in lighting, hence it is equally important to preprocess the images prior to actual processing and experimentations. This paper proposes a novel method of illumination normalization based on histogram of an image and scaling function. It helps in construction of an optimal global lighting space from these images which improve accuracy of face recognition system. The proposed method helps in recognition of sparsely sampled images with different lighting too. Also, most valuable information of an image, i.e. gray scale value, is not discarded and person's discriminative information in face image is strengthened. Hence recognition can be carried out using preserved illumination invariant features. (Vasudha, Patil & Lokesh, 2013)

Image enhancement is one of the most important issues in low-level image processing. The goal of image enhancement is to improve the quality of an image such that enhanced image is better than the original image. Conventional Histogram equalization (HE) is one of the most algorithms used in the contrast enhancement of medical images, this due to its simplicity and effectiveness. However, it causes the unnatural look and visual artifacts, where it tends to change the brightness of an image. The Histogram Based Fast

Enhancement Algorithm (HBFE) tries to enhance the CT head images, where it improves the water-washed effect caused by conventional histogram equalization algorithms with less complexity. It depends on using full gray levels to enhance the soft tissues ignoring other image details. We present a modification of this algorithm to be valid for most CT image types with keeping the degree of simplicity. Experimental results show that The Modified Histogram Based Fast Enhancement Algorithm (MHBFE) enhances the results in term of PSNR, AMBE and entropy. We use also the Statistical analysis to ensure the improvement of the proposed modification that can be generalized. ANalysis Of VAriance (ANOVA) is used as first to test whether or not all the results have the same average. Then we find the significant improvement of the modification. (Kandeel, Abbas, Hadhoud & El-Saghir, 2014)

Precision agriculture is area with lack of cheap technology. The refinement of the production system brings large advantages to the producer and the use of images makes the monitoring a more cheap methodology. Macronutrients monitoring can to determine the health and vulnerability of the plant in specific stages. In this paper is analyzed the method based on computational intelligence to work with image segmentation in the identification of symptoms of plant nutrient deficiency. Artificial neural networks are evaluated for image segmentation and filtering, several variations of parameters and insertion impulsive noise were evaluated too. Satisfactory results are achieved with artificial neural for segmentation same with high noise levels. (Satin & da Silva, 2014)

Image compression is minimizing the size in bytes of a graphics file without degrading the quality of the image to an unacceptable level, the reduction in file size allows more images to be stored in a given amount of disk or memory space, it

also reduces the time required for images to be sent over the ground. This paper presents a new coding scheme for satellite images. In this study we apply the fast Fourier transform and the scalar quantization for standard LENA image and satellite image. The results obtained after the (SQ) phase are encoded using entropy encoding, after decompression, the results show that it is possible to achieve higher compression ratios, more than 78%, the results are discussed in the paper. (Sahnoun & Benabadji, 2014)

The purpose of this project was to determine whether Contrast Limited Adaptive Histogram Equalization (CLAHE) improves detection of simulated speculations in dense mammograms. Lines simulating the appearance of speculations, a common marker of malignancy when visualized with masses, were embedded in dense mammograms digitized at 50 micron pixels, 12 bits deep. Film images with no CLAHE applied were compared to film images with nine different combinations of clip levels and region sizes applied. A simulated speculation was embedded in a background of dense breast tissue, with the orientation of the speculation varied. The key variables involved in each trial included the orientation of the speculation, contrast level of the speculation and the CLAHE settings applied to the image. Combining the 10 CLAHE conditions, 4 contrast levels and 4 orientations gave 160 combinations. The trials were constructed by pairing 160 combinations of key variables with 40 backgrounds. Twenty student observers were asked to detect the Orientation of the speculation in the image. There was a statistically significant improvement in detection performance for speculations with CLAHE over unenhanced images when the region size was set at 32 with a clip level of 2, and when the region size was set at 32 with a clip level of 4. The selected CLAHE settings should be tested in the clinic with digital mammograms to determine whether detection of speculations associated with masses detected at

mammography can be improved. (Pisano, Zong, Hemminger, DeLuca, Johnson, Muller & Pizer, 1998)

Since edge detection is in the forefront of image processing for object detection, it is crucial to have a good understanding of edge detection algorithms. This paper introduces a new classification of most important and commonly used edge detection algorithms, namely ISEF, Canny, Marr-Hildreth, Sobel, Kirsch, Lapla1 and Lapla2. Five categories are included in our classification, and then advantages and disadvantages of some available algorithms within this category are discussed. A representative group containing the above seven algorithms are the implemented in C++ and compared subjectively, using 30 images out of 100 images. Two sets of images resulting from the application of those algorithms are then presented. It is shown that under noisy conditions, ISEF, Canny, Marr-Hildreth, Kirsch, Sobel, Lapla2, Lapla1 exhibit better performance, respectively. (Sharifi, Fathy & Tayefeh, 2002)

Edges are image attributes which are useful for image analysis and classification in a wide range of applications. The numerous applications and the subjective approach to edge definition and characterization have promoted the development of a large number of edge detectors which may perform well in given applications but poorly in others. In this work we describe a variety of edge detectors and evaluate their performance in terms of different shapes, slopes and background noise levels. The performed evaluation together with results in other related works helps to categorize the different edge detection schemes, as well as to better understand the usefulness and limitations of the performance measures used. (Peli & Malah , 1982)

Image segmentation is a relevant research area in Computer Vision, and several methods of segmentation have been proposed in the last 40 years. This paper presents the implementation using the GUI feature of the MATLAB and one best result can be selected for any algorithm using the subjective evaluation. This process can help to find out the best suitable value of parameters for the segmentation of different types of imagery. In this paper, one best algorithm has considered for each method of image segmentation. The interactive based method provides the facility to select the desired area as an object and produces better result. The proposed process also displays the duration of segmentation of each algorithm. (Agrawal , Shriwastava & Limaye , 2010)

A neuro-fuzzy network based impulse noise filtering for gray scale images is presented. The proposed filter is constructed by combining two neuro-fuzzy filters with a postprocessor, which generates the final output. Each neuro-fuzzy filter is a first order *Sugeno* type fuzzy inference system with 4-inputs and 1-output. The proposed impulse noise filter consists of two modes of operation, namely, training and testing (filtering). As demonstrated by the experimental results, the proposed filter not only has the ability of noise attenuation but also possesses desirable capability of detail preservation. It significantly outperforms other conventional filters. (Li, Sun & Luo, 2014)

A novel blind deconvolution technique for the restoration of linearly degraded images without explicit knowledge of either the original image or the point spread function is presented in this paper. The technique applies to situations in which the scene consists of a finite support object against a uniformly black, grey, or white background. This occurs in certain types of astronomical imaging, medical imaging, and one-dimensional (1-D) gamma ray spectra processing,

among others. The only information required is the non negativity of the true image and the support size of the original object. The restoration procedure involves recursive filtering of the blurred image to minimize a convex cost function. The proof of convexity of the cost function, establish sufficient conditions to guarantee a unique solution, and examine the performance of the technique in the presence of noise. The new approach is experimentally shown to be more reliable and to have faster convergence than existing nonparametric finite support blind deconvolution methods. For situations in which the exact object support is unknown so a novel support finding algorithm is proposed. (Kundur & Hatzinakos, 1998)

Image segmentation is a fundamental problem in computer vision. Despite many years of research, general purpose image segmentation is still a very challenging task because segmentation is inherently ill-posed. Among different segmentation schemes, graph theoretical ones have several good features in practical applications. It explicitly organizes the image elements into mathematically sound structures, and makes the formulation of the problem more flexible and the computation more efficient. In this paper, we conduct a systematic survey of graph theoretical methods for image segmentation, where the problem is modeled in terms of partitioning a graph into several sub-graphs such that each of them represents a meaningful object of interest in the image. These methods are categorized into five classes under a uniform notation: the minimal spanning tree based methods, graph cut based methods with cost functions, graph cut based methods on Markov random field models, and the shortest path based methods and the other methods that do not belong to any of these classes. We present motivations and detailed technical descriptions for each category of methods. The quantitative evaluation is carried by using five indices – Probabilistic Rand (PR)

index, Normalized Probabilistic Rand (NPR) index, Variation of Information (VI), Global Consistency Error (GCE) and Boundary Displacement Error (BDE) – on some representative automatic and interactive segmentation methods. (Peng, Zhang & Zhang, 2013)

The use of image analysis algorithms continuously grows as the reliability and robustness of systems using these algorithms increase. An important field of interest for image analysis is medical applications. They demand high reliability together with the ability to handle large data amounts. Automatic image segmentation is of special interest since it can simplify the classification process to a large extent. This survey addresses the basics of segmentation algorithms followed by an example of how segmentation of a cell can be performed. (Hedberg, 2010)

Low-dimensional feature representation with enhanced discriminatory power is of paramount importance to face recognition (FR) systems. Most of traditional linear discriminant analysis (LDA) based methods suffer from the disadvantage that their optimality criteria are not directly related to the classification ability of the obtained feature representation. Moreover, their classification accuracy is affected by the “small sample size” (SSS) problem which is often encountered in FR tasks. In this short paper, we propose a new algorithm that deals with both of the shortcomings in an efficient and cost effective manner. The proposed here method is compared, in terms of classification accuracy, to other commonly used FR methods on two face databases. Results indicate that the performance of the proposed method is overall superior to those of traditional FR approaches, such as the Eigen faces, Fisher faces and D-LDA methods. (Lu, Plataniotis & Venetsanopoulos, 2003)

While researchers in computer vision and pattern recognition have worked on automatic techniques for recognition faces for the 20 years most systems specialize on frontal views of the face. We present a face recognizer that works under varying pose, the difficult part of which is to handle face rotations in depth. Building of successful template-based systems, our basic approach is to represent faces with templates from multiple model views that cover different poses from the viewing sphere. Our system has achieved a recognition rate of 98% on a data base of 62 people containing 10 testing and 15 modeling views per person. (Beymer, 1994)

Two groups of algorithms are presented generalizing the Fast Fourier Transform (FFT) to the case of non-integer frequencies and non-equi-spaced nodes on the interval $[-\pi, \pi]$. These schemes are based on combinations of certain analytical considerations with the classical fast Fourier transform, and generalize both the forward and backward FFTs. The number of arithmetic operations required by each of the algorithms is proportional to $\log N + N \log \frac{1}{\varepsilon}$, where ε is the desired precision of computations and N is the number of nodes. Several related algorithms are also presented, each of which utilizes a similar set of techniques from analysis and linear algebra. These include an efficient version of the Fast Multiple Method in one dimension and fast algorithms for the evaluation, integration and differentiation of Lagrange polynomial inter-polants. Several numerical examples are used to illustrate the efficiency of the approach, and to compare the performance of the two sets of non-uniform FFT algorithms. (Dutt & Rokhlin, 1993)

A component-based method and two global methods for face recognition is presented and evaluated with respect to robustness against pose changes. In the

component system first locates facial components, extract them and combine them into a single feature vector which is classified by a Support Vector Machine (SVM). The two global systems recognize faces by classifying a single feature vector consisting of the gray values of the whole face image. In the first global system, a single SVM classifier for each person in the database is trained. The second system consists of sets of viewpoint-specific SVM classifiers and involves clustering during training. Extensive tests on a database which included faces rotated up to about 40 °in depth are performed. The component system clearly outperformed both global systems on all tests (Heisele, Ho &Poggio, 2001)

Adaptive histogram equalization (ahe) is a contrast enhancement method designed to be broadly applicable and having demonstrated effectiveness. However, slow speed and the over enhancement of noise it produces in relatively homogeneous regions are two problems. We report algorithms designed to overcome these and other concerns. These algorithms included interpolated ahe, to speed up the method on general purpose computers; a version of interpolated ahe designed to run in a few seconds on feedback processors; a version of full ahe designed to run in under one second on custom VLSI hardware; weighted ahe, designed to improve the quality of the result by emphasizing pixels' contribution to the histogram in relation to their nearness to the result pixel and; clipped ahe, designed to overcome the problem of over enhancement of noise contrast. The conclusion specifies that the clipped ahe should become a method of choice in medical imaging and probably also in other areas of digital imaging, and that clipped ahe can be made adequately fast to be routinely applied in the normal display sequence. (Pizer , Amburn , Austin , Cromartie, Geselowitz, Greer & Zuiderveld,1987)

This paper proposes a scheme for adaptive image contrast enhancement based on a generalization of histogram equalization (HE). HE is a useful technique for improving image contrast, but its effect is too severe for many purposes. However, dramatically different results can be obtained with relatively minor modifications. A concise description of adaptive HE is set out, and this framework is used in a discussion of past suggestions for variations on HE. A key feature of this formalism is a “cumulation function,” which is used to generate a grey level mapping from the local histogram. By choosing alternative forms of cumulation function one can achieve a wide variety of effects. A specific form is proposed. Through the variation of one or two parameters, the resulting process can produce a range of degrees of contrast enhancement, at one extreme leaving the image unchanged, at another yielding full adaptive equalization. (Stark, 2000)

A significant improvement of seismic image resolution can be obtained by setting the shot-profile migration imaging condition as a 2-D deconvolution in the shot position-time dimension (x_s, t) domain. (Valenciano & Biondi, 2003)

A stable algorithm is proposed for image restoration based on the “mean curvature motion” equation. Existence and uniqueness of the viscosity solution of the equation are proved, a L^∞ stable algorithm is given, experimental results are shown and the subjacent vision model is compared with those introduced recently by several researchers. The algorithm presented appears to be the sharpest possible among the multi-scale image smoothing methods preserving uniqueness and stability. (Alvarez, Lions & Morel, 1992)

This paper focuses on no-reference image sharpness/blurriness metrics due to their importance in image, video, and biomedical applications. Simulation results show that existing no-reference objective image sharpness metrics fail to

predict correctly the sharpness of images in the presence of noise. A noise-immune wavelet-based sharpness metric is proposed based on the Lipschitz regularity for differentiating between edges and noise singularities. Comparison results reveal the superiority of the proposed method when dealing with a moderate noisy environment. (Ferzli & Karam, 2005)

A new median-based filter, progressive switching median (PSM) filter, is proposed to restore images corrupted by salt–pepper impulse noise. The algorithm is developed by the following two main points: 1) switching scheme—an impulse detection algorithm is used before filtering, thus only a proportion of all the pixels will be filtered and 2) progressive methods—both the impulse detection and the noise filtering procedures are progressively applied through several iterations. Simulation results demonstrate that the proposed algorithm is better than traditional median-based filters and is particularly effective for the cases where the images are very highly corrupted. (Wang & Zhang, 1999)

Soft Computing is an emerging field that consists of complementary elements of fuzzy logic, neural computing and evolutionary computation. Soft computing techniques have found wide applications. One of the most important applications is edge detection for image segmentation. The process of partitioning a digital image into multiple regions or sets of pixels is called image segmentation. Edge is a boundary between two homogeneous regions. Edge detection refers to the process of identifying and locating sharp discontinuities in an image. In this paper, the main aim is to survey the theory of edge detection for image segmentation using soft computing approach based on the Fuzzy logic, Genetic Algorithm and Neural Network. (Senthilkumaran & Rajesh, 2009)

Gradient based edge detection techniques can be extended to multispectral images in various ways: difference operators can be applied to each component of a multi-image, and the results can be combined, e.g., taking the RMS, or the sum, or the maximum of their absolute values. In all of these approaches the image-components do not actually cooperate with one another, i.e., edge evidence along a given direction in one component does not reinforce edge evidence along the same direction in other components. To avoid this, the use of the tensor gradient of multi-images regarded as vector fields is suggested. Explicit formulas for the direction along which the rate of change is maximum, as well as for the maximum rate of change itself are derived. Digital approximations are obtained by surface fitting. (Di Zenzo, 1986)

Wavelets have been used in image processing and their ability to capture localized spatial-frequency information of image motivates their use for feature extraction. An overview of using wavelets in the face recognition technology is given in this paper. (Dai & Yan, 2007)

In this work experiments with Eigen faces for recognition and interactive search in a large-scale face database are described. Accurate visual recognition is demonstrated using a database of $O(10^3)$ faces. The problem of recognition under general viewing orientation is also examined. A view-based multiple-observer Eigen space technique is proposed for use in face recognition under variable pose. In addition, a modular Eigen space description technique is used which incorporates salient features such as the eyes, nose and mouth, in an Eigen feature layer. This modular representation yields higher recognition rates as well as a more robust framework for face recognition. An automatic feature extraction technique

using feature Eigen templates is also demonstrated. (Pentland, Moghaddam & Starner, 1994)

In this paper, an advanced histogram-equalization algorithm for contrast enhancement is presented. Histogram equalization is the most popular algorithm for contrast enhancement due to its effectiveness and simplicity. It can be classified into two branches according to the transformation function used: global or local. Global histogram equalization is simple and fast, but its contrast-enhancement power is relatively low. Local histogram equalization, on the other hand, can enhance overall contrast more effectively, but the complexity of computation required is very high due to its fully overlapped sub-blocks. In this paper, a low-pass filter-type mask is used to get a non-overlapped sub-block histogram-equalization function to produce the high contrast associated with local histogram equalization but with the simplicity of global histogram equalization. This mask also eliminates the blocking effect of non-overlapped sub-block histogram-equalization. The low-pass filter-type mask is realized by partially overlapped sub-block histogram-equalization (POSHE). With the proposed method, since the sub-blocks are much less overlapped, the computation overhead is reduced by a factor of about 100 compared to that of local histogram equalization while still achieving high contrast. The proposed algorithm can be used for commercial purposes where high efficiency is required, such as camcorders, closed-circuit cameras, etc. (Kim, Kim & Hwang, 2001)

Extension of the theory of edge detection based upon second-order differential operators to the multi-band case is presented, and the analysis shows that this extension is feasible. Some results from one-band theory do not extend to

this case; for example, closeness of the zero-crossing lines is no more guaranteed. (Cumani, 1991)

Video streams are ubiquitous in applications such as surveillance, games, and live broadcast. Processing and analyzing these data is challenging because algorithms have to be efficient in order to process the data on the fly. From a theoretical standpoint, video streams have their own specificities – they mix spatial and temporal dimensions, and compared to standard video sequences, half of the information is missing, i.e. the future is unknown. The theoretical part of our work is motivated by the ubiquitous use of the Gaussian kernel in tools such as bilateral filtering and mean-shift segmentation. We formally derive its equivalent for video streams as well as a dedicated expression of isotropic diffusion. Building upon this theoretical ground, we adapt a number of classical powerful algorithms to video streams: bilateral filtering, mean-shift segmentation, and anisotropic diffusion. (Paris, 2008)

A new algorithm for removing motion blur from a single image is presented. Our method computes a de-blurred image using a unified probabilistic model of both blur kernel estimation and un-blurred image restoration. An analysis of the causes of common artifacts found in current de-blurring methods, and then introduce several novel terms within this probabilistic model that are inspired by the analysis are presented. These terms include a model of the spatial randomness of noise in the blurred image, as well a new local smoothness prior that reduces ringing artifacts by constraining contrast in the un-blurred image wherever the blurred image exhibits low contrast. Finally, we describe an efficient optimization scheme that alternates between blur kernel estimation and un-blurred image restoration until convergence. As a result of these steps, we are able to produce

high quality de-blurred results in low computation time. We are even able to produce results of comparable quality to techniques that require additional input images beyond a single blurry photograph, and to methods that require additional hardware. (Shan, Jia & Agarwala, 2008)

A novel statistical and variational approach to image segmentation based on a new algorithm named region competition is presented. This algorithm is derived by minimizing a generalized Bayes/MDL criterion using the variational principle. The algorithm is guaranteed to converge to a local minimum and combines aspects of snakes / balloons and region growing. Indeed the classic snakes / balloons and region growing algorithms can be directly derived from the approach. Theoretical analysis of region competition including accuracy of boundary location, criteria for initial conditions, and the relationship to edge detection using filters is provided. It is straight forward to generalize the algorithm to multi band segmentation and demonstrates it on grey level images, color images and texture images. The novel color model allows us to eliminate intensity gradients and shadows, thereby obtaining segmentation based on the albedos of objects. It also helps detect highlight regions. (Zhu & Yuille, 1996)

Taking satisfactory photos under dim lighting conditions using a hand-held camera is challenging. If the camera is set to a long exposure time, the image is blurred due to camera shake. On the other hand, the image is dark and noisy if it is taken with a short exposure time but with a high camera gain. By combining information extracted from both blurred and noisy images, however, we show in this paper how to produce a high quality image that cannot be obtained by simply de-noising the noisy image, or de-blurring the blurred image alone. Our approach is image de-blurring with the help of the noisy image. First, both images are used

to estimate an accurate blur kernel, which otherwise is difficult to obtain from a single blurred image. Second and again using both images, a residual deconvolution is proposed to significantly reduce ringing artifacts inherent to image deconvolution. Third, the remaining ringing artifacts in smooth image regions are further suppressed by a gain-controlled deconvolution process. We demonstrate the effectiveness of our approach using a number of indoor and outdoor images taken by off-the-shelf hand-held cameras in poor lighting environments. (Yuan, Sun, Quan & Shum, 2007)

The publication of the Cooley-Tukey fast Fourier transform (FIT) algorithm in 1965 has opened a new area in digital signal processing by reducing the order of complexity of some crucial computational tasks like Fourier transform and convolution from N^2 to $N \cdot \log_2 N$, where N is the problem size. The development of the major algorithms (Cooley-Tukey and split-radix FFT, prime factor algorithm and Winograd fast Fourier transform) is reviewed. Then, an attempt is made to indicate the state of the art on the subject, showing the standing of research, open problems and implementations. (Duhamel & Vetterli, 1990)

This paper studies different methods proposed so far for segmentation evaluation. Most methods can be classified into three groups: the analytical, the empirical goodness and the empirical discrepancy groups. Each group has its own characteristics. After a brief description of each method in every group, some comparative discussions about different method groups are first carried out. An experimental comparison for some empirical (goodness and discrepancy) methods commonly used is then performed to provide a rank of their evaluation abilities. In addition, some special methods are also discussed. This study is helpful for an

appropriate use of existing evaluation methods and for improving their performance as well as for systematically designing new evaluation methods. (Zhang, 1996)

In this paper, a face recognition technique “Sub-Holistic Hidden Markov Model” has been proposed. The technique divides the face image into three logical portions. The proposed technique, which is based on Hidden Markov Model (HMM), is then applied to these portions. The recognition process involves three steps i.e. pre-processing, template extraction and recognition. The experiments were conducted on images with different resolutions of the two standard databases (YALE and ORL) and the results were analyzed on the basis of recognition time and accuracy. The accuracy of proposed technique is also compared with SHPCA algorithm, which shows better recognition rates. (Sharif, Shah, Moshin & Raza, 2013)

Dense disparity map is required by many great 3D applications. In this paper, a novel stereo matching algorithm is presented. The main contributions of this work are three-fold. Firstly, a new cost-volume filtering method is proposed. A novel concept named “two-level local adaptation” is introduced to guide the proposed filtering approach. Secondly, a novel post-processing method is proposed to handle both occlusions and texture-less regions. Thirdly, a parallel algorithm is proposed to efficiently calculate an integral image on GPU, and it accelerates the whole cost-volume filtering process. The overall stereo matching algorithm generates the state-of-the-art results. At the time of submission, it ranks the 10th among about 152 algorithms on the Middlebury stereo evaluation benchmark, and takes the 1st place in all local methods. By implementing the entire algorithm on

the NVIDIA Tesla C2050 GPU, it can achieve over 30 million disparity estimates per second (MDE/s). (Yang, Ji, Li, Yao & Zhang, 2014)

Many image processing problems are ill posed and must be regularized. Usually, a roughness penalty is imposed on the solution. The difficulty is to avoid the smoothing of edges, which are very important attributes of the image. In this paper, first the conditions for the design of such an edge-preserving regularization are given. Under these conditions, it is possible to introduce an auxiliary variable whose role is twofold. First, it marks the discontinuities and ensures their preservation from smoothing. Second, it makes the criterion half-quadratic. The optimization is then easier. A deterministic strategy, based on alternate minimizations on the image and the auxiliary variable is presented. This leads to the definition of an original reconstruction algorithm, called ARTUR. Some theoretical properties of ARTUR are discussed. Experimental results illustrate the behavior of the algorithm. These results are shown in the field of tomography, but this method can be applied in a large number of applications in image processing. (Charbonnier, Blanc-Feraud, Aubert & Barlaud, 1997)

In this paper the detection of human face and eye in still frontal color images is discussed. Firstly; the preprocessing required step is accomplished. It includes image resize, RGB to gray-scale conversion, image binarization, noise removing and small objects removing. Then a proposed algorithm is applied for face localization by detecting the face edges using the detection of the pixel color change in the binary image. Finally, the normalized cross correlation is applied to find the accurate position of eyes within the localized area of the face. (Ismaeel & Ahmad, 2013)

Over the last 20 years, several different techniques have been proposed for computer recognition of human faces. The purpose of this paper is to compare two simple but general strategies on a common database (frontal images of faces of 47 people: 26 males and 21 females, four images per person). We have developed and implemented two new algorithms; the first one is based on the computation of a set of geometrical features, such as nose width and length, mouth position, and chin shape, and the second one is based on almost-grey-level template matching. The results obtained on the testing sets (about 90% correct recognition using geometrical features and perfect recognition using template matching) favor our implementation of the template-matching approach. (Brunelli & Poggio, 1993)

A novel approach for solving the perceptual grouping problem in vision is presented. Rather than focusing on local features and their consistencies in the image data is proposed, the approach aims at extracting the global impression of an image. Image segmentation is treated as a graph partitioning problem and proposes a novel global criterion, the normalized cut, for segmenting the graph. The normalized cut criterion measures both the total dissimilarity between the different groups as well as the total similarity within the groups. We show that an efficient computational technique based on a generalized Eigen value problem can be used to optimize this criterion. This approach is used in segmenting static images, as well as motion sequences. (Shi & Malik, 2000)

The Fast Fourier Transform (FFT) is one of the rudimentary operations in field of digital signal and image processing. Some of the applications of the fast Fourier transform include Signal analysis, Sound filtering, Data compression, Partial differential equations, Multiplication of large integers, Image

filtering etc. Fast Fourier transform (FFT) is an efficient implementation of the discrete Fourier transform (DFT). This paper concentrates on the development of the Fast Fourier Transform (FFT), based on Decimation –In Time (DIT) domain, Radix-2 algorithm, this paper uses VERILOG as a design entity. The input of Fast Fourier transform has been given by a keyboard using a test bench and output has been displayed using the waveforms on the Xilinx Design Suite 13.1 and synthesis results in Xilinx show that the computation for calculating the 32 - point Fast Fourier transform is efficient in terms of speed. (Fatima, 2014)

The non-equispaced Fourier transform arises in a variety of application areas, from medical imaging to radio astronomy to the numerical solution of partial differential equations. In a typical problem, one is given an irregular sampling of N data in the frequency domain and one is interested in reconstructing the corresponding function in the physical domain. When the sampling is uniform, the fast Fourier transform (FFT) allows this calculation to be computed in $O(N \log N)$ operations rather than $O(N^2)$ operations. Unfortunately when the sampling is non-uniform, the FFT does not apply. Over the last few years, a number of algorithms have been developed to overcome this limitation and are often referred to as non-uniform FFTs (NUFFTs). In this paper, we observe that one of the standard interpolation or “gridding” schemes, based on Gaussians, can be accelerated by a significant factor without pre-computation and storage of the interpolation weights. This is of particular value in two- and three dimensional settings, saving either $10^d N$ in storage in d dimensions or a factor of about 5–10 in CPU time (independent of dimension). (Greengard & Lee, 2004)

Existing state-of-the-art switching-based median filters are commonly found to be non-adaptive to noise density variations and prone to misclassifying pixel

characteristics at high noise density interference. This reveals the critical need of having a sophisticated switching scheme and an adaptive weighted median filter. In this paper, we propose a novel switching-based median filter with incorporation of fuzzy-set concept, called the noise adaptive soft-switching median (NASM) filter, to achieve much improved filtering performance in terms of effectiveness in removing impulse noise while preserving signal details and robustness in combating noise density variations. The proposed NASM filter consists of two stages. A soft-switching noise-detection scheme is developed to classify each pixel to be uncorrupted pixel, isolated impulse noise, non-isolated impulse noise or image object's edge pixel. "No filtering" (or identity filter), standard median (SM) filter or our developed fuzzy weighted median (FWM) filter will then be employed according to the respective characteristic type identified. Experimental results show that our NASM filter impressively outperforms other techniques by achieving fairly close performance to that of ideal-switching median filter across a wide range of noise densities, ranging from 10% to 70 %.(Eng & Ma, 2001)

Fast algorithm for two-dimensional median filtering is presented. It is based on storing and updating the gray level histogram of the picture elements in the window. The algorithm is much faster than conventional sorting methods. For a window size of $m \times n$, the computer time required is $O(n)$. (Huang, Yang & Tang, 1979)

The technique of scale multiplication is analyzed in the framework of canny edge detection. A scale multiplication function is defined as the product of the responses of the detection filter at two scales. Edge maps are constructed as the local maxima by thresholding the scale multiplication results. The detection and localization criteria of the scale multiplication are derived. At a small loss in the

detection criterion, the localization criterion can be much improved by scale multiplication. The product of the two criteria for scale multiplication is greater than that for a single scale, which leads to better edge detection performance. (Bao, Zhang & Wu, 2005)

In this paper, the performance of image Denoising algorithms using wavelet transforms can be improved by a post-processing deconvolution step that takes into account the inherent blur function created by the considered wavelet based denoising system is shown. The interest of the proposed de-blurring procedure is illustrated on de-noised images reconstructed by shrinkage of curvelet and undecimated wavelet coefficients. Experimental results reported here show that the proposed post-processing technique yields improvements in term of image quality and lower mean square error, especially when the image is corrupted by strong additive white Gaussian noise. (Mignotte, 2007)

Image Segmentation refers to the process of partitioning an image into non-overlapping different regions with similar attributes, for gray level images, the most basic attribute used is the luminance amplitude, and for color or multispectral images, color or information components are used, so as to provide more details of an image .Segmentation has become a prominent objective in image analysis and computer vision. This paper reviews some of the Technologies used for image segmentation for different images and survey of recent segmentation techniques. (Kaur Seerha, 2013)

This paper addresses the problem of segmenting an image into regions. It defines a predicate for measuring the evidence for a boundary between two regions using a graph-based representation of the image, then develops an efficient segmentation algorithm based on this predicate, and shows that although this

algorithm makes greedy decisions it produces segmentations that satisfy global properties. The algorithm to image segmentation using two different kinds of local neighborhoods in constructing the graph, and illustrating the results with both real and synthetic images has been applied. The algorithm runs in time nearly linear in the number of graph edges and is also fast in practice. An important characteristic of the method is its ability to preserve detail in low-variability image regions while ignoring detail in high-variability regions. (Felzenszwalb & huttnlocher, 2004)

The main focus of image mining is concerned with the classification of brain tumor in the brain MRI images. The proposed method is used to classify the medical images for diagnosis. Steps involved in this system are: pre-processing, feature extraction, association rule mining and classification. Here, we present some experiments for tumor detection in MRI images. The pre-processing step has been done using the median filtering process and features have been extracted using texture feature extraction technique. The extracted features from the CT scan images are used to mine the association rules. In this system we are going to use Decision Tree classification algorithm. The proposed method improves the efficiency than the traditional image mining methods. Here, results which we get are compared with Naive Bayesian classification algorithm. (Naik & Patel, 2011)

Image Segmentation is an important basis process in image analysis. It is used in several processes, which receive the input of more advanced processes, the result of which will affect the accuracy of overall results significantly. Edge detection is the basic process of image segmentation. The Sobel Filter, Derivative of Gaussian and Laplace of Gaussian are well-known methods of edge detection. However, these methods cannot detect edge details and it remains difficult to segment thin areas because the edge pixels obliterate details. For example, in a text

image, the details of the characters are obliterated by using these methods. We propose an image segmentation method by using boundary code to solve this problem. Thin areas are segmented continuously by using our proposed segmentation method. In an experiment, we compare the proposed method with existing method. We use binarization with a discriminant analysis method and a sobel filter to compare our proposed method. According to the experimental result, the proposed method segments more accurately than existing methods in images that has a narrow elongated object, shading and blurring. (Uemura,Koutaki & Uchimura,2011)

In order to preferably identify infrared image of refuge chamber, reduce image noises of refuge chamber and retain more image details, we propose the method of combining two-dimensional discrete wavelet transform and bilateral de-noising. First, the wavelet transform is adopted to decompose the image of refuge chamber, of which low frequency component remains unchanged. Then, three high-frequency components are treated by bilateral filtering, and the image is reconstructed. The result shows that the combination of bilateral filtering and wavelet transform for image de-noising can better retain the details which are included in the image, while providing better visual effect. This is superior to using either bilateral filtering or wavelet transform alone. It is useful for perfecting emergency refuge system of coal mines. (Zhang, 2013)

Image segmentation has played an important role in computer vision especially for human tracking. The result of image segmentation is a set of segments that collectively cover the entire image or a set of contours extracted from the image. Its accuracy but very elusive is very crucial in areas as medical, remote sensing and image retrieval where it may contribute to save, sustain and

protect human life. This paper presents the analysis and implementation using MATLAB features and one best result can be selected for any algorithm using the subjective evaluation. We considered the techniques under the following five groups: Edge-based, Clustering-based, Region-based, Threshold-based and Graph-based. (Verma, Khare, Gupta & Chandel, 2013)

A method that combines region growing and edge detection for image segmentation is presented. It is started with a split and merge algorithm where the parameters have been set up so that an over-segmented image results. Then region boundaries are eliminated or modified on the basis of criteria that integrate contrast with boundary smoothness, variation of the image gradient along the boundary, and a criterion that penalizes for the presence of artifacts reflecting the data structure used using segmentation. (Pavlidis & Liow, 1990)

An ensemble of descriptors for face recognition is proposed in this paper. Starting from the base patterns of the oriented edge magnitudes (POEM) descriptor, different ensembles by varying the preprocessing techniques, the parameters for extracting the accumulated magnitude images (AM), and the parameters of the local binary patterns (LBP) applied to AM are developed. The best proposed ensemble works well regardless of whether dimensionality reduction by principal component analysis (PCA) is performed or not before the matching step. It was validated using the FERET datasets and the Labeled Faces in the Wild (LFW) dataset. (Nanni, Lumini, Brahman & Migliaridi, 2013)

This literature review attempts to provide a brief overview of some of the most common segmentation techniques, and a comparison between them. It discusses the “Grab-Cut” technique, and reviews some of the common matting techniques. The graph cut approaches to segmentation can be extended to 3-D data

and can be used for segmenting 3-D volumes. Other segmentation techniques use either contour or edge segmentation to perform segmentation. The graph cut techniques use both contour and edge information. The main matting techniques are Poisson matting and probabilistic alpha matting using color statistics. Poisson matting works directly on the alpha matte of the image, and is interactive. The statistical approach uses Gaussians to model color statistics in the image and is not interactive. (Marsh)

Histogram is the basis for numerous spatial domain processing techniques. Histogram manipulation is used for image enhancement. Histogram are simple technique to calculate in software and also lend themselves to economic hardware implementations, thus can be used as popular tool for real-time image processing. The focus of this paper is attempt to improve the quality of digital images using Histogram Equalization in MATLAB version R2007a software and result obtained are discussed and highlights the performance of method. (Patil & Thakare, 2014)

Blind deconvolution is the recovery of a sharp version of a blurred image when the blur kernel is unknown. Recent algorithms have afforded dramatic progress, yet many aspects of the problem remain challenging and hard to understand. The goal of this paper is to analyze and evaluate recent blind deconvolution algorithms both theoretically and experimentally. We explain the previously reported failure of the naive MAP approach by demonstrating that it mostly favors no-blur explanations. On the other hand we show that since the kernel size is often smaller than the image size a MAP estimation of the kernel alone can be well constrained and accurately recover the true blur. The plethora of recent deconvolution techniques makes an experimental evaluation on ground-truth data important. We have collected blur data with ground truth and compared recent

algorithms under equal settings. Additionally, our data demonstrates that the shift-invariant blur assumption made by most algorithms is often violated. (Levin, Weiss, Durand & Freema, 2009)

A neural network-based upright frontal face detection system is presented. A retinally connected neural network examines small windows of an image and decides whether each window contains a face. The system arbitrates between multiple networks to improve performance over a single network. A straightforward procedure for aligning positive face examples for training is presented. To collect negative examples, we use a bootstrap algorithm, which adds false detections into the training set as training progresses. This eliminates the difficult task of manually selecting non-face training examples, which must be chosen to span the entire space of non-face images. Simple heuristics, such as using the fact that faces rarely overlap in images, can further improve the accuracy. Comparisons with several other state-of-the-art face detection systems are presented, showing that our system has comparable performance in terms of detection and false-positive rates. (Rowley, Baluja & Kanade, 1998)

A discrete cosine transform (DCT) is defined and an algorithm to compute it using the fast Fourier transform is developed. It is shown that the discrete cosine transform can be used in the area of digital processing for the purposes of pattern recognition and Wiener filtering. Its performance is compared with that of a class of orthogonal transforms and is found to compare closely to that of the Karhunen-Lo'eve transform, which is known to be optimal. The performances of the Karhunen-Lo'eve and discrete cosine transforms are also found to compare closely with respect to the rate-distortion criterion. (Ahmed, Natarajan & Rao, 1974)

The computational tools and a hardware prototype for 3D face recognition are presented. Full automation is provided through the use of advanced multistage alignment algorithms, resilience to facial expressions by employing a deformable model framework, and invariance to 3D capture devices through suitable preprocessing steps. In addition, scalability in both time and space is achieved by converting 3D facial scans into compact metadata. We present our results on the largest known, and now publicly available, Face Recognition Grand Challenge 3D facial database consisting of several thousand scans. To the best of our knowledge, this is the highest performance reported on the FRGC v2 database for the 3D modality. (Kakadiaris, Passalis, Toderici, Murtuza, Lu, Karampatziakis & Theoharis, 2007)

Face recognition algorithms have to deal with significant amounts of illumination variations between gallery and probe images. State-of-the-art commercial face recognition algorithms still struggle with this problem. A new image preprocessing algorithm that compensates for illumination variations in images is proposed. From a single brightness image the algorithm first estimates the illumination field and then compensates for it to mostly recover the scene reflectance. Unlike previously proposed approaches for illumination compensation, our algorithm does not require any training steps, knowledge of 3D face models or reflective surface models. We apply the algorithm to face images prior to recognition. We demonstrate large performance improvements with several standard face recognition algorithms across multiple, publicly available face databases. (Gross & Brajovic, 2003)

This paper presented a review on different image segmentation techniques. Segmentation is the stage where a significant commitment is made during

automated analysis by delineating structures of interest and discriminating them from back ground tissue. It is also useful for feature extraction, image measurements and image display. The aim of this paper is to give a detailed review on digital image segmentation techniques in three major fields of images as gray scale images, hyper-spectral images and medical images. It has been useful in medical image processing as well as hyper-spectral image processing. This evaluation on image segmentation techniques will be very useful for the development and improvement of new techniques. (Tripathi, Kumar, Singh & Singh, 2012)

The scale-space technique introduced by Witkin involves generating coarser resolution images by convolving the original image with a Gaussian kernel. This approach has a major drawback: it is difficult to obtain accurately the locations of the “semantically meaningful” edges at coarse scales. This paper suggests a new definition of scale-space, and introduces a class of algorithms that realize it using a diffusion process. The diffusion coefficient is chosen to vary spatially in such a way as to encourage intra-region smoothing in preference to inter-region smoothing. It is shown that the “no new maxima should be generated at coarse scales” property of conventional scale space is pre-served. As the region boundaries in our approach remain sharp, we obtain a high quality edge detector which successfully exploits global information. Experimental results are shown on a number of images. The algorithm involves elementary, local operations replicated over the image making parallel hardware implementations feasible. (Perona & Malik,1990)

This paper discusses an extension of the well-known phase correlation technique to cover translation, rotation, and scaling. Fourier scaling properties and

Fourier rotational properties are used to find scale and rotational movement. The phase correlation technique determines the translational movement. This method shows excellent robustness against random noise. (Reddy & Chatterji, 1996)

Many image segmentation techniques are available in the literature. Some of these techniques use only gray level histogram, some use spatial details while others use fuzzy set theoretic approaches. Most of these techniques are not suitable for noisy environments. Some works have been done using the Markov Random Field (MRF) model which is robust to noise, but is computationally involved. Neural network architectures which help to get the output in real time because of their parallel processing ability, have also been used for segmentation and they work fine even when the noise level is very high. The literature on color image segmentation is not that rich as it is gray tone images. This paper critically reviews and summarizes some of these techniques. Attempts have been made to cover both fuzzy and non-fuzzy techniques including color images and magnetic resonance images. It also addresses the issue of quantitative evaluation of segmentation results. (Pal & Pal, 1993)

Differences in illumination conditions cause significant challenges for any 2-D face recognition algorithm. One of the methods to counter these effects is image preprocessing before feature extraction. In this paper we present a new preprocessing approach that uses custom filters obtained through an optimization procedure striving for most suitable preprocessing filters for the selected feature extractor and distance measure. We experiment with it using Local Binary Pattern texture features and χ^2 histogram distance metric. Results are provided for Face Recognition Grand Challenge (FRGC) 1.0.4 dataset. (Holappa , Ahonen & Pietikainen, 2008)

In a recent publication, it was shown that median filtering is an optimization process in which a two-term cost function is minimized. Based on this functional optimization property of the median filtering process, a new approach for designing the recursive median filter for image processing applications is introduced in this paper. We prove that the new approach is guaranteed to converge to root within a finite number of iterations. The new method is applied to process a real image corrupted by pseudorandom impulsive noise, and the results show that the new scheme provides improved mean square error (MSE) performance over the standard recursive median filters. (Qiu, 1996)

Image segmentation is the process of partitioning an image into multiple segments, so as to change the representation of an image into something that is more meaningful and easier to analyze. Several general-purpose algorithms and techniques have been developed for image segmentation. This paper describes the different segmentation techniques used in the field of ultrasound and SAR Image Processing. Firstly this paper investigates and compiles some of the technologies used for image segmentation. Then a bibliographical survey of current segmentation techniques is given in this paper and finally general tendencies in image segmentation are presented. (Dass & Devi, 2012)

Making recognition more reliable under uncontrolled lighting conditions is one of the most important challenges for practical face recognition systems. We tackle this by combining the strengths of robust illumination normalization, local texture based face representations, and distance transform based matching, kernel-based feature extraction and multiple feature fusion. (Tan & Triggs, 2010)

Bilateral filtering smoothes images while preserving edges, by means of a nonlinear combination of nearby image values. The method is non-iterative, local,

and simple. It combines gray levels or colors based on both their geometric closeness and their photometric similarity, and prefers near values to distant values in both domain and range. In contrast with filters that operate on the three bands of a color image separately, a bilateral filter can enforce the perceptual metric underlying the CIE-Lab color space, and smooth colors and preserve edges in a way that is tuned to human perception. Also, in contrast with standard filtering, bilateral filtering produces no phantom colors along edges in color images, and reduces phantom colors where they appear in the original image. (Tomasi & Manduchi, 1998)

Quantitative evaluation and comparison of image segmentation algorithms is now feasible owing to the recent availability of collections of hand-labeled images. However, little attention has been paid to the design of measures to compare one segmentation result to one or more manual segmentations of the same image. Existing measures in statistics and computer vision literature suffer either from intolerance to labeling refinement, making them unsuitable for image segmentation, or from the existence of degenerate cases, making the process of training algorithms using the measures to be prone to failure. This paper surveys previous work on measures of similarity and illustrates scenarios where they are applicable for performance evaluation in computer vision. For the image segmentation problem, we propose a measure that addresses the above concerns and has desirable properties such as accommodation of labeling errors at segment boundaries, region sensitive refinement, and compensation for differences in segment ambiguity between images. (Unnikrishnan & Hebert, 2005)

In computer vision and image processing, edge detection concerns the localization of significant variations of the grey level image and the identification

of the physical phenomena that originated them. This information is very useful for applications in 3D reconstruction, motion, recognition, image enhancement and restoration, image registration, image compression, and so on. Usually, edge detection requires smoothing and differentiation of the image. Differentiation is an ill-conditioned problem and smoothing results in a loss of information. It is difficult to design a general edge detection algorithm which performs well in many contexts and captures the requirements of subsequent processing stages. Consequently, over the history of digital image processing a variety of edge detectors have been devised which differ in their mathematical and algorithmic properties. This paper is an account of the current state of our understanding of edge detection. We propose an overview of research in edge detection: edge definition, properties of detectors, the methodology of edge detection, the mutual influence between edges and detectors, and existing edge detectors and their implementation. (Ziou & Tabbone, 1998)



A Fast Discrete Cosine Transform algorithm has been developed which provides a factor of six improvements in computational complexity when compared to conventional Discrete Cosine Transform algorithms using the Fast Fourier Transform. The algorithm is derived in the form of matrices and illustrated by a signal-flow graph, which may be readily translated to hardware or software implementations. (Wen-Hsiung, Harrison & Fraclik, 1977)







DATA COLLECTION







3. Data Collection





The facial photographs were collected from two different sources. The photographs with Indian ethnicity were mostly photographed of an age group of 18-22 in Women's Christian College. The photographs of people with British ethnicity were taken from (Burton et al.). The total numbers of samples considered are 200.

Table 1 : Data Collection

S.NO.	ORIGINAL	ETHNICITY	GENDER	AGE
1		INDIAN	FEMALE	22
2		INDIAN	FEMALE	22
3		INDIAN	FEMALE	22
4		INDIAN	FEMALE	45







5		INDIAN	FEMALE	77
6		INDIAN	FEMALE	22
7		INDIAN	MALE	15
8		INDIAN	FEMALE	22
9		INDIAN	FEMALE	22
10		INDIAN	FEMALE	22







11		INDIAN	FEMALE	22
12		WHITE BRITISH	MALE	47
13		WHITE BRITISH	MALE	19
14		WHITE BRITISH	MALE	20
15		WHITE BRITISH	MALE	20
16		WHITE BRITISH	MALE	20

17		WHITE BRITISH	FEMALE	20
18		WHITE BRITISH	FEMALE	19
19		WHITE BRITISH	FEMALE	24
20		WHITE BRITISH	FEMALE	18
21		WHITE BRITISH	FEMALE	33
22		WHITE BRITISH	MALE	40

23		WHITE BRITISH	MALE	21
24		WHITE BRITISH	FEMALE	19
25		WHITE BRITISH	MALE	26
26		WHITE BRITISH	FEMALE	24
27		ASIAN BRITISH	FEMALE	19
28		WHITE BRITISH	MALE	20

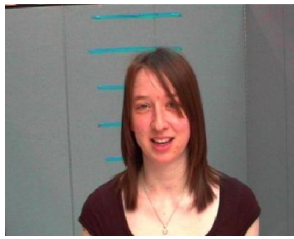
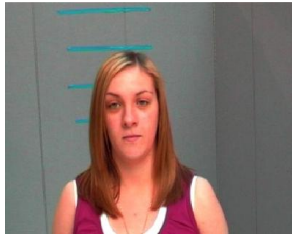




29		WHITE BRITISH	MALE	20
30		WHITE BRITISH	MALE	20
31		WHITE BRITISH	MALE	20
32		WHITE BRITISH	FEMALE	22
33		WHITE BRITISH	FEMALE	22
34		WHITE BRITISH	FEMALE	22

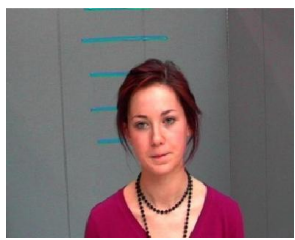





35		WHITE BRITISH	FEMALE	20
36		WHITE BRITISH	FEMALE	22
37		ASIAN BRITISH	MALE	18
38		WHITE BRITISH	MALE	18
39		WHITE BRITISH	FEMALE	19
40		WHITE BRITISH	FEMALE	19



41		INDIAN	FEMALE	22
42		INDIAN	MALE	45
43		INDIAN	FEMALE	22
44		INDIAN	FEMALE	22
45		INDIAN	FEMALE	21
46		INDIAN	FEMALE	21







47	 A portrait of a woman with dark hair pulled back, wearing a light blue V-neck shirt. The background is a plain, light-colored wall. A small yellow timestamp '02/08/2014' is visible in the bottom right corner of the photo.	INDIAN	FEMALE	22
48	 A portrait of a woman wearing a white and yellow sari. She is standing in front of a wooden door. A small yellow timestamp '02/08/2014' is visible in the bottom right corner of the photo.	INDIAN	FEMALE	23
49	 A portrait of a woman wearing a green patterned short-sleeved shirt. The background is a plain, light-colored wall. A small yellow timestamp '02/08/2014' is visible in the bottom right corner of the photo.	INDIAN	FEMALE	22
50	 A portrait of a man with glasses and a mustache, wearing a yellow shirt. He is indoors, with a staircase and a doorway visible in the background. A small yellow timestamp '02/08/2014' is visible in the bottom right corner of the photo.	INDIAN	MALE	50
51	 A portrait of a woman wearing a black top with white polka dots. She is outdoors, with trees and a bench in the background. A small yellow timestamp '11/02/2014' is visible in the bottom right corner of the photo.	INDIAN	FEMALE	19
52	 A portrait of a woman wearing glasses and a blue button-down shirt. She is outdoors, with green foliage and a building in the background. A small yellow timestamp '11/02/2014' is visible in the bottom right corner of the photo.	INDIAN	FEMALE	19

53		INDIAN	FEMALE	20
54		INDIAN	FEMALE	20
55		INDIAN	FEMALE	20
56		WHITE BRITISH	FEMALE	21
57		WHITE BRITISH	MALE	21
58		WHITE BRITISH	FEMALE	24

59		WHITE BRITISH	FEMALE	20
60		WHITE BRITISH	FEMALE	20
61		WHITE BRITISH	MALE	22
62		WHITE BRITISH	MALE	25
63		WHITE BRITISH	FEMALE	19
64		WHITE BRITISH	MALE	18







65		WHITE BRITISH	FEMALE	18
66		WHITE BRITISH	FEMALE	18
67		WHITE BRITISH	MALE	18
68		WHITE BRITISH	FEMALE	17
69		WHITE BRITISH	MALE	38
70		WHITE BRITISH	MALE	19

71		WHITE BRITISH	MALE	19
72		WHITE BRITISH	MALE	19
73		WHITE BRITISH	MALE	21
74		WHITE BRITISH	MALE	20
75		WHITE BRITISH	MALE	23
76		WHITE BRITISH	FEMALE	22


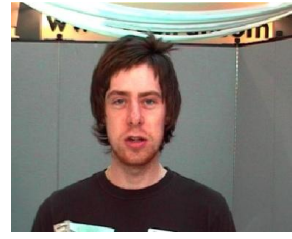

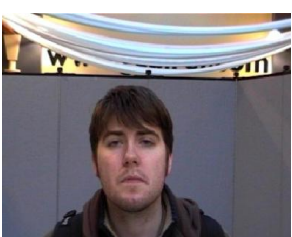
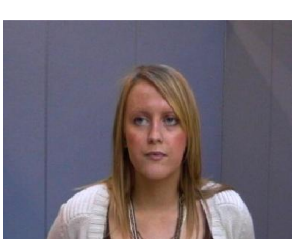
77		WHITE BRITISH	MALE	20
78		WHITE BRITISH	MALE	19
79		WHITE BRITISH	MALE	19
80		WHITE BRITISH	FEMALE	18
81		WHITE BRITISH	FEMALE	36
82		WHITE BRITISH	MALE	35

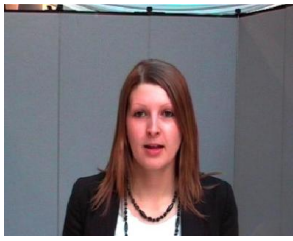





83		WHITE BRITISH	FEMALE	41
84		WHITE BRITISH	MALE	31
85		WHITE BRITISH	FEMALE	21
86		WHITE BRITISH	FEMALE	30
87		WHITE BRITISH	FEMALE	47
88		WHITE BRITISH	FEMALE	22


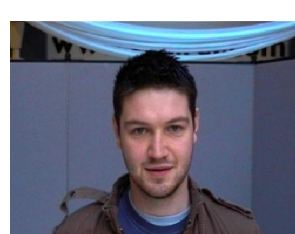
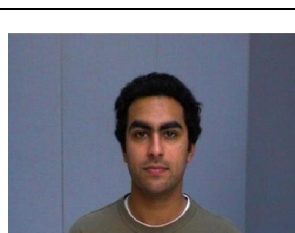
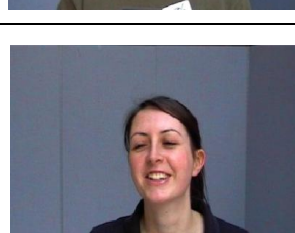


89		WHITE BRITISH	FEMALE	25
90		WHITE BRITISH	MALE	21
91		WHITE BRITISH	FEMALE	47
92		WHITE BRITISH	FEMALE	35
93		WHITE BRITISH	FEMALE	46
94		WHITE BRITISH	FEMALE	55

95		WHITE BRITISH	MALE	60
96		WHITE BRITISH	MALE	20
97		WHITE BRITISH	FEMALE	20
98		WHITE BRITISH	FEMALE	21
99		WHITE BRITISH	MALE	21
100		WHITE BRITISH	MALE	37

101		WHITE BRITISH	MALE	40
102		WHITE BRITISH	MALE	20
103		WHITE BRITISH	MALE	25
104		WHITE BRITISH	MALE	21
105		WHITE BRITISH	MALE	20
106		WHITE BRITISH	MALE	21


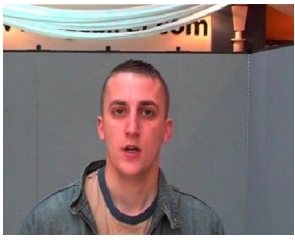
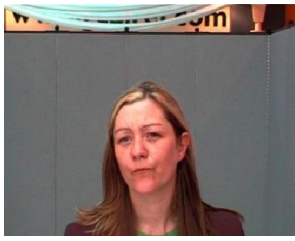
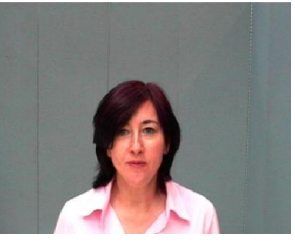
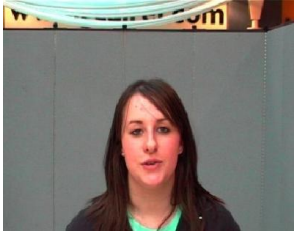
107		WHITE BRITISH	MALE	21
108		WHITE BRITISH	MALE	26
109		WHITE BRITISH	MALE	21
110		WHITE BRITISH	FEMALE	23
111		WHITE BRITISH	MALE	22
112		WHITE BRITISH	FEMALE	24



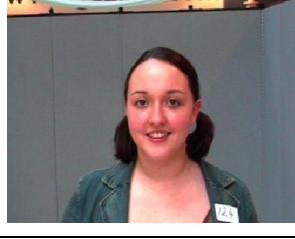
113		WHITE BRITISH	FEMALE	22
114		WHITE BRITISH	FEMALE	22
115		WHITE BRITISH	MALE	23
116		WHITE BRITISH	MALE	20
117		WHITE BRITISH	MALE	23
118		WHITE BRITISH	MALE	59


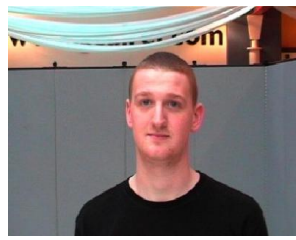



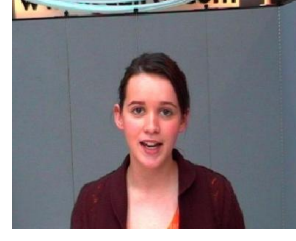
119		WHITE BRITISH	FEMALE	20
120		WHITE BRITISH	MALE	22
121		ASIAN BRITISH	MALE	21
122		WHITE BRITISH	FEMALE	22
123		WHITE BRITISH	FEMALE	21
124		WHITE BRITISH	FEMALE	23






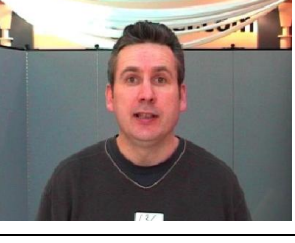
125		WHITE BRITISH	FEMALE	27
126		WHITE BRITISH	MALE	24
127		WHITE BRITISH	MALE	26
128		WHITE BRITISH	FEMALE	28
129		WHITE BRITISH	FEMALE	19
130		WHITE BRITISH	MALE	24







131		WHITE BRITISH	MALE	20
132		WHITE BRITISH	MALE	23
133		WHITE BRITISH	FEMALE	18
134		WHITE BRITISH	FEMALE	18
135		WHITE BRITISH	FEMALE	25
136		WHITE BRITISH	FEMALE	27


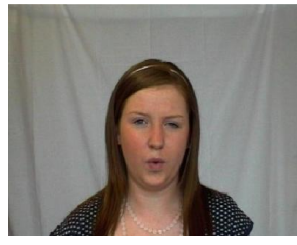
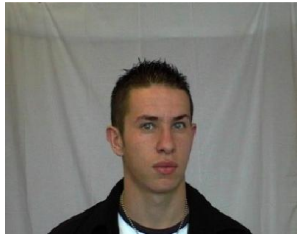
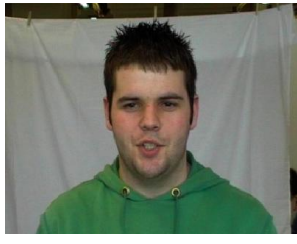

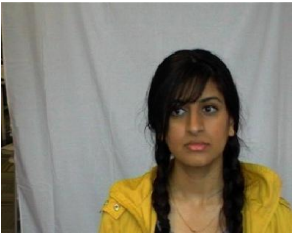
137		WHITE BRITISH	MALE	23
138		WHITE BRITISH	MALE	23
139		WHITE BRITISH	FEMALE	37
140		WHITE BRITISH	FEMALE	42
141		WHITE BRITISH	FEMALE	20
142		WHITE BRITISH	FEMALE	21



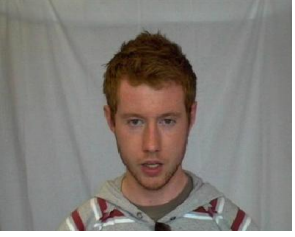
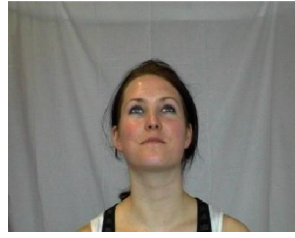


143		WHITE BRITISH	MALE	38
144		WHITE BRITISH	MALE	33
145		WHITE BRITISH	MALE	34
146		ASIAN BRITISH	MALE	20
147		WHITE BRITISH	FEMALE	21
148		WHITE BRITISH	FEMALE	18



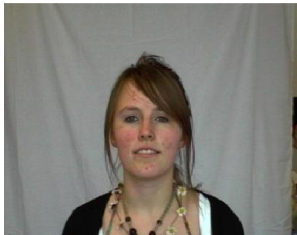



149		WHITE BRITISH	MALE	21
150		WHITE BRITISH	MALE	19
151		WHITE BRITISH	FEMALE	26
152		WHITE BRITISH	MALE	22
153		WHITE BRITISH	MALE	18
154		WHITE BRITISH	FEMALE	18






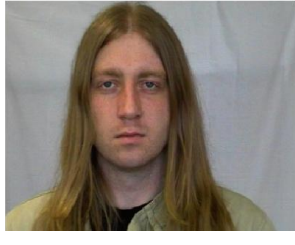
155		WHITE BRITISH	FEMALE	18
156		WHITE BRITISH	FEMALE	19
157		WHITE BRITISH	MALE	28
158		WHITE BRITISH	MALE	18
159		WHITE BRITISH	FEMALE	27
160		WHITE BRITISH	MALE	43

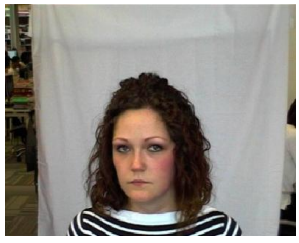
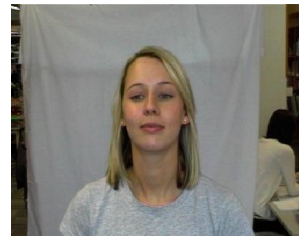
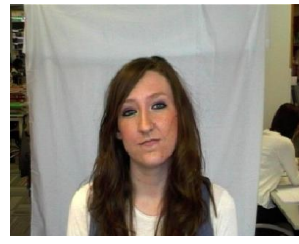

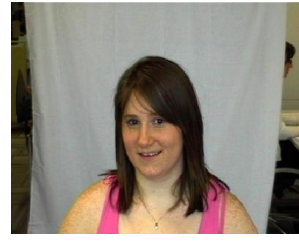

161		WHITE BRITISH	FEMALE	22
162		WHITE BRITISH	MALE	53
163		WHITE BRITISH	MALE	18
164		WHITE BRITISH	MALE	18
165		WHITE BRITISH	MALE	18
166		WHITE BRITISH	FEMALE	31

167		WHITE BRITISH	FEMALE	18
168		WHITE BRITISH	FEMALE	19
169		WHITE BRITISH	MALE	20
170		WHITE BRITISH	MALE	19
171		WHITE BRITISH	MALE	20
172		ASIAN BRITISH	FEMALE	20

173		ASIAN BRITISH	FEMALE	18
174		ASIAN BRITISH	FEMALE	21
175		WHITE BRITISH	MALE	20
176		WHITE BRITISH	FEMALE	18
177		WHITE BRITISH	FEMALE	18
178		WHITE BRITISH	FEMALE	22

179		WHITE BRITISH	MALE	20
180		WHITE BRITISH	MALE	20
181		WHITE BRITISH	FEMALE	20
182		WHITE BRITISH	MALE	25
183		WHITE BRITISH	MALE	19
184		WHITE BRITISH	FEMALE	20

185		WHITE BRITISH	MALE	20
186		ASIAN BRITISH	MALE	26
187		ASIAN BRITISH	MALE	25
188		ASIAN BRITISH	MALE	24
189		ASIAN BRITISH	MALE	26
190		WHITE BRITISH	MALE	26

191		WHITE BRITISH	FEMALE	21
192		WHITE BRITISH	FEMALE	21
193		WHITE BRITISH	FEMALE	22
194		WHITE BRITISH	MALE	19
195		WHITE BRITISH	FEMALE	19
196		WHITE BRITISH	MALE	20



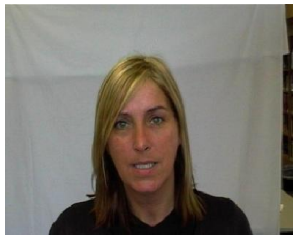
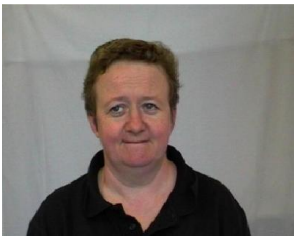
197		ASIAN BRITISH	MALE	22
198		WHITE BRITISH	MALE	21
199		WHITE BRITISH	FEMALE	41
200		WHITE BRITISH	MALE	40

IMAGE TRANSFORMATION

4. Image Transformation

4.1 Introduction

Image transformations typically involve the manipulation of multiple bands of data, whether from a single multispectral image or from two or more images of the same area acquired at different times. Either way, image transformations generate "new" images from two or more sources which highlight particular features or properties of interest, better than the original input images.

4.2 Fourier Transformation

The Fourier Transform was developed by Jean Baptiste Joseph Fourier to explain the distribution of temperature and heat conduction. Fourier is widely used in the field of image processing. An image is a spatially varying function. It is used to convert image data from time domain to frequency domain. Transformation doesn't lose data present in the signal. The main reason this transformation is used is to isolate critical components of the image pattern so that they are directly accessible for analysis.

Let $g(x)$ be a continuous function of a real variable x , the Fourier transform of $g(x)$ is defined as $F\{g(x)\}$ by the equation

$$F\{g(x)\} = F(u) = \int_{-\infty}^{\infty} E[-j2\pi ua] dx \quad \text{where } j = \sqrt{-1}$$

----- [Eq. 4.1]

Given $F(u)$, $g(x)$ can be obtained by using the inverse Fourier transform

$$F^{-1}\{F(u)\} = g(x) = \int_{-\infty}^{\infty} F(u)E[-j2\pi ua]du$$

----- [Eq. 4.2]

[Eq. 4.1] and [Eq. 4.2] form the Fourier Transform pair. This exists if and only if $g(x)$ is continuous and integratable and $F(u)$ is integratable. $g(x)$ is assumed to be a real function. The Fourier transform of a real function. However is generally complex in nature.

$$F(u) = \text{Real}(u) + j \text{Imag}(u)$$

$\text{Real}(u) \rightarrow \text{Real part of } u$

$\text{Imag}(u) \rightarrow \text{Imaginary part of } u$

$$\text{So } F(u) = |F(u)| e^{j\phi(u)}$$

$$\text{where } |F(u)| = \sqrt{\text{Real}^2(u) + \text{Imag}^2(u)}$$

$$\phi(u) = \tan^{-1} \frac{\text{Imag}(u)}{\text{Real}(u)}$$

$|F(u)|$ is defined as the magnitude function, and it is called as the Fourier spectrum of $g(u)$ and $\phi(u)$ is known as phase angel of $g(u)$.

The power of the spectrum or spectral density of $g(a)$ is given as

$$P(u) = |F(u)|^2$$

where u is the frequency variable.

The given expression $E[-j2\pi ux]$ is Euler's formula and can be given by

$$E[-j2\pi ux] = \cos 2\pi ux - j \sin 2\pi ux$$

Interpreting [I] as the limit summation of discrete terms makes evident that $F(u)$ is composed of an infinite sum of sine and cosine terms and that each value of u determines the frequency of its sine-cosine pair.

Discrete Transformation pair in terms of [I] and [II] is given by

$$F(u) = \frac{1}{N} \sum_{x=0}^{N-1} g(x) E[-j2\pi ux/N] \text{ for } u = 0,1,2 \dots N-1$$

$$g(x) = \sum_{u=0}^{N-1} F(u) E\left[\frac{j2\pi ux}{N}\right] \text{ where } x = 0,1,2 \dots N-1$$

----- [Eq. 4.3]

4.4 Fast Fourier Transformation

The number of complex multiplication and additions required to implement Discrete Fourier Transform [III] is proportional to N^2 . That is for each of the N values of u expansion of the summation requires N complex multiplication of $g(x)$ by $E[-j2\pi ux/N]$ and $N-1$ additions of the results. The terms of $E[-j2\pi ux/N]$ can be computed once and stored in a table for all subsequent application. For this reason, the multiplication of u by x in these terms is usually not considered a direct part of the implementation.

Proper decomposition of [III] can make the number of multiplication and addition operations proportional to $N \log_2 N$. The decomposition procedure is called Fast Fourier Transform algorithm. The reduction in proportionality from N^2 to $N \log_2 N$ operations represents a significant saving in computational effort.

4.4 Fast Fourier Transformation

By the fast fourier transform, the magnitude and phase of an image can be separated

4.6 Direct Cosine Transformation (DCT)

The $N \times N$ cosine transform matrix $C = \{C(k,n)\}$ also called the direct cosine transform is defined as

$$C(k, n) = \begin{cases} \frac{1}{\sqrt{N}} & \text{for } k = 0, 0 \leq n \leq N - 1 \\ \sqrt{\frac{2}{N}} \cos \frac{\pi(2n+1)k}{2N} & \text{for } 1 \leq k \leq N - 1, 0 \leq n \leq N - 1 \end{cases}$$

The one dimensional DCT of a sequence $\{u(n), 0 \leq n \leq N-1\}$ is defined as

$$V(k) = \alpha(k) \sum_{n=0}^{N-1} u(n) \cos \left[\frac{\pi(2n+1)k}{2N} \right] \text{ For } 0 \leq k \leq N - 1$$

$$\text{where } \alpha(0) \triangleq \sqrt{\frac{1}{N}}, \alpha(k) \triangleq \sqrt{\frac{2}{N}} \text{ for } 1 \leq k \leq N - 1$$

The inverse transformation is given by

$$u(n) = \sum_{k=0}^{N-1} \alpha(k) v(k) \cos \frac{\pi(2n+1)k}{2N} \text{ for } 0 \leq n \leq N - 1$$

IMAGE ENHANCEMENT

5. Image Enhancement

5.1 Introduction

Image Enhancement refers to sharpening of image features such as edges, boundaries or contrast to make a graphic display more useful to display and analysis. The enhancement process doesn't increase the inherent information content in the data. But it does increase the dynamic range of the chosen features so that they can be detected easily. Image enhancement includes gray level and contrast manipulation, noise reduction, edge crispening and sharpening, filtering, interpolation and magnification, pseudo-coloring and so on. The greatest difficulty in image enhancement is quantifying the criterion for enhancement. Therefore, a large number of image enhancement techniques are empirical and require interactive procedures to obtain satisfactory results. The principal objective of enhancements techniques is to process an image so that the result is more suitable than the original image for a specific application.

There different types of Image Enhancement techniques

1. Point Operation
 - a. Contrast Stretching
 - b. Noise clipping
 - c. Window Slicing
 - d. Histogram Modeling
2. Spatial Ordering
 - a. Noise smoothing
 - b. Median filtering

- c. Un-sharp masking
 - d. Low-pass filtering
 - e. Band-pass filtering
 - f. High-pass filtering
 - g. Zoom
3. Transform operation
- a. Linear filtering
 - b. Root filtering
 - c. Homo-morphic filtering
4. Pseudo Coloring
- a. False coloring
 - b. Pseudo coloring

In the list of different enhancement techniques, two techniques are used in this project

- 1. Histogram Modeling
- 2. Median Filtering

5.2 Histogram Modeling

The histogram of a digital image with gray levels in the range $[0, L-1]$ is a discrete function $p(r_k) = n_k/n$, where r_k is the k^{th} gray level, n_k is the number of pixels in the image with that gray level, n is the total number of pixels in the image and $k=0,1,2\dots L-1$. Loosely speaking $p(r_k)$ gives an estimate of the probability of occurrence of gray level v_k . A plot of this function for all values of k provides a global description of the appearance of an image.

Higher-order histograms have also been found useful in image analysis applications. A second-order histogram is an estimate of the joint probability density function of pairs of pixels. The pairs may originate from different locations in the same grayscale image or from the same location in two channels of a color or multispectral image. In the former case we get what is commonly called a co-occurrence matrix (also known as the gray-tone spatial dependence matrix), in the latter the joint histogram of a pair of color channels. In a co-occurrence matrix the value at the coordinate $\{i,j\}$ is the number of pixel pairs having gray level i at position $\{x,y\}$ and gray level j at position $\{x,y\}+v$, where v is some fixed displacement vector. In a joint histogram, the value at position i, j is the number of pixels with value i in one channel and value j at the same location in the other. For an 8-bit image (256 luminance levels), the dimensionality of the resulting histogram matrix is 256×256 , which may be prohibitive for many applications. For this reason, prior to processing, pixel values are typically quantized to reduce the number of levels.

5.2.1 Grey Level Histogram

The gray-scale histogram of an image represents the distribution of the pixels in the image over the gray-level scale. It can be visualised as if each pixel is placed in a bin corresponding to the colour intensity of that pixel. All of the pixels in each bin are then added up and displayed on a graph. This graph is the histogram of the image. Figure below illustrates the histogram of a sample image. The frequencies of all the intensity levels can be seen, and the image can be analysed based on this.



Figure 2: Input image for histogram

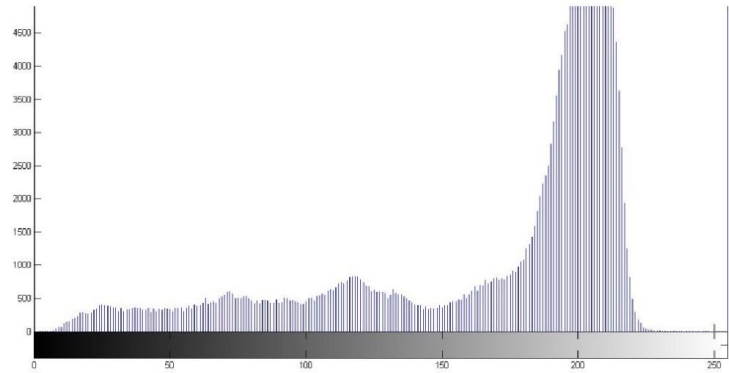


Figure 3: Grey level histogram

5.2.2 Histogram Equalization

Let the variable r represent the gray levels in the image to be enhanced. In the initial part of discussion, the assumption is that pixel values are continuous quantities that have been normalized so that they lie in the interval $[0, 1]$, with $r=0$ representing black and $r=1$ representing white. Later it is considered a discrete formulation and allows pixel values to be in the interval $[0, L-1]$.

For r satisfying these conditions, transformation of the form

$$s = T(r) \text{ for } 0 \leq r \leq L - 1$$

It produces an output intensity s for every pixel in the input image having intensity r . It is assumed that $T(r)$ is a monotonically increasing function in the interval $0 \leq r \leq L - 1$ and $0 \leq T(r) \leq L - 1$ for $0 \leq r \leq L - 1$.

The requirement in condition that $T(r)$ be monotonically increasing guarantees that output intensity values will never be less than corresponding input values, thus preventing artifacts created by reversals of intensity.

5.3 Median Filtering

This filtering technique involves the replacement of the input pixel by the median of the pixels contained in a window around the pixel that is

$$v(m, n) = \text{median}\{y(m - k, n - l), (k, l) \in W\}$$

where W is a suitably chosen window. The algorithm of median filtering requires arranging the pixel values in the window in increasing or decreasing order and picking the middle value.

Generally the window size is chosen so that N_w is odd. If N_w is even then the median is taken as the average of the two values in the middle. N_w is the number of pixels for chosen window. Typical windows are 3×3 , 5×5 , 7×7 etc. The 5 point window is considered for spatial averaging.



Figure 4: Input image for median filtering



Figure 5: Median Filtering of image effected by salt and pepper noise

IMAGE SEGMENTATION

6. Image Segmentation

6.1 Introduction

Image segmentation is the process of partitioning a digital image into multiple segments (sets of pixels, also known as super pixels). The goal of segmentation is to simplify and/or change the representation of an image into something that is more meaningful and easier to analyze. Image segmentation is typically used to locate objects and boundaries (lines, curves, etc.) in images. More precisely, image segmentation is the process of assigning a label to every pixel in an image such that pixels with the same label share certain visual characteristics.

The result of image segmentation is a set of segments that collectively cover the entire image, or a set of contours extracted from the image. Each of the pixels in a region is similar with respect to some characteristic or computed property, such as color, intensity, or texture. Adjacent regions are significantly different with respect to the same characteristics. When applied to a stack of images, typical in medical imaging, the resulting contours after image segmentation can be used to create 3D reconstructions with the help of interpolation algorithms like marching cubes.

The following are few methods of image segmentation:

- Edge Detection
- Corner Detection
- Blob Detection

- Ridge Detection
- Hough Detection

6.2 Edge Detection

Edge detection is the name for a set of mathematical methods which aim at identifying points in a digital image at which the image brightness changes sharply or, more formally, has discontinuities. The points at which image brightness changes sharply are typically organized into a set of curved line segments termed edges. The same problem of finding discontinuities in 1D signal is known as step detection and the problem of finding signal discontinuities over time is known as change detection. Edge detection is a fundamental tool in image processing, machine vision and computer vision, particularly in the areas of feature detection examples of operators such as Canny, Sobel, Kayyali, etc. and feature extraction.

6.2.1 Importance of Edge Detection

Edge detection is a problem of fundamental importance in image analysis. The purpose of edge detection is to identify areas of an image where a large change in intensity occurs. These changes are often associated with some physical boundary in the scene from which the image is derived. In typical images, edges characterize object boundaries and are useful for segmentation, registration and identification of objects in a scene.

6.3 Types of Edge Detection

6.3.1 Sobel

The Sobel operator represents a rather inaccurate approximation of the image gradient, but is still of sufficient quality to be of practical use in many applications. More precisely, it uses intensity values only in a 3×3 region around each image point to approximate the corresponding image gradient, and it uses only integer values for the coefficients which weight the image intensities to produce the gradient approximation. The following is example of the 3×3 filter.

$$\begin{bmatrix} -1 & 0 & 1 \\ 0 & 0 & 0 \\ 1 & 0 & -1 \end{bmatrix} \quad \left| \quad \begin{bmatrix} 1 & 2 & 1 \\ 0 & 0 & 0 \\ -1 & -2 & -1 \end{bmatrix} \right.$$

6.3.2 Roberts Kernel

The produced edges should be well-defined, the background should contribute as little noise as possible, and the intensity of edges should correspond as close as possible to what a human would perceive.

$$\begin{bmatrix} 1 & 0 & -1 \\ 0 & 1 & -1 \end{bmatrix} \quad \left| \quad \begin{bmatrix} 1 & 0 & -1 \\ 0 & 1 & -1 \end{bmatrix}^2$$

where x is the initial intensity value in the image, z is the computed derivative and i, j represent the location in the image.

6.3.3 Prewitt Kernel

The gradient of a two-variable function (here the image intensity function) is at each image point a 2D vector with the components given by the derivatives in

the horizontal and vertical directions. At each image point, the gradient vector points in the direction of largest possible intensity increase, and the length of the gradient vector corresponds to the rate of change in that direction.

This implies that the result of the Prewitt operator at an image point which is in a region of constant image intensity is a zero vector and at a point on an edge is a vector which points across the edge, from darker to brighter values

6.3.4 Laplacian of Gaussian (LoG)

The Laplacian is a 2-D isotropic measure of the 2nd spatial derivative of an image. The Laplacian of an image highlights regions of rapid intensity change and is therefore often used for edge detection (see zero crossing edge detectors). The Laplacian is often applied to an image that has first been smoothed with something approximating a Gaussian smoothing filter in order to reduce its sensitivity to noise, and hence the two variants will be described together here. The operator normally takes a single gray level image as input and produces another gray level image as output.

The Laplacian $L(x, y)$ of an image with pixel intensity values $I(x, y)$ is given by:

$$L(x, y) = \frac{\partial^2 I}{\partial x^2} + \frac{\partial^2 I}{\partial y^2}$$

This can be calculated using a convolution filter. Since the input image is represented as a set of discrete pixels, we have to find a discrete convolution kernel that can approximate the second derivatives in the definition of the Laplacian. Two commonly used small kernels given below

0	-1	0	-1	-1	-1
-1	4	-1	-1	8	-1
0	-1	0	-1	-1	-1

6.3.5 Canny Edge Detector

Canny algorithm aims to discover the optimal edge detection algorithm. In this situation, an "optimal" edge detector means:

- good detection – the algorithm should mark as many real edges in the image as possible.
- good localization – edges marked should be as close as possible to the edge in the real image.
- minimal response – a given edge in the image should only be marked once, and where possible, image noise should not create false edges.

To satisfy these requirements Canny used the calculus of variations – a technique which finds the function which optimizes a given functional. The optimal function in Canny's detector is described by the sum of four exponential terms, but it can be approximated by the first derivative of a Gaussian.

6.3.5.1 Stages of the Canny algorithm

Noise reduction: The image after a 5x5 Gaussian mask has been passed across each pixel. Because the Canny edge detector is susceptible to noise present in raw unprocessed image data, it uses a filter based on a Gaussian (bell) curve, where the raw image is convolved with a Gaussian filter. The result is a slightly blurred version of the original which is not affected by a single noisy pixel to any

significant degree. Here is an example of a 5x5 Gaussian filter, used to create the image to the right, with $\sigma = 1.4$.

$$E = \frac{1}{256} \begin{pmatrix} 0.22 & 0.42 & 0.61 & 0.78 & 0.91 \\ 0.42 & 0.81 & 1.26 & 1.67 & 2.04 \\ 0.61 & 1.26 & 1.99 & 2.69 & 3.34 \\ 0.78 & 1.67 & 2.69 & 3.76 & 4.38 \\ 0.91 & 2.04 & 3.34 & 4.38 & 5.09 \end{pmatrix} \quad \text{etc.}$$

Finding the intensity gradient of the image: An edge in an image may point in a variety of directions, so the Canny algorithm uses four filters to detect horizontal, vertical and diagonal edges in the blurred image. The edge detection operator (Roberts, Prewitt, Sobel for example) returns a value for the first derivative in the horizontal direction (G_x) and the vertical direction (G_y). From this the edge gradient and direction can be determined:

$$G = \sqrt{G_x^2 + G_y^2}$$

$$\Theta = \text{atan2}(G_y, G_x)$$

where G can be computed using the hypot function and atan2 is the arctangent function with two arguments. The edge direction angle is rounded to one of four angles representing vertical, horizontal and the two diagonals (0, 45, 90 and 135 degrees for example).

Non-maximum suppression: Non-maximum suppression is an edge thinning technique. Given estimates of the image gradients, a search is carried out to determine if the gradient magnitude assumes a local maximum in the gradient

direction. In some implementations, the algorithm categorizes the continuous gradient directions into a small set of discrete directions, and then moves a 3x3 filter over the output of the previous step (that is, the edge strength and gradient directions). At every pixel, it suppresses the edge strength of the center pixel (by setting its value to 0) if its magnitude is not greater than the magnitude of the two neighbors in the gradient direction. For example, if the rounded gradient angle is zero degrees (i.e. the edge is in the north-south direction) the point will be considered to be on the edge if its gradient magnitude is greater than the magnitudes at pixels in the north and south directions, if the rounded gradient angle is 90 degrees (i.e. the edge is in the east-west direction) the point will be considered to be on the edge if its gradient magnitude is greater than the magnitudes at pixels in the east and west directions, if the rounded gradient angle is 135 degrees (i.e. the edge is in the north east-south west direction) the point will be considered to be on the edge if its gradient magnitude is greater than the magnitudes at pixels in the north east and south west directions, if the rounded gradient angle is 45 degrees (i.e. the edge is in the north west-south east direction) the point will be considered to be on the edge if its gradient magnitude is greater than the magnitudes at pixels in the north west and south east directions. In more accurate implementations, linear interpolation is used between the two neighboring pixels that straddle the gradient direction. For example, if the gradient angle is between 45 degrees and 90 degrees interpolation between gradients at the north east and east pixels will give one interpolated value, and interpolation between the south west and west pixels will give the other (using the conventions of last paragraph). The gradient magnitude at the central pixel must be greater than both of these for it to mark as an edge.

Tracing edges through the image and hysteresis thresholding: Large intensity gradients are more likely to correspond to edges than small intensity gradients. It is in most cases impossible to specify a threshold at which a given intensity gradient switches from corresponding to an edge into not doing so. Therefore Canny uses thresholding with hysteresis. Thresholding with hysteresis requires two thresholds – high and low. Making the assumption that important edges should be along continuous curves in the image allows us to follow a faint section of a given line and to discard a few noisy pixels that do not constitute a line but have produced large gradients. Therefore we begin by applying a high threshold. These marks out the edges we can be fairly sure are genuine. Starting from these, using the directional information derived earlier, edges can be traced through the image. While tracing an edge, we apply the lower threshold, allowing us to trace faint sections of edges as long as we find a starting point. Once this process is complete we have a binary image where each pixel is marked as either an edge pixel or a non-edge pixel. From complementary output from the edge tracing step, the binary edge map obtained in this way can also be treated as a set of edge curves, which after further processing can be represented as polygons in the image domain.

RESULTS & DISCUSSION

7. Results & Discussion

7.1 Descriptive Statistics

As given in the data collection, a total number 200 samples. The following is the descriptive analysis of the data being considered.

7.1.1 Gender Based

Table 2: Gender Distribution

		Frequency	Percent	Valid Percent	Cumulative Percent
Valid	FEMALE	104	52.0	52.0	52.0
	MALE	96	48.0	48.0	100.0
	Total	200	100.0	100.0	

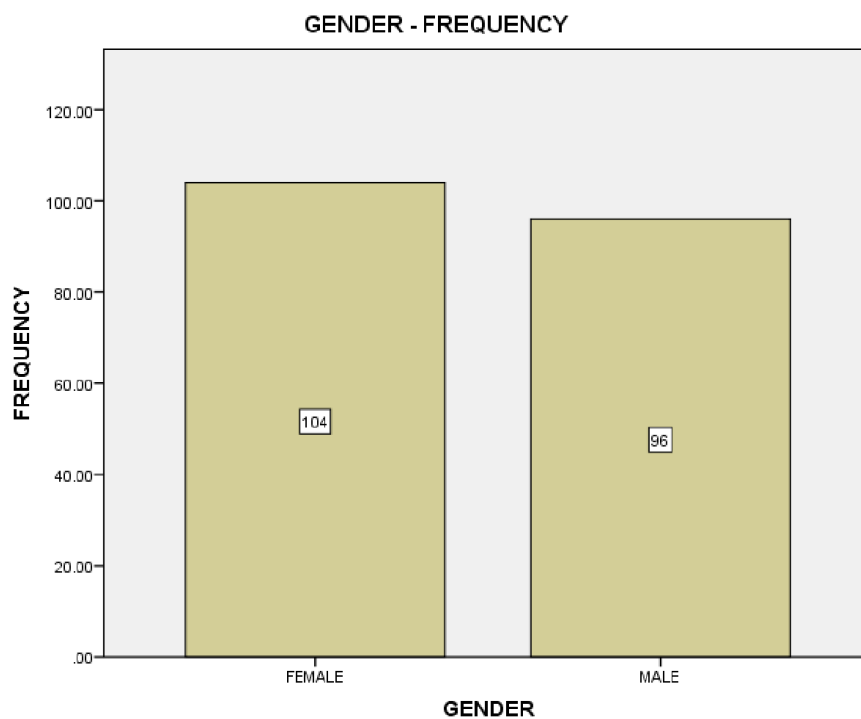


Figure 6: Gender Frequency Bar graph

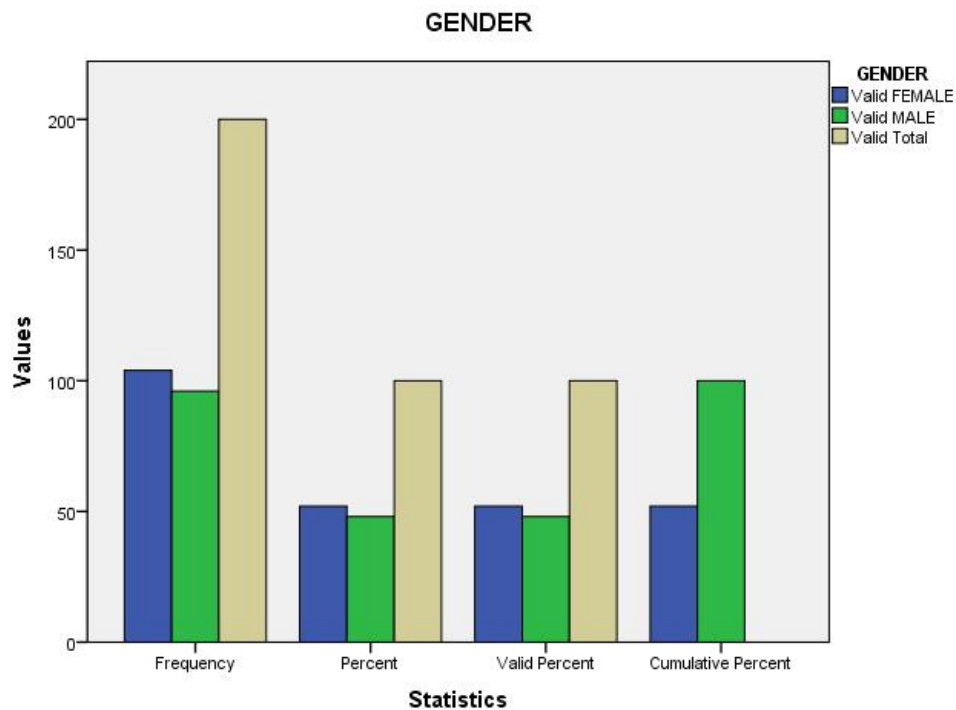


Figure 7: Gender Statistics

7.1.2 Ethnicity Based

Table 3: Ethnicity Distribution

		Frequency	Percent	Valid Percent	Cumulative Percent
Valid	ASIAN BRITISH	12	6.0	6.0	6.0
	INDIAN	26	13.0	13.0	19.0
	WHITE BRITISH	162	81.0	81.0	100.0
	Total	200	100.0	100.0	

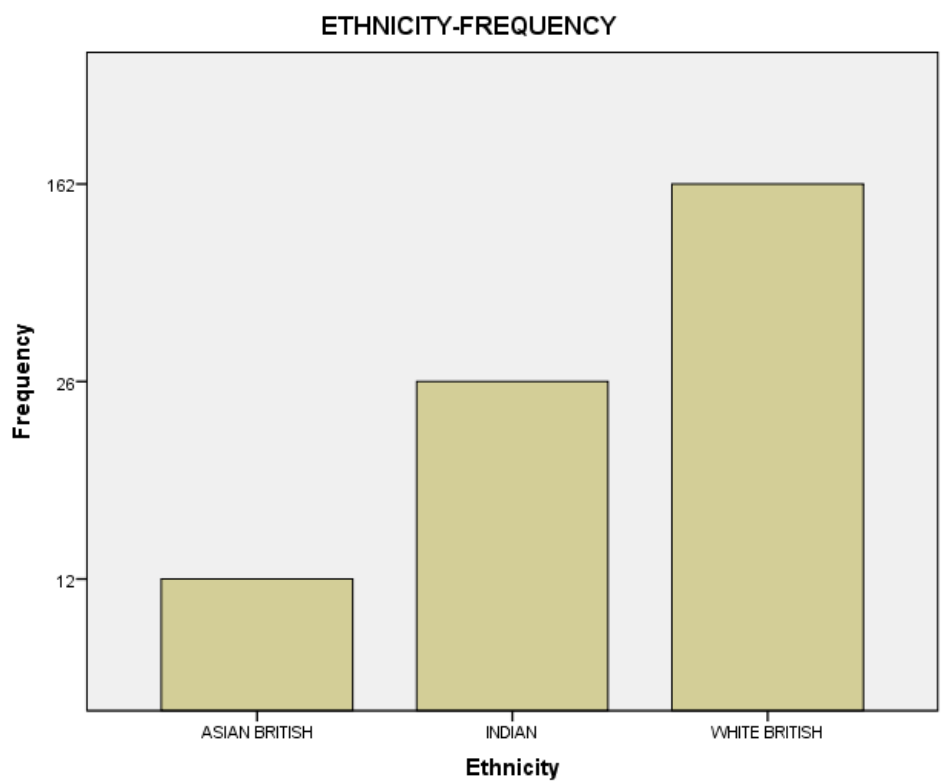


Figure 8: Ethnicity-Frequency Bar Graph

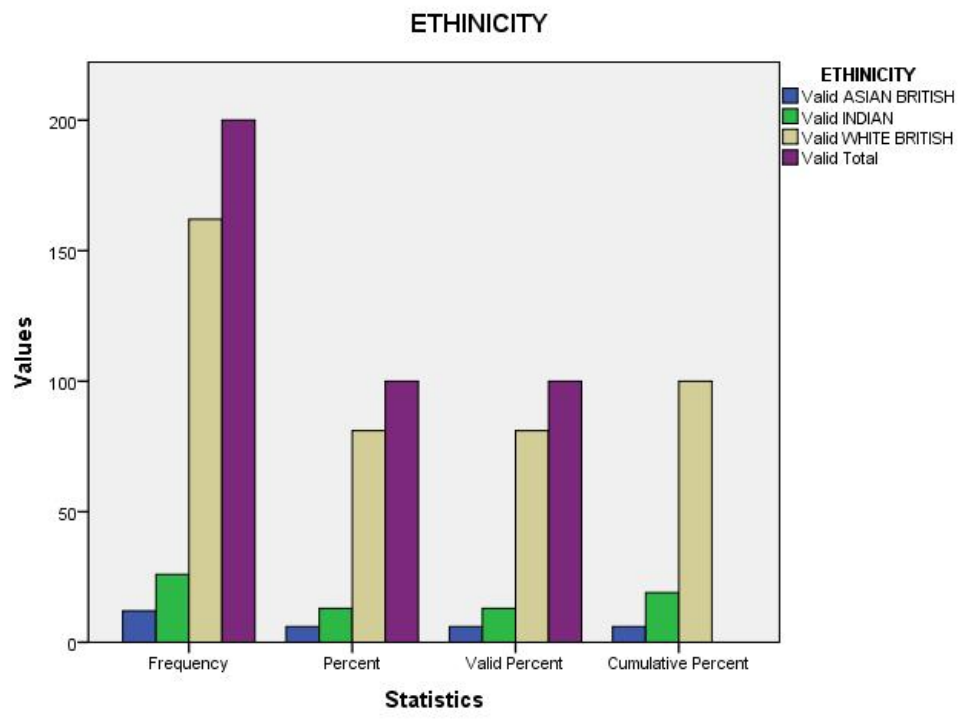


Figure 9: Ethnicity Statistics

7.1.3 Age Based

Table 3: Age Distribution

		Frequency	Percent	Valid Percent	Cumulative Percent
Valid	15.0	1	.5	.5	.5
	17.0	1	.5	.5	1.0
	18.0	22	11.0	11.0	12.0
	19.0	22	11.0	11.0	23.0
	20.0	35	17.5	17.5	40.5
	21.0	23	11.5	11.5	52.0
	22.0	30	15.0	15.0	67.0
	23.0	9	4.5	4.5	71.5
	24.0	7	3.5	3.5	75.0
	25.0	6	3.0	3.0	78.0
	26.0	7	3.5	3.5	81.5
	27.0	3	1.5	1.5	83.0
	28.0	2	1.0	1.0	84.0
	30.0	1	.5	.5	84.5
	31.0	2	1.0	1.0	85.5
	33.0	2	1.0	1.0	86.5
34.0	1	.5	.5	87.0	
35.0	2	1.0	1.0	88.0	

36.0	1	.5	.5	88.5
37.0	2	1.0	1.0	89.5
38.0	2	1.0	1.0	90.5
40.0	3	1.5	1.5	92.0
41.0	2	1.0	1.0	93.0
42.0	1	.5	.5	93.5
43.0	1	.5	.5	94.0
45.0	2	1.0	1.0	95.0
46.0	1	.5	.5	95.5
47.0	3	1.5	1.5	97.0
50.0	1	.5	.5	97.5
53.0	1	.5	.5	98.0
55.0	1	.5	.5	98.5
59.0	1	.5	.5	99.0
60.0	1	.5	.5	99.5
77.0	1	.5	.5	100.0
Total	200	100.0	100.0	

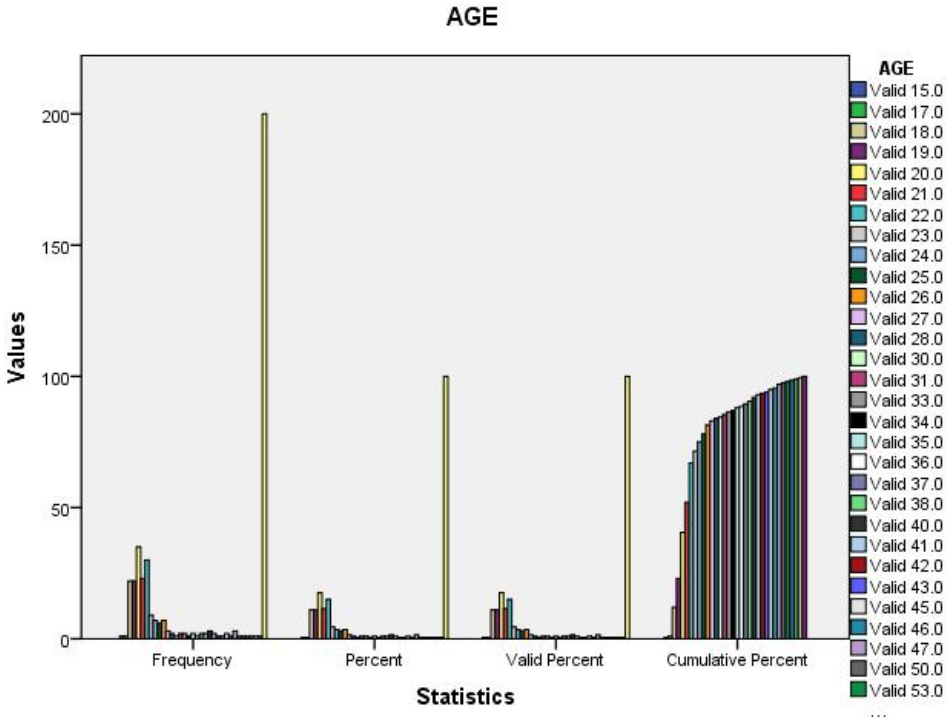


Figure 10: Age Statistics

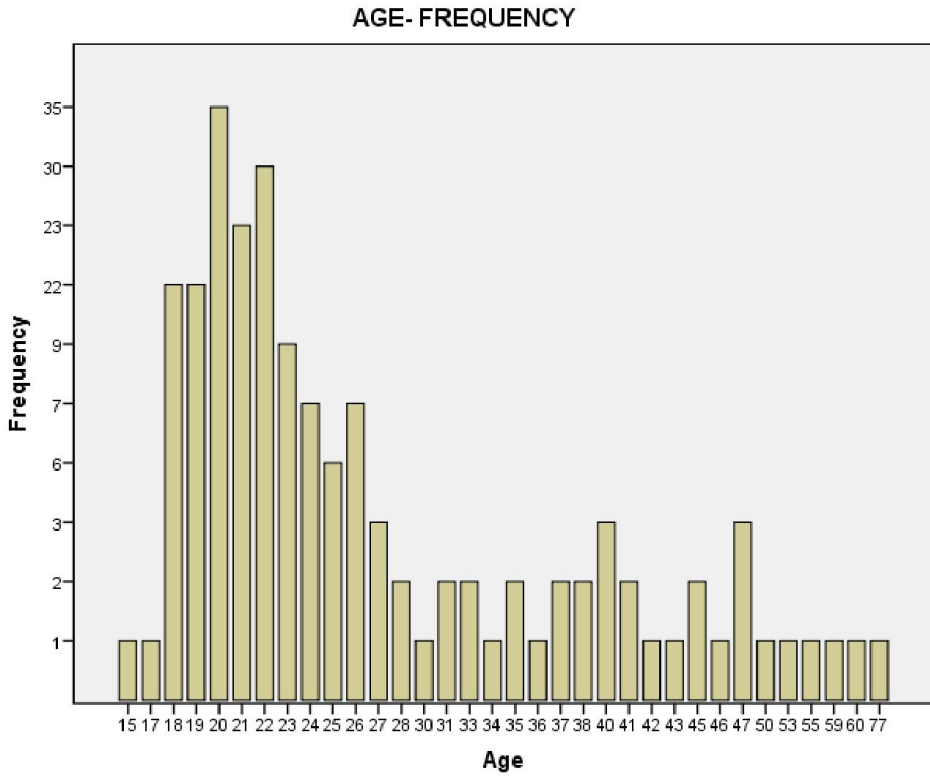


Figure 11: Age Frequency Bar Graph

7.2 Adding Noise to the Images

The following is sample data of the size 100 (the first 100 in data collection are considered here) in which 4 different kinds of noises are added namely Speckle, Poisson, Gaussian and Salt & Pepper. For the Pre-Processing for Facial Recognition System, the Salt & Pepper is considered as it would provide the maximum disorientation to facial images (Disorientation is considered based on feature extraction). From the following the data, the above stated statement can be proved. Refer to column 1:4 in the results table provided later in this chapter.

7.3 Adding Fast Fourier Transformation

After Salt & Pepper addition to the image is transformed into frequency domain. The main reason the step is included is that using the frequency domain, the user can later on extract specific feature. Feature extraction is easier in frequency domain rather than the spatial domain. The following is a sample image of fast fourier transformation and its inverse.

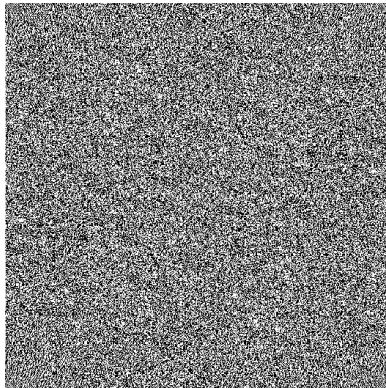


Figure 12: Fast Fourier Transformation of image



Figure 13: Inverse Fast Fourier Transformation

7.4 Histogram Equalization

The method is used to reduce the problem due to lighting conditions as discussed in the problem definition. In this method, the whole image is equalized to avoid the ambiguity caused by the lighting conditions. The histogram of the original image and equalized image show the difference in the frequency of grey levels in the image. Refer to column 5:7 in the results table provided later in this chapter.

7.5 Median Filtering

The median filtering method is the enhancement used to remove the noise from the image. It is considered most effective method as feature details are not lost during the process of filtering. The loss of the image data is very low. Refer to column 8 in the results table provided later in this chapter.

7.6 Edge Detection Methods

Five different edge detection methods are tested in the sample data (size: 100). In which Canny Edge Detector is proved to be best for face detection and feature extraction. The edge detectors used are Laplacian of Gaussian, Sobel, Roberts, Prewitt and Canny.

The following are Value Distribution Statistical Data shown below for a single image, the sample data (No. 1) is considered for the distribution here.

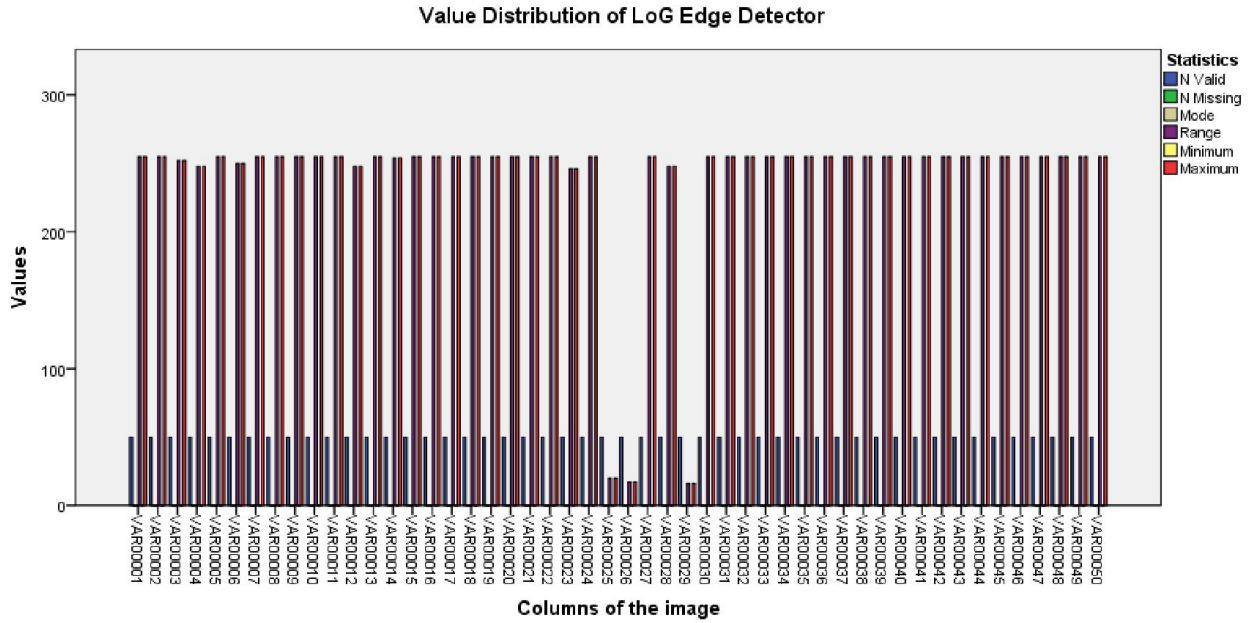


Figure 14: Value Distribution of LoG Edge Detector

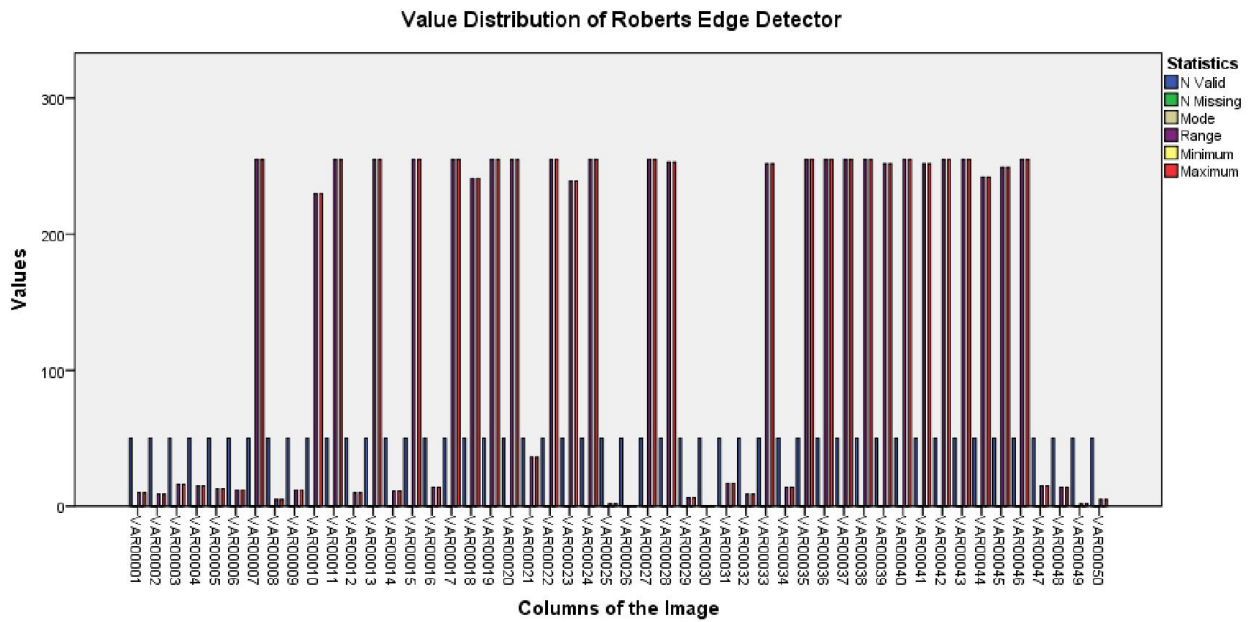


Figure 15: Value Distribution of Roberts Edge Detector

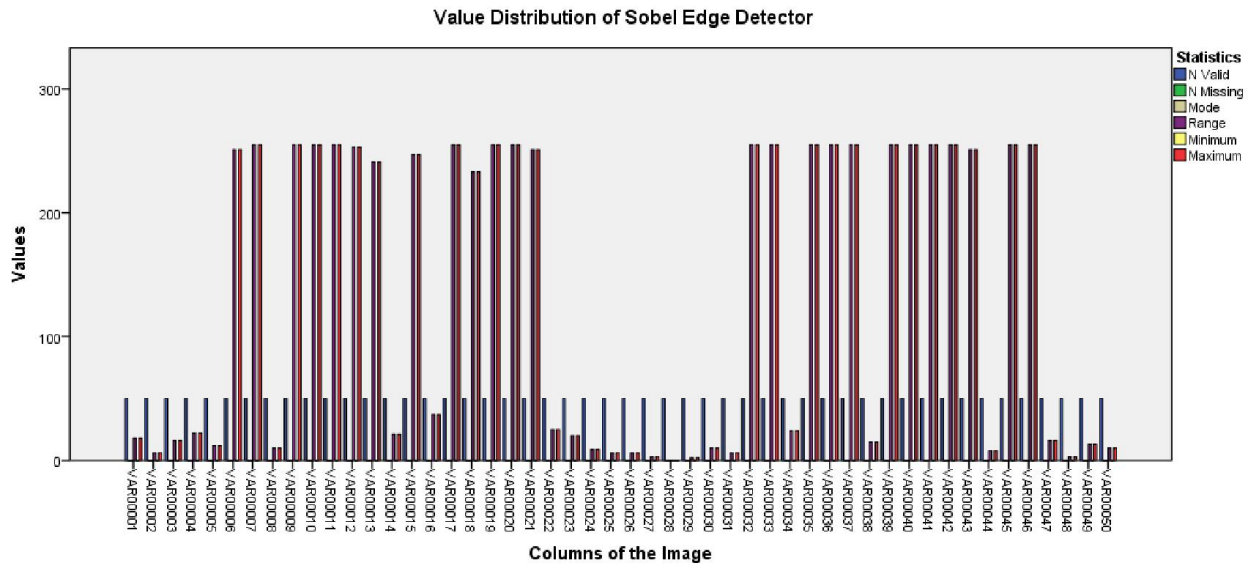


Figure 16: Value Distribution of Sobel Edge Detector

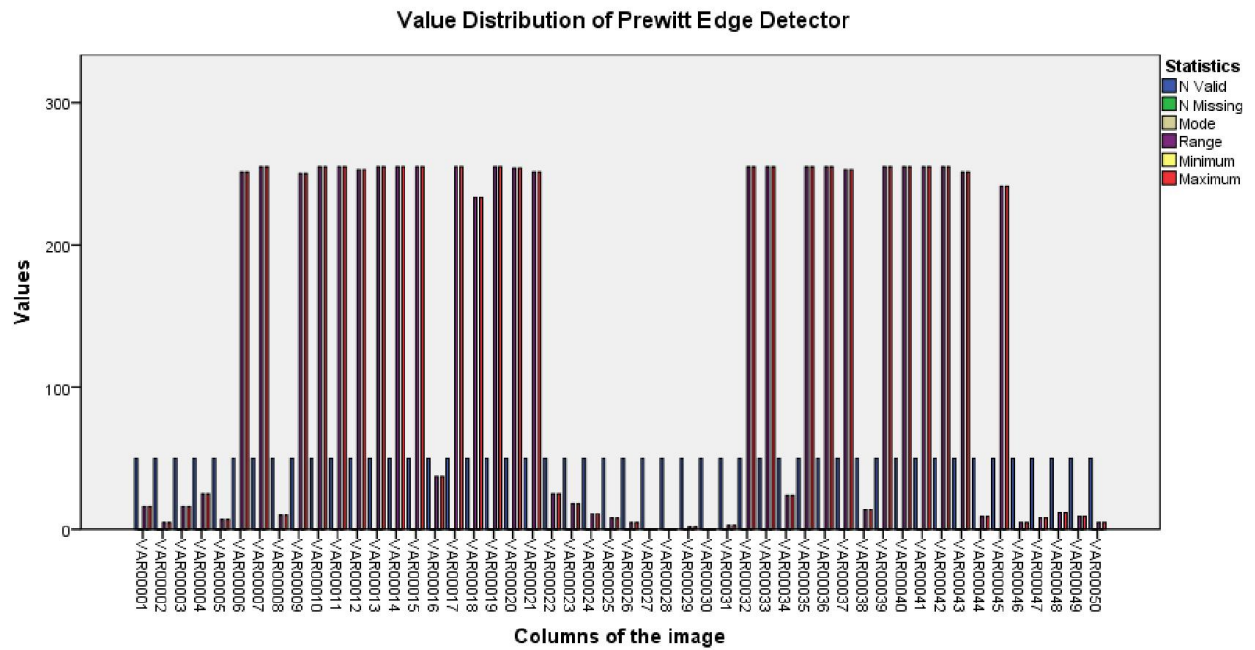


Figure 17: Value Distribution of Prewitt Edge Detector

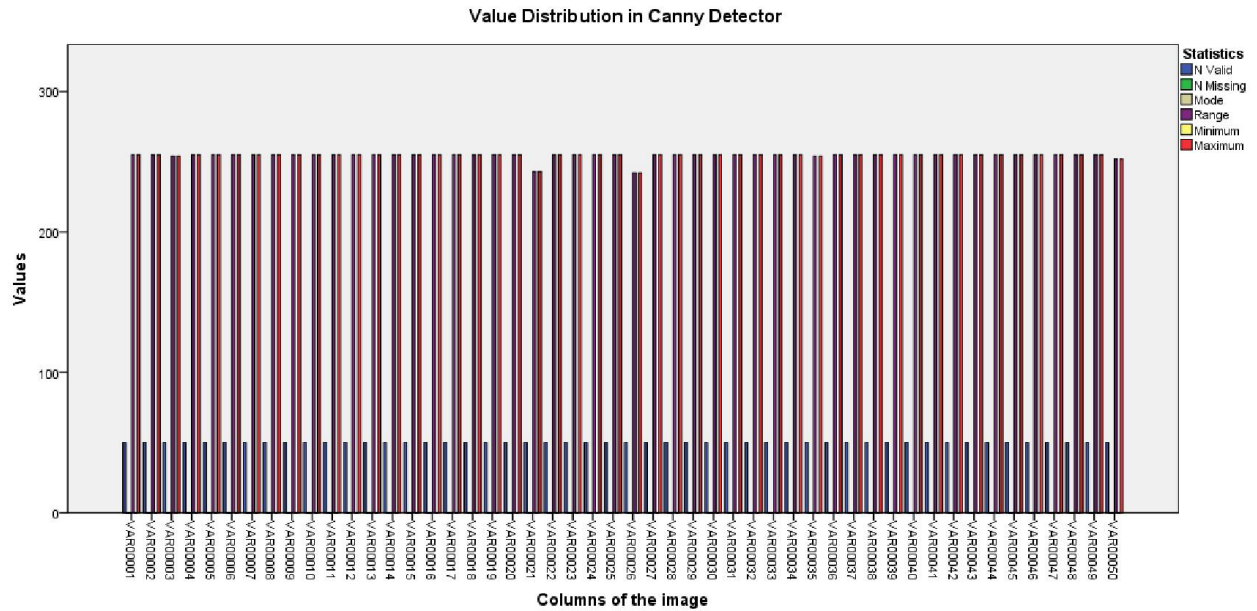
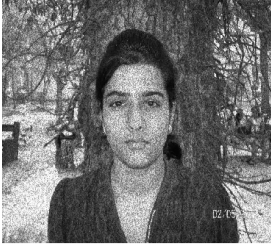
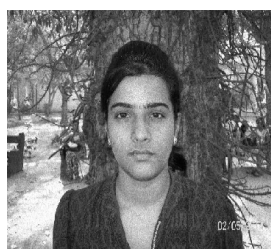
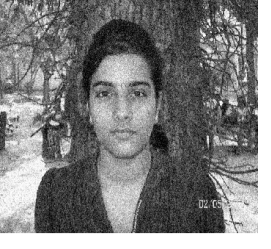
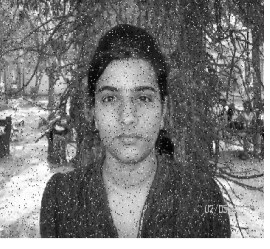









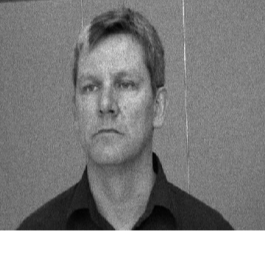

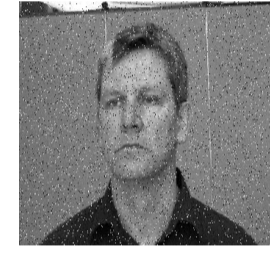

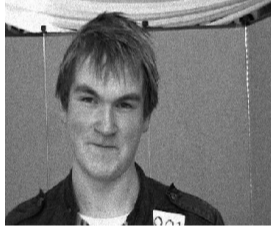
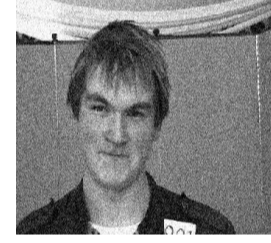
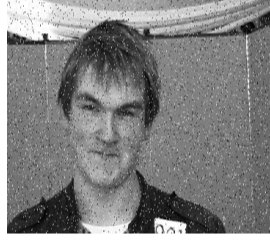






























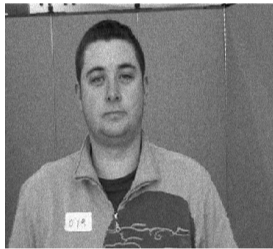






















Figure 18: Value Distribution of Prewitt Edge Detector

Comparing the value distribution charts provided, it is obvious that canny provides in depth information. LoG detector can also be considered but as seen in the sample distribution, the essential central columns have lost data. Refer to column 9:13 in the results table provided later in this chapter.

S.NO	SPECKLE	POISSON	GAUSSIAN	SALT & PEPPER
1				
2				
3				
4				
5				
6				
7				
8				

9				
10				
11				
12				
13				
14				
15				
16				
17				

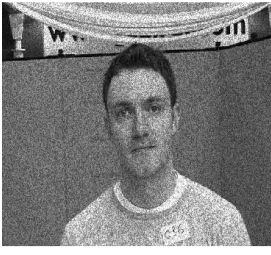
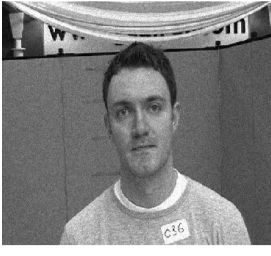
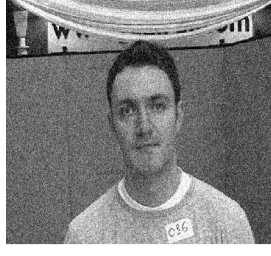


























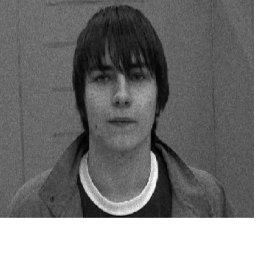


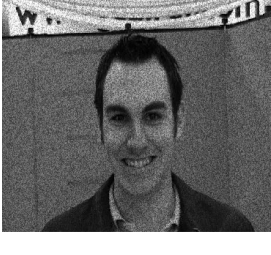
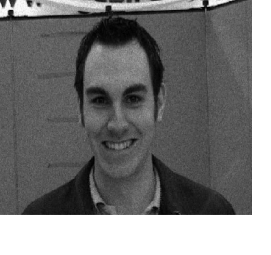


18				
19				
20				
21				
22				
23				
24				
25				
26				

27				
28				
29				
30				
31				
32				
33				
34				
35				

36				
37				
38				
39				
40				
41				
42				
43				
44				

45				
46				
47				
48				
49				
50				
51				
52				
53				

54				
55				
56				
57				
58				
59				
60				
61				
62				

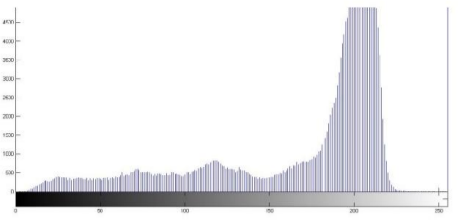

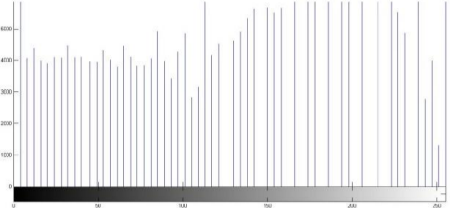

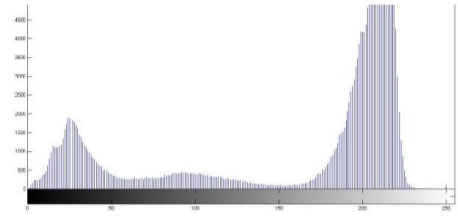

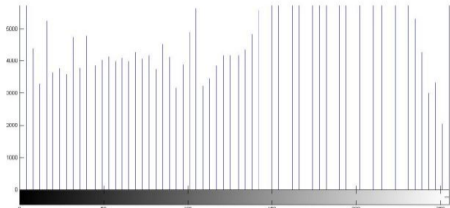
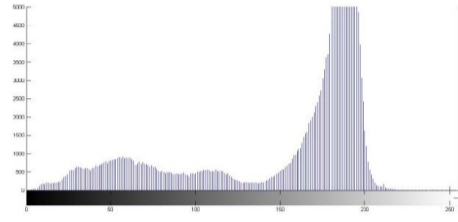

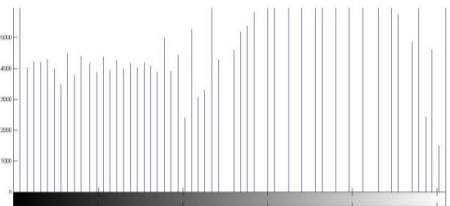

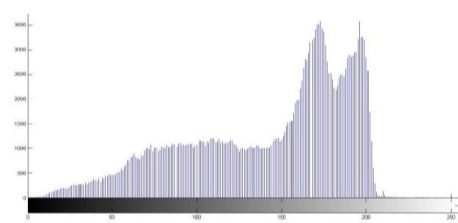
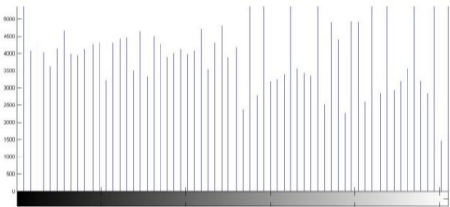

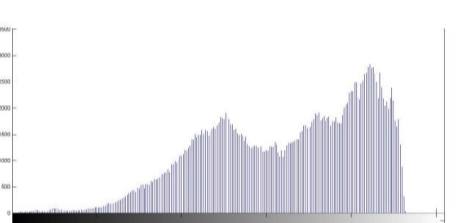

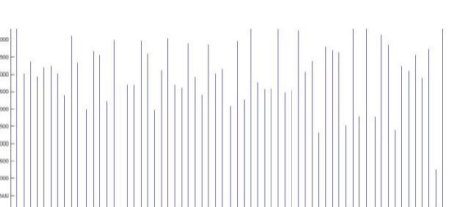

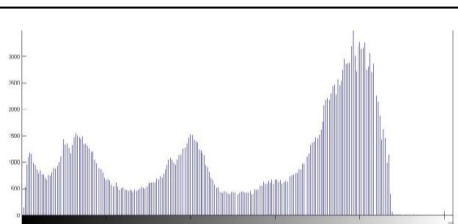

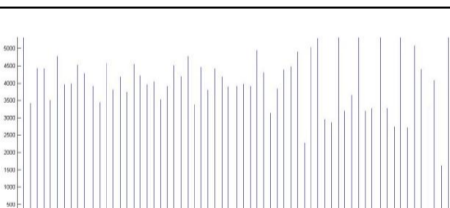

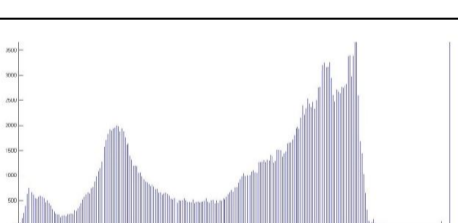

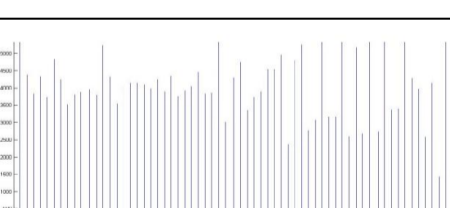

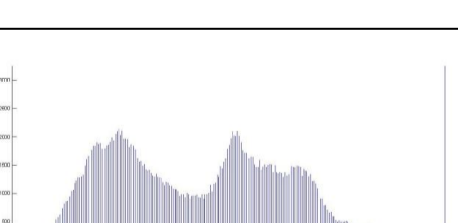

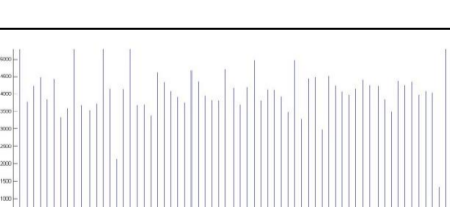

63				
64				
65				
66				
67				
68				
69				
70				
71				

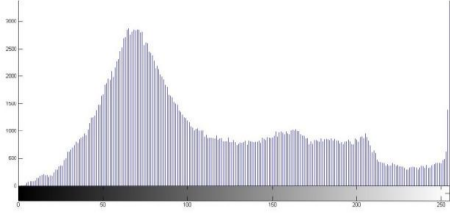
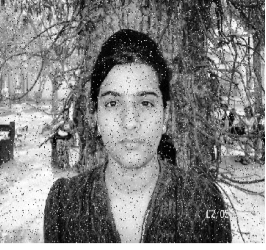
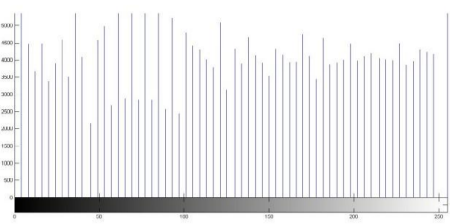

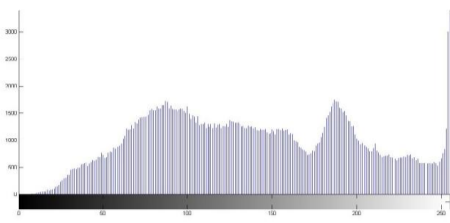

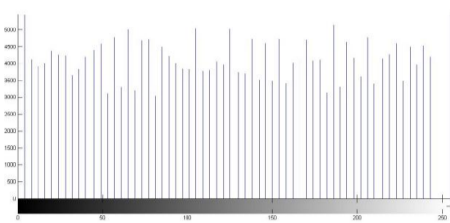

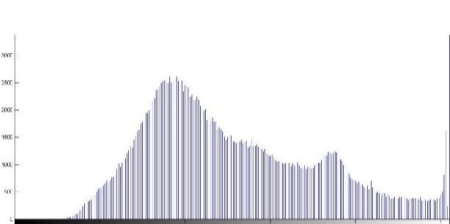

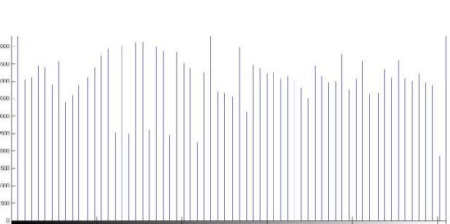

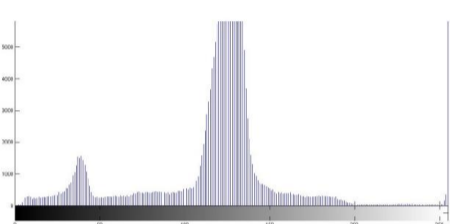

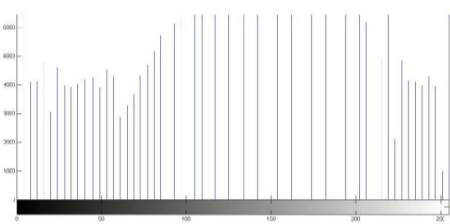

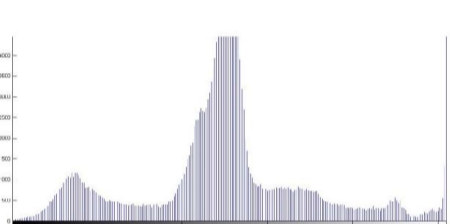
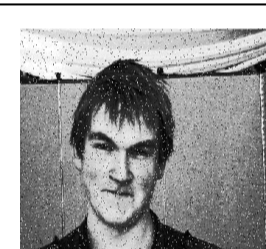
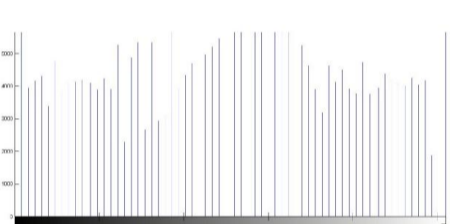
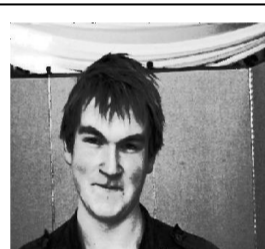
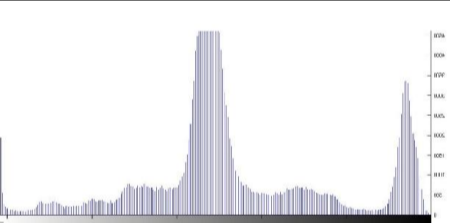

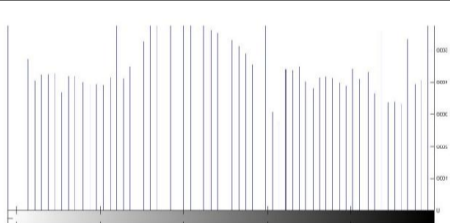

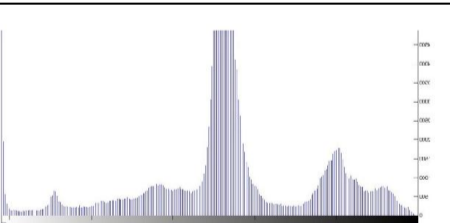

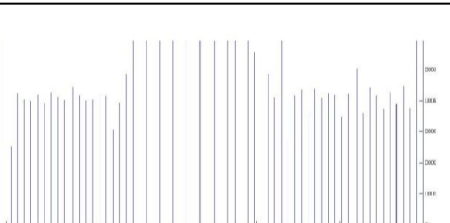
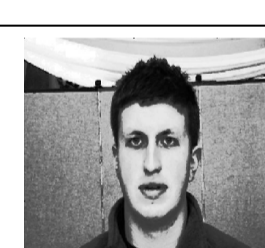
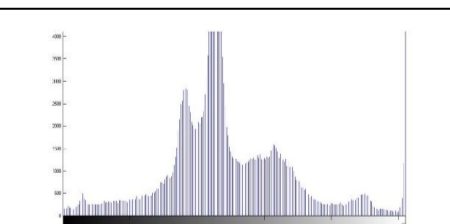
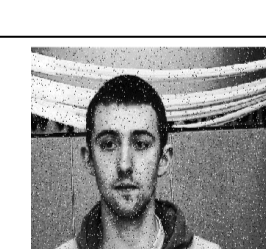
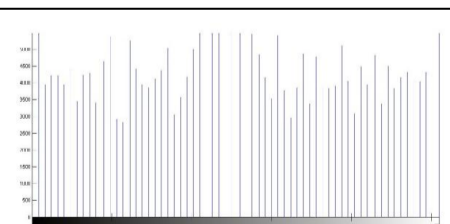
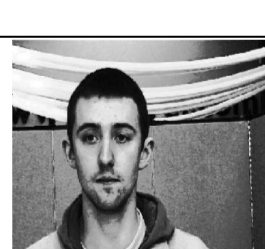
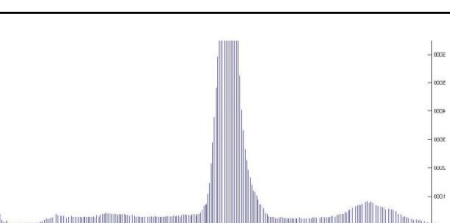
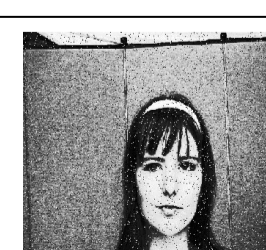
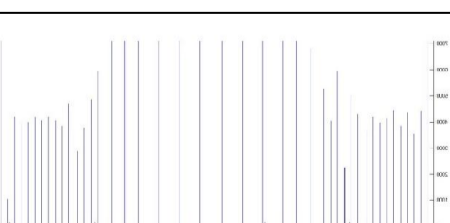

72				
73				
74				
75				
76				
77				
78				
79				
80				

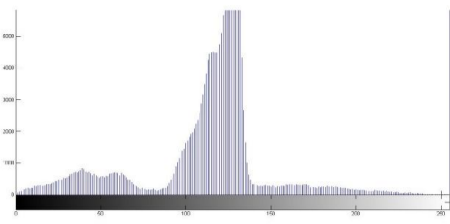

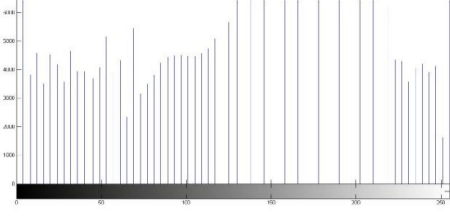

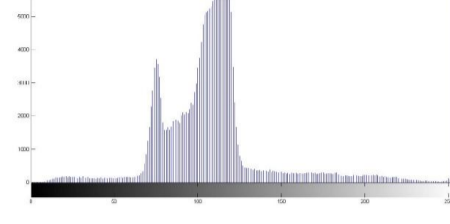

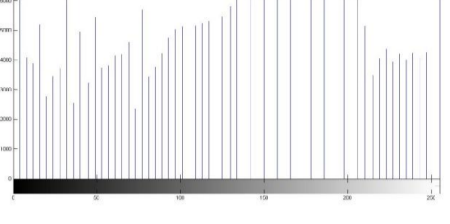

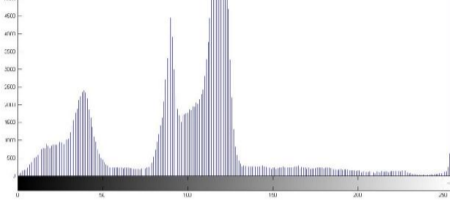

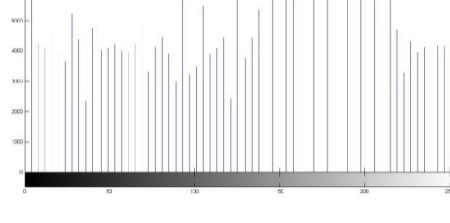

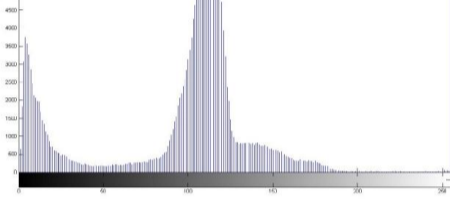

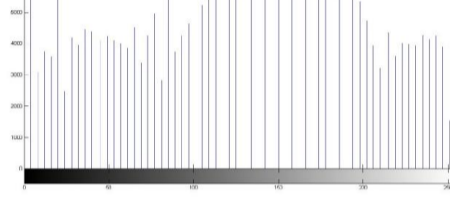

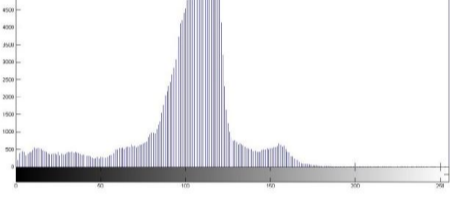
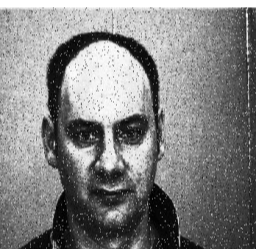
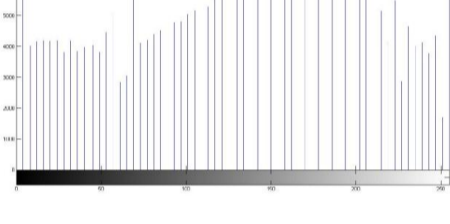

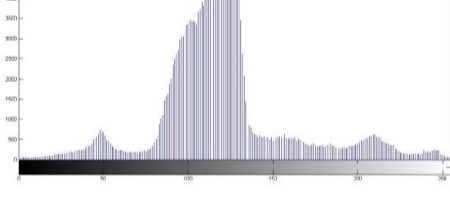

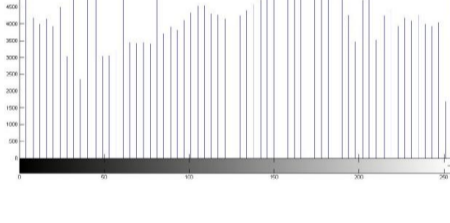

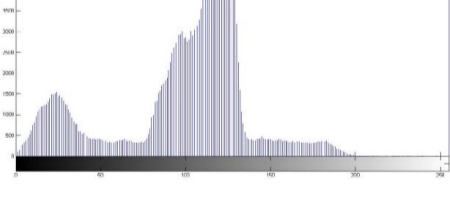

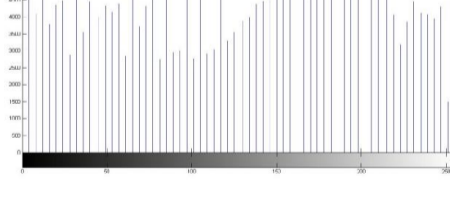

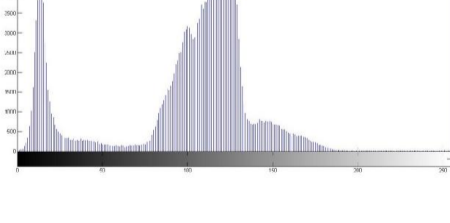
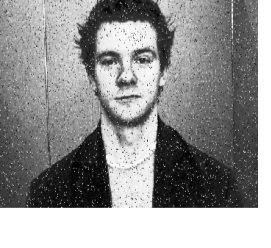
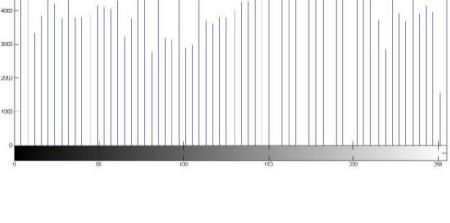
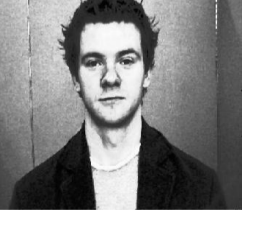
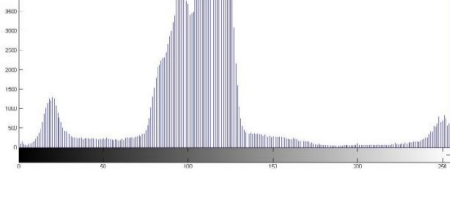

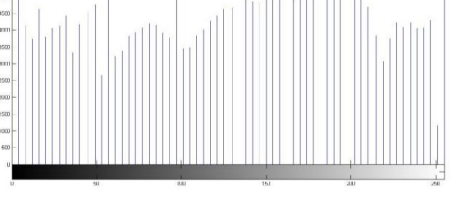

81				
82				
83				
84				
85				
86				
87				
88				
89				


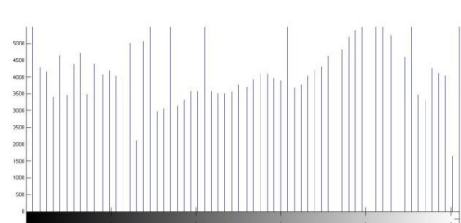

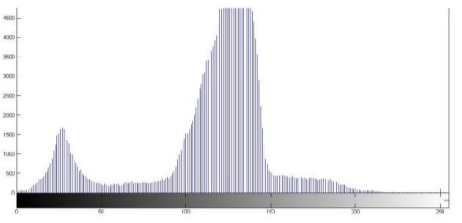

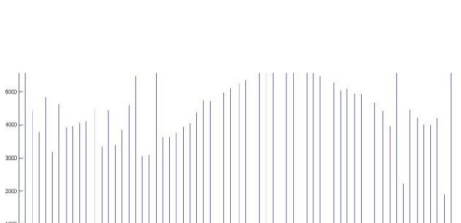

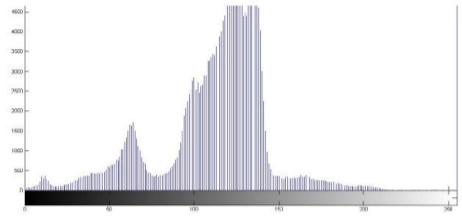

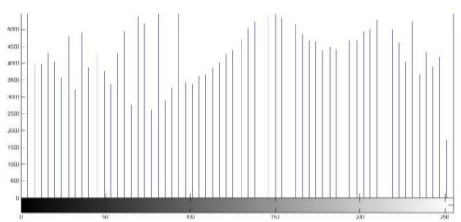

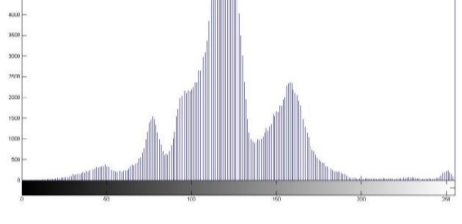
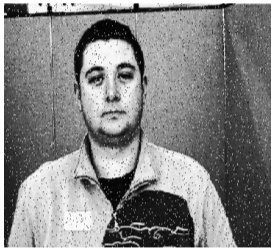
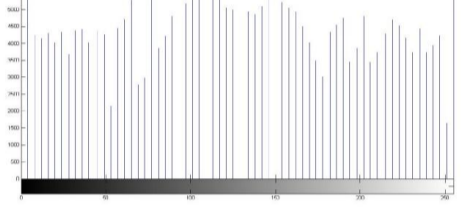

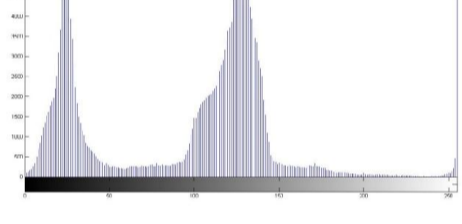

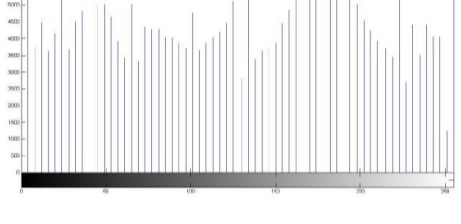

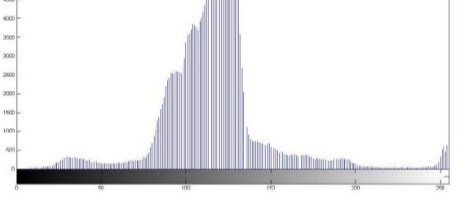

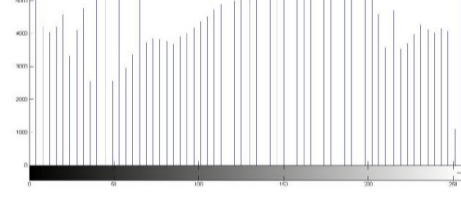

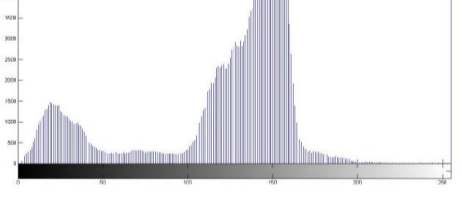

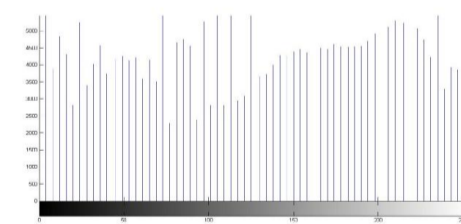

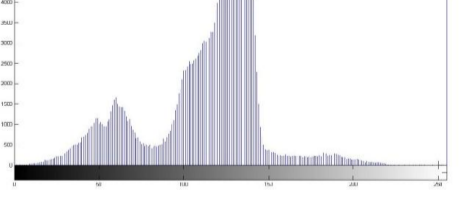

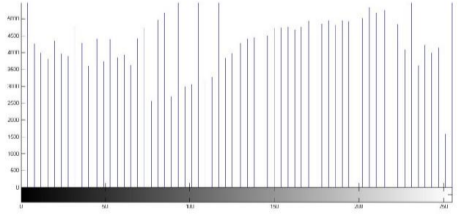

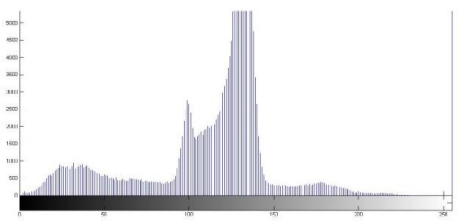

90				
91				
92				
93				
94				
95				
96				
97				
98				

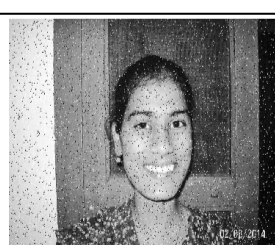
99				
100				


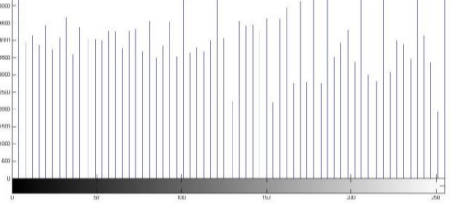

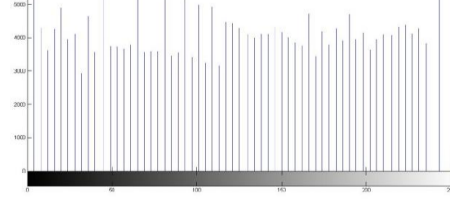
S.NO	HISTOGRAM BEFORE EQUALIZATION	PICTURE AFTER EQUALIZATION	HISTOGRAM AFTER EQUALIZATION	MEDIAN FILTERING
1				
2				
3				
4				
5				
6				
7				
8				


9				
10				
11				
12				
13				
14				
15				
16				
17				

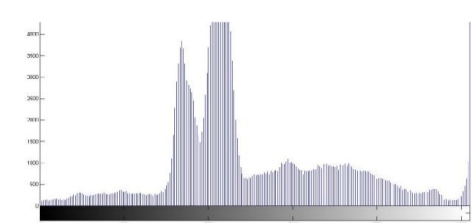
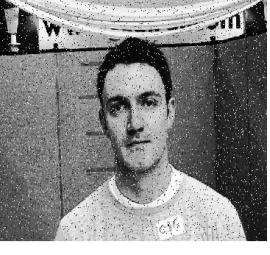
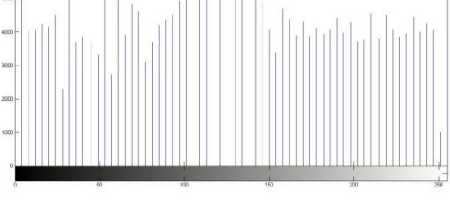

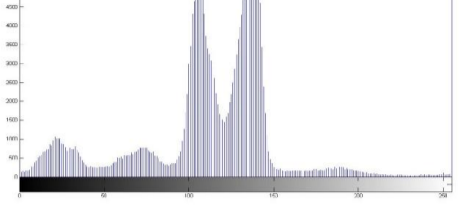

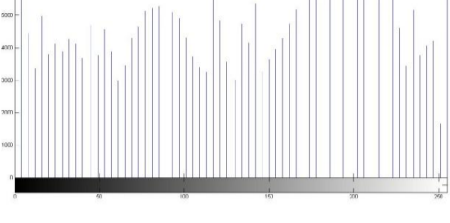

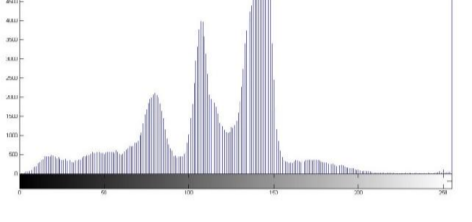

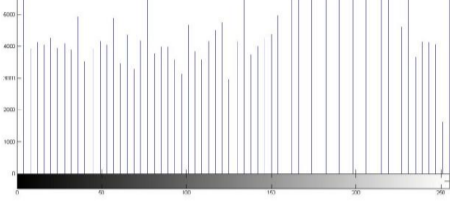

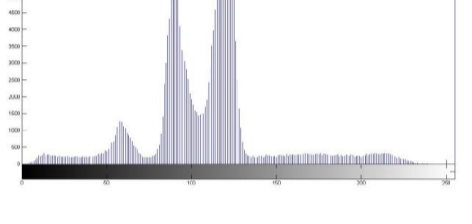

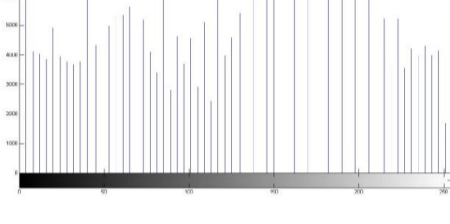

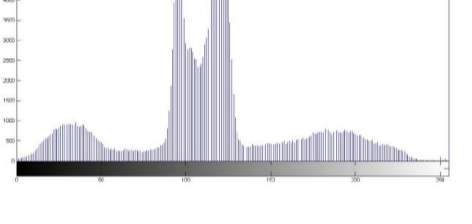

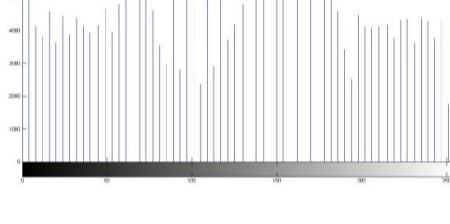

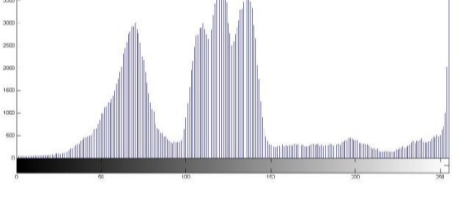

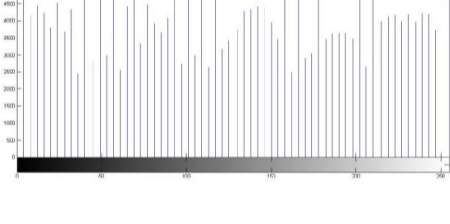
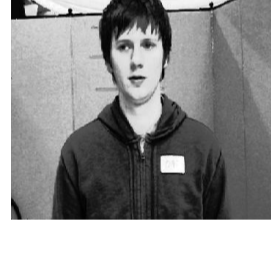
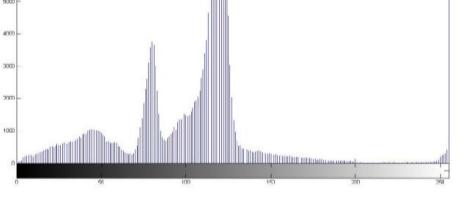

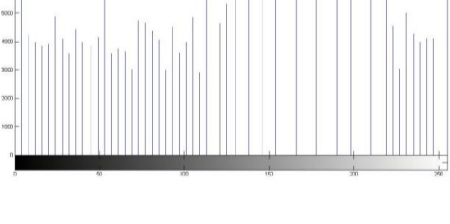

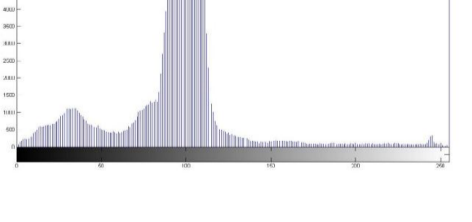

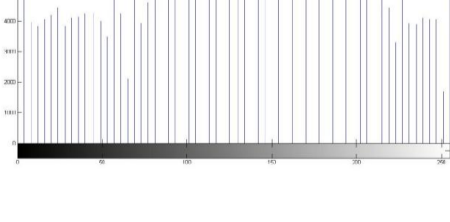

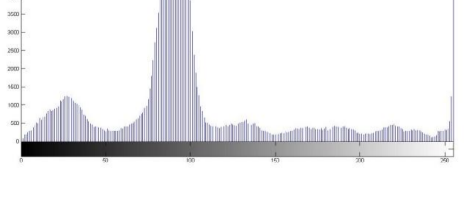

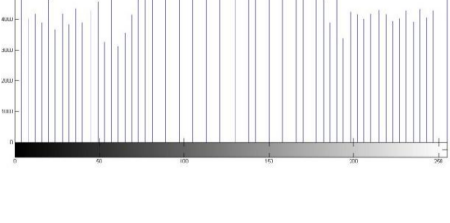
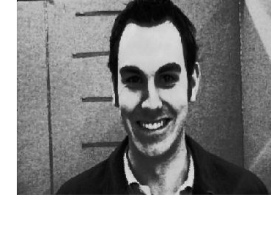
18				
19				
20				
21				
22				
23				
24				
25				
26				

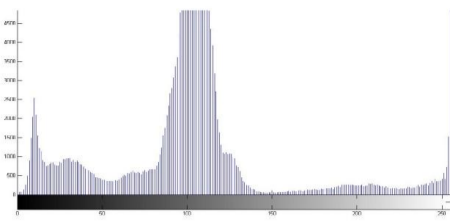

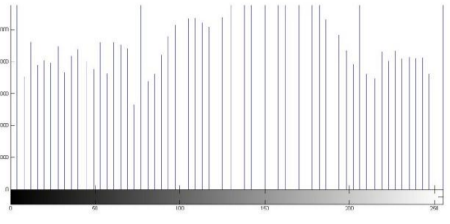

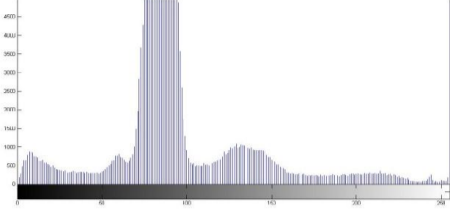

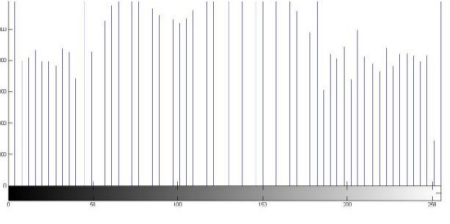

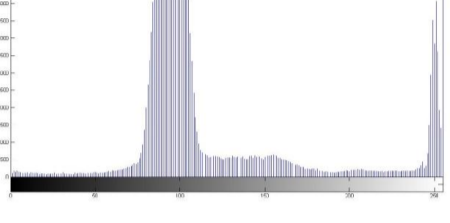
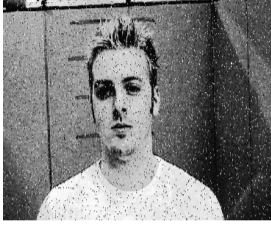
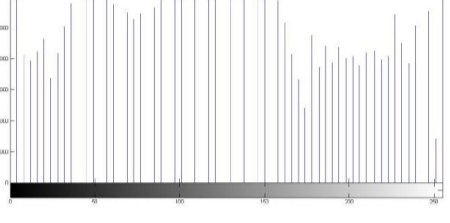

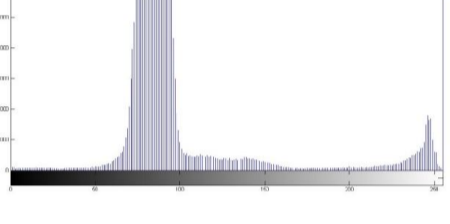
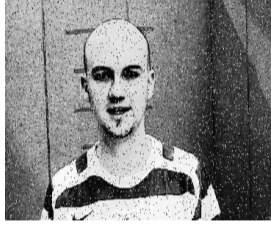
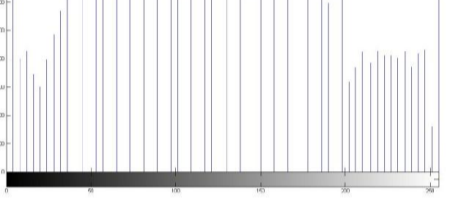

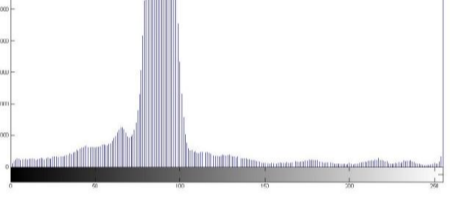

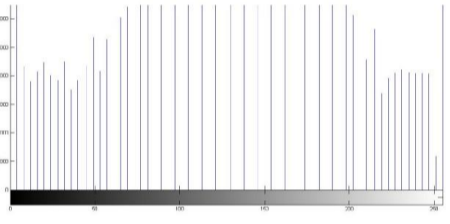

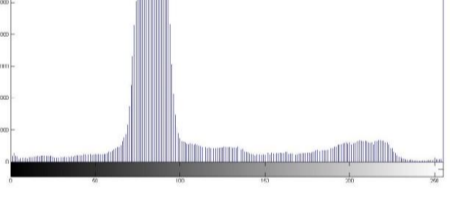

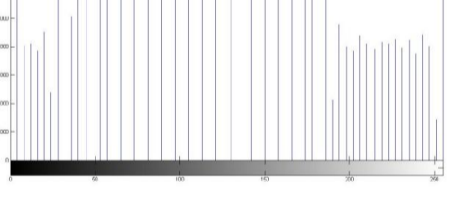

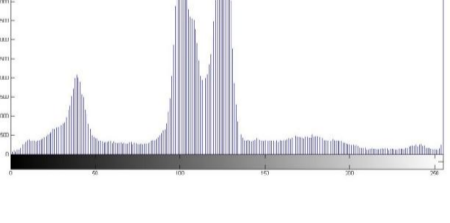
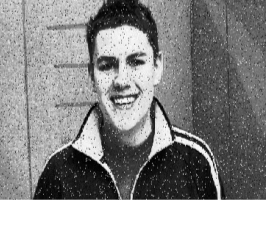
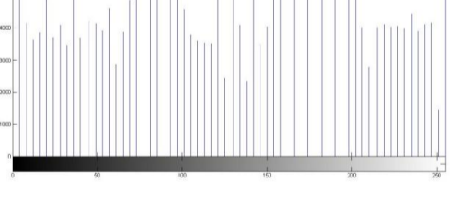

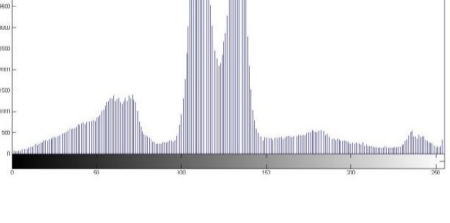
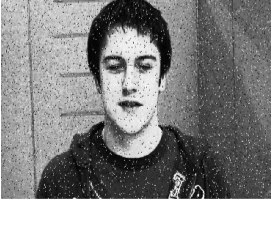
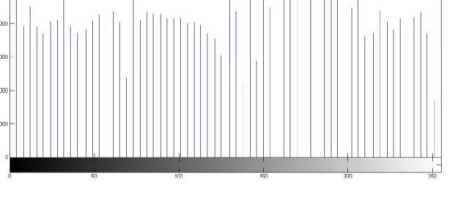
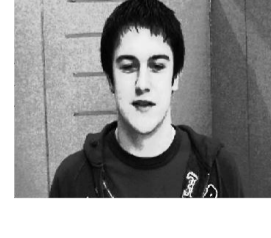
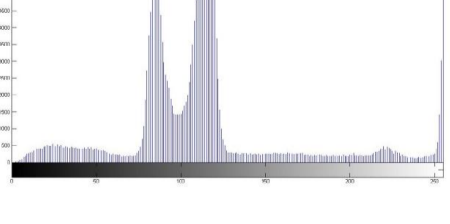

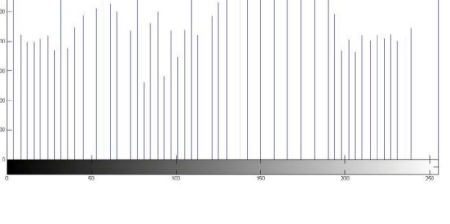

27				
28				
29				
30				
31				
32				
33				
34				
35				

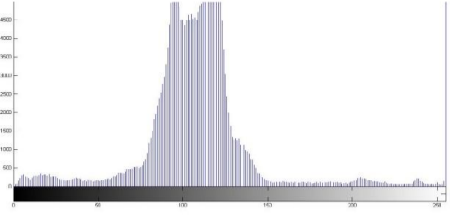
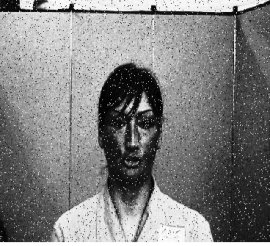
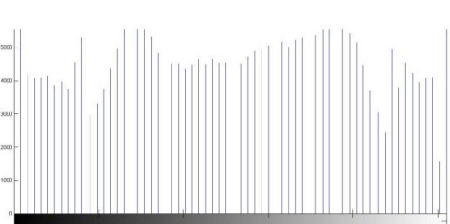

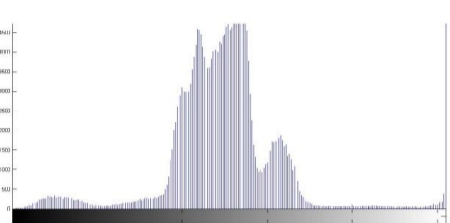
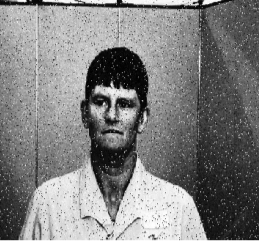
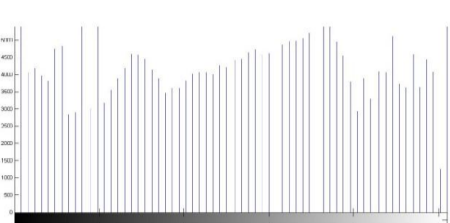

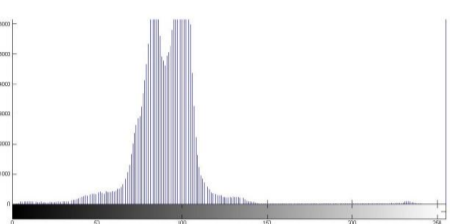

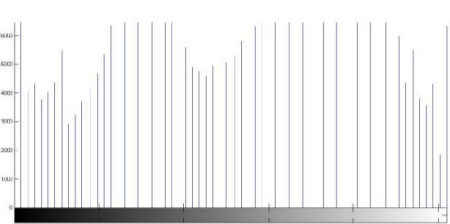

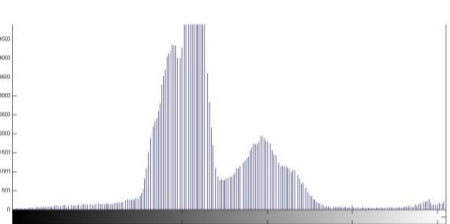

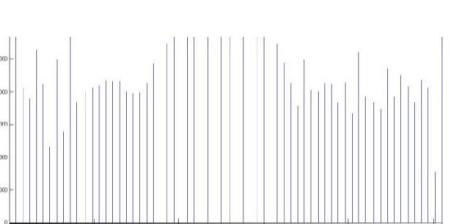

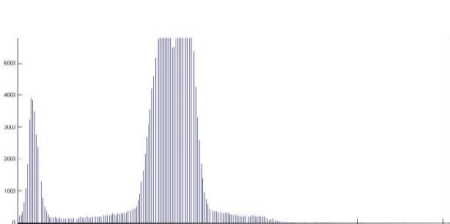

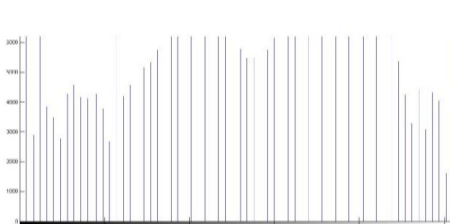

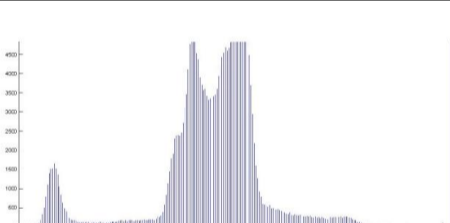

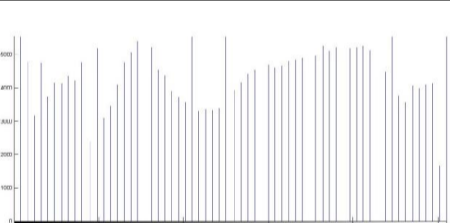

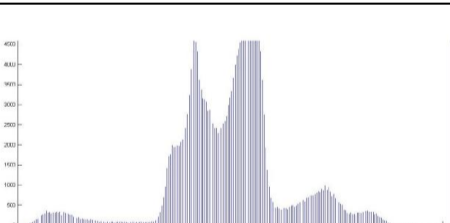
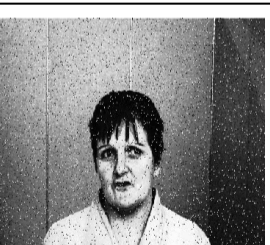


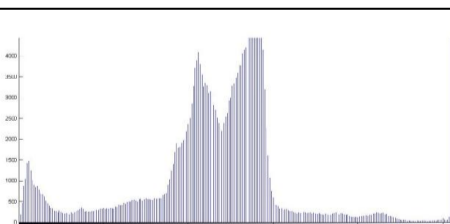

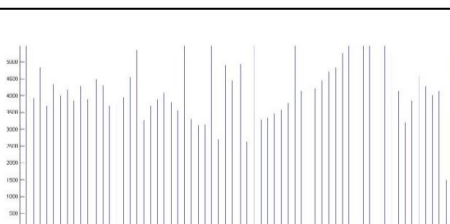

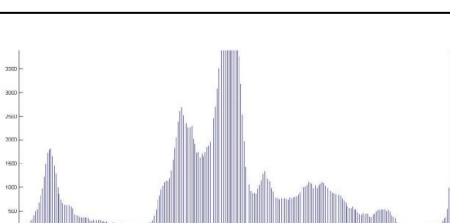
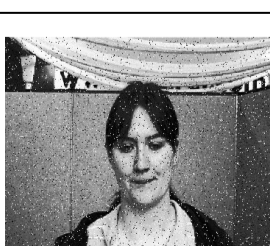
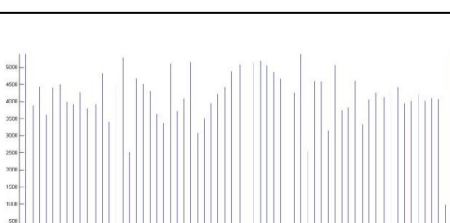

36				
37				
38				
39				
40				
41				
42				
43				
44				

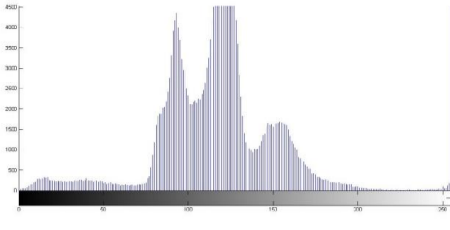
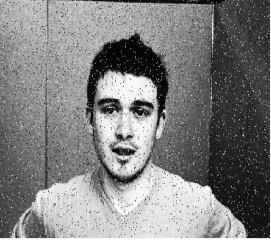
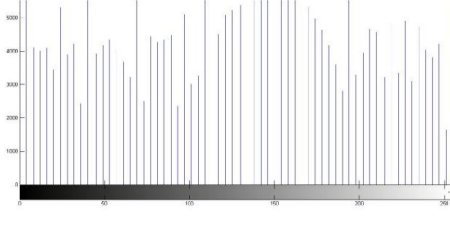

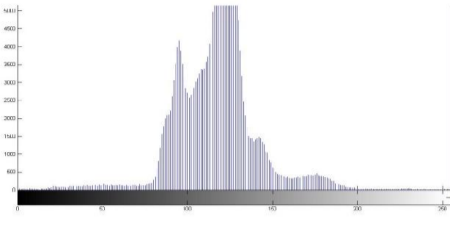


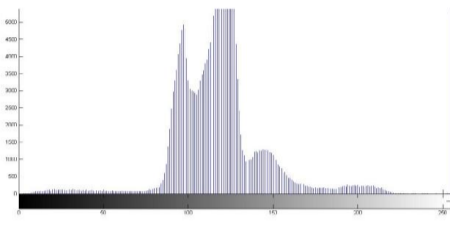

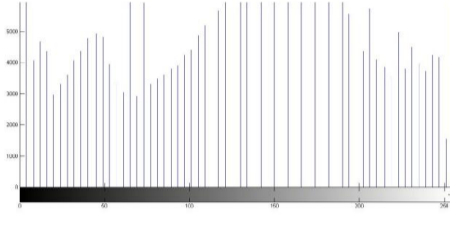

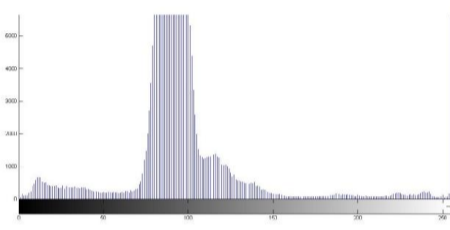

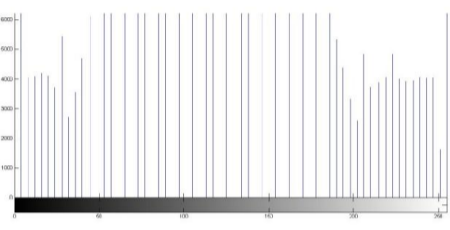

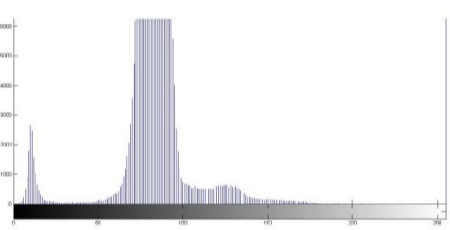

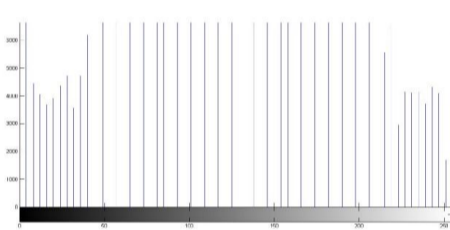

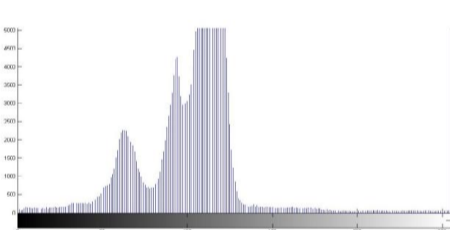
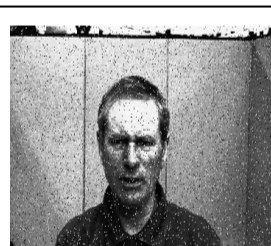
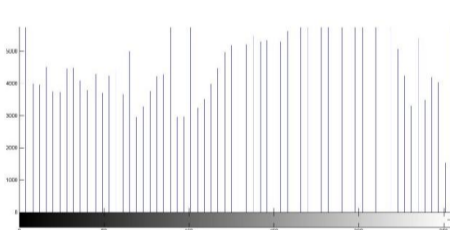

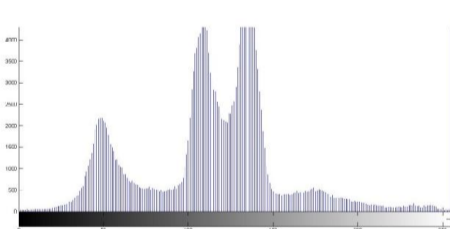

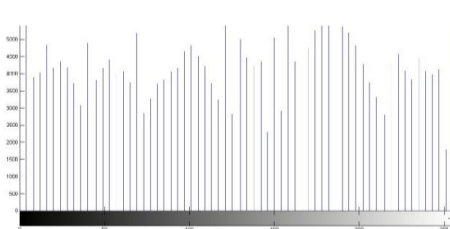

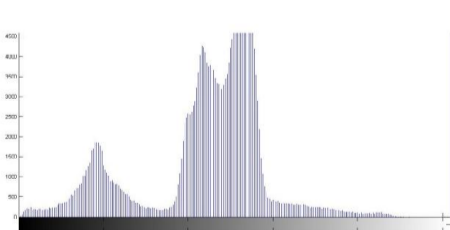

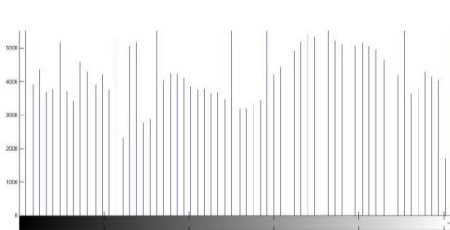
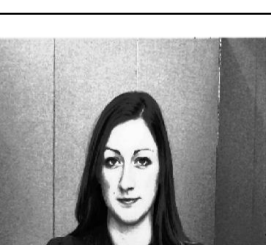
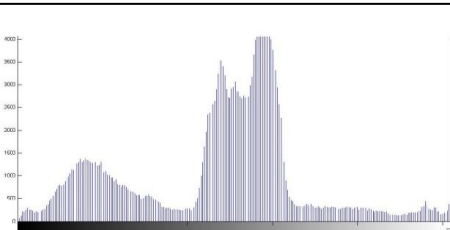

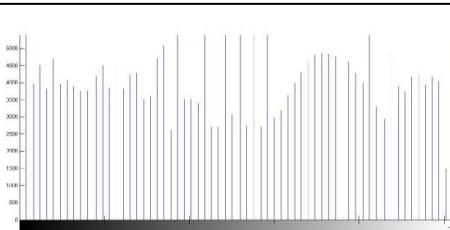
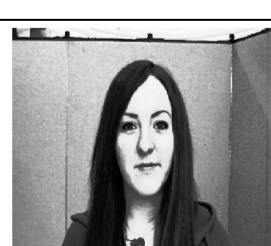
45				
46				
47				
48				
49				
50				
51				
52				
53				

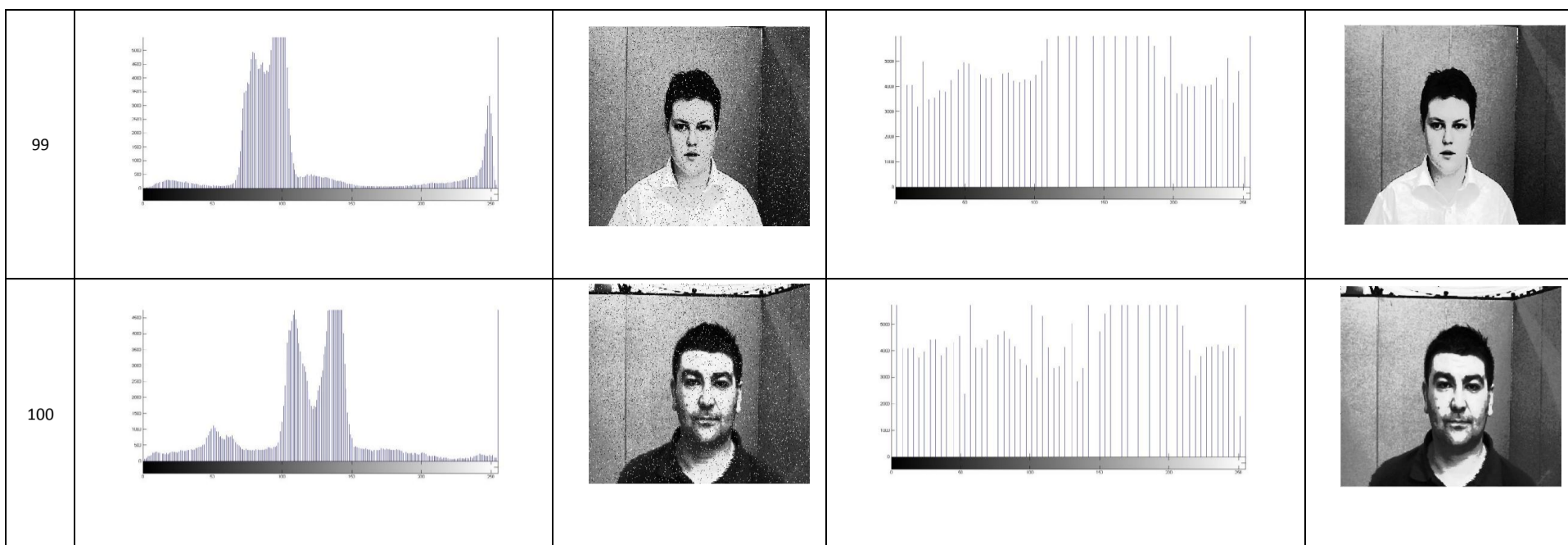
54				
55				
56				
57				
58				
59				
60				
61				
62				



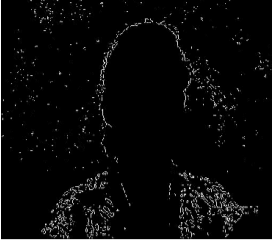
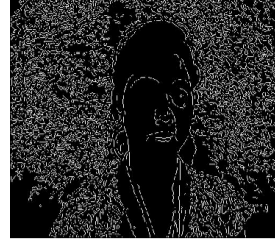






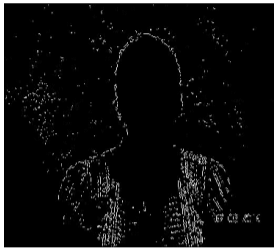
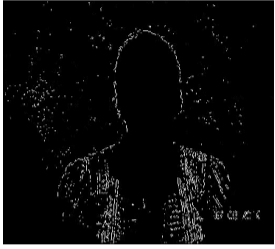


















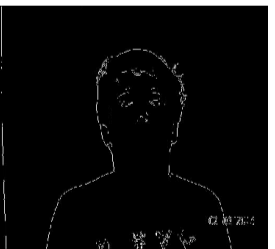


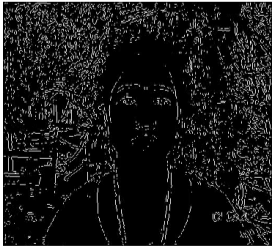




63				
64				
65				
66				
67				
68				
69				
70				
71				





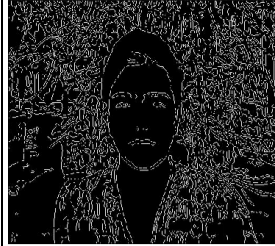
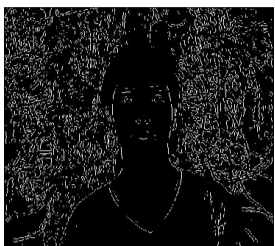



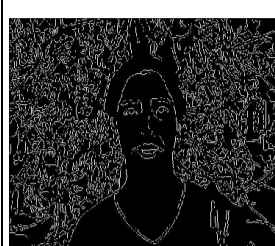




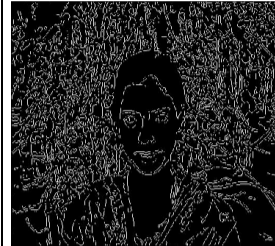


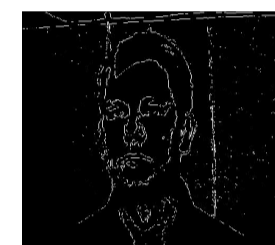



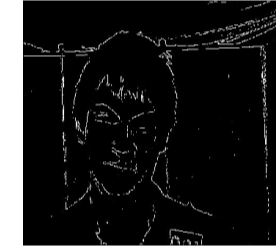




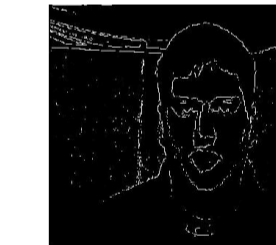



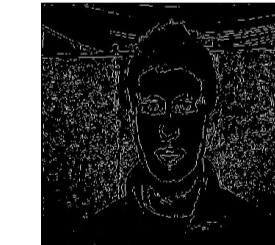
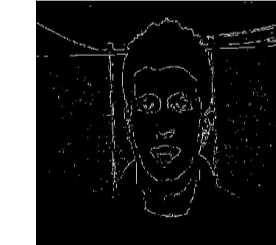
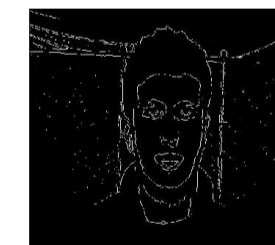

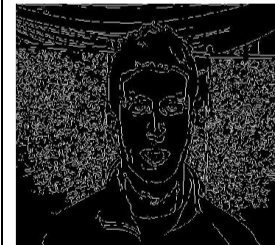







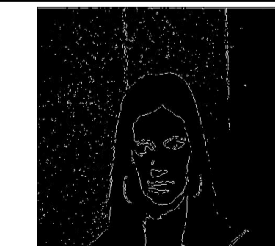

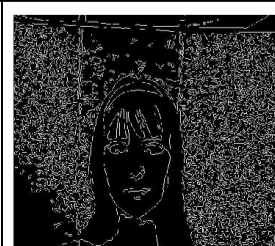
72				
73				
74				
75				
76				
77				
78				
79				
80				




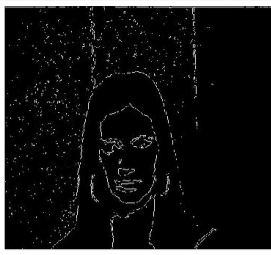


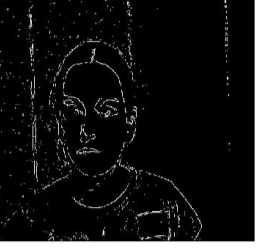


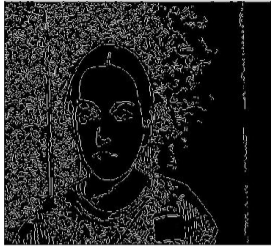





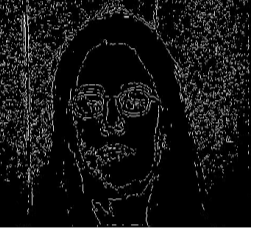





























81				
82				
83				
84				
85				
86				
87				
88				
89				






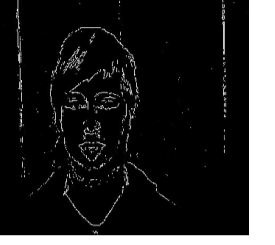
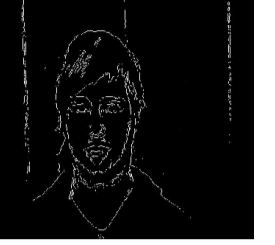
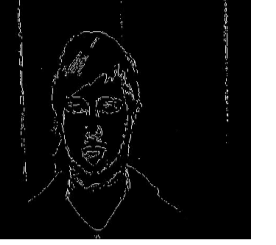













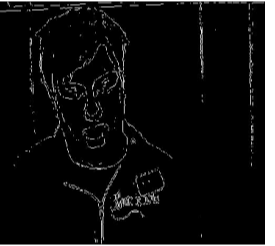








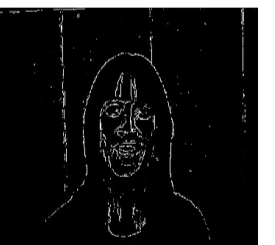



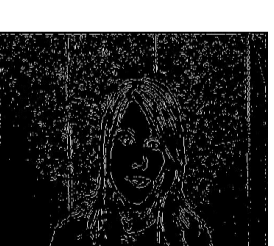



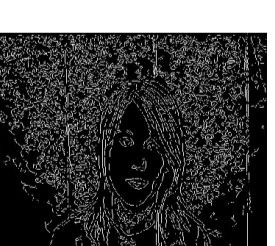
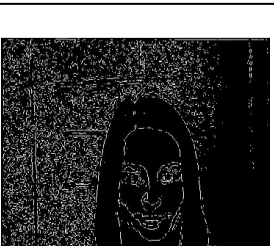
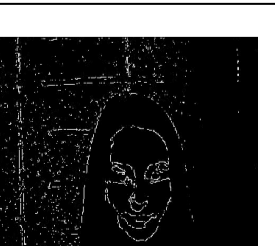
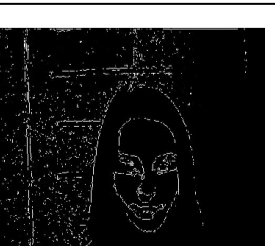

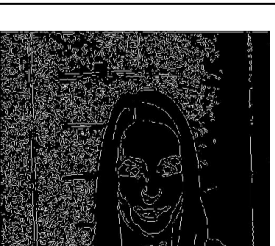
90				
91				
92				
93				
94				
95				
96				
97				
98				







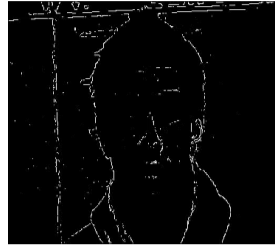
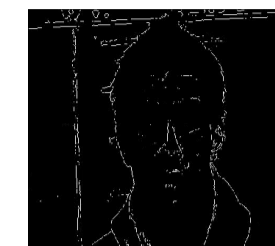
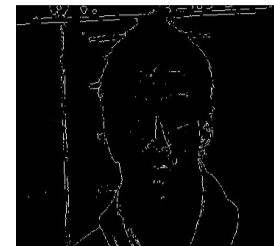




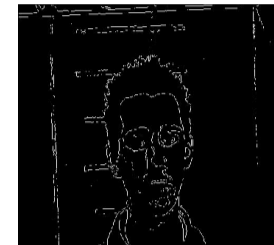






















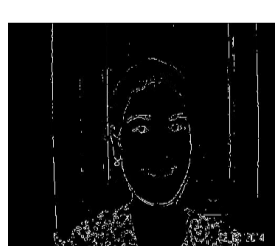

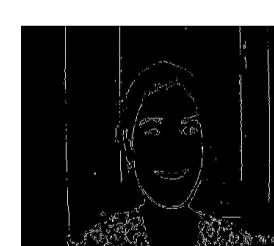
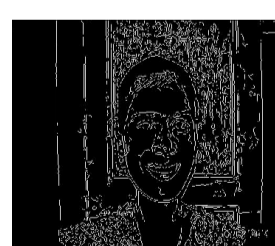




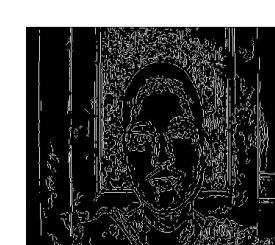





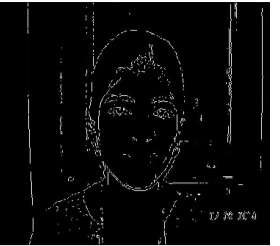








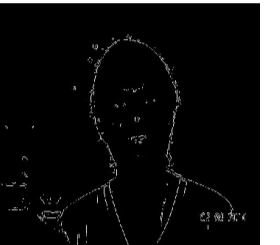
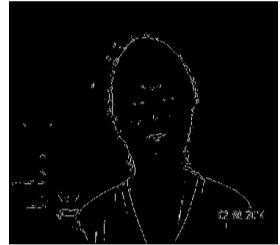







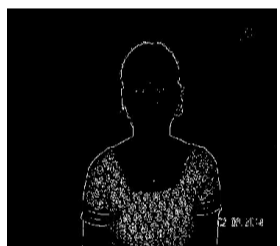
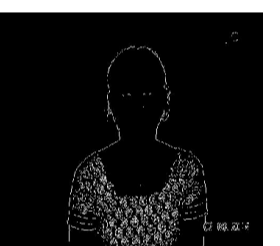
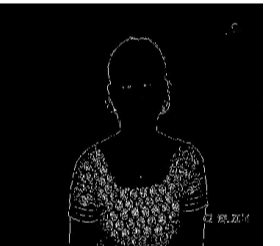



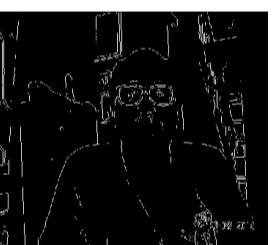

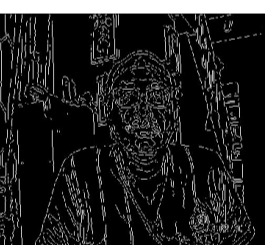















S.NO	LOG	ROBERTS	SOBEL	PREWITT	CANNY
1					
2					
3					
4					
5					
6					
7					
8					

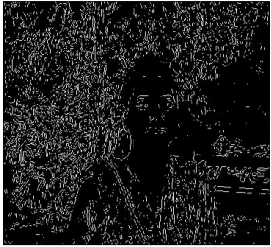








































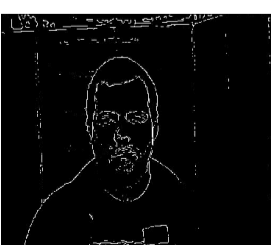
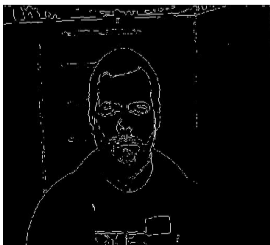


9					
10					
11					
12					
13					
14					
15					
16					
17					
































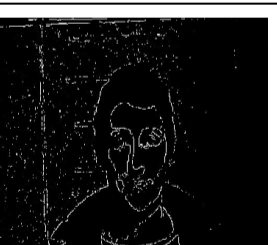
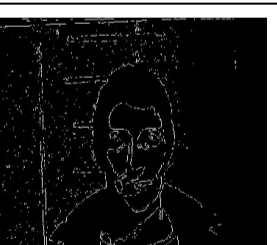



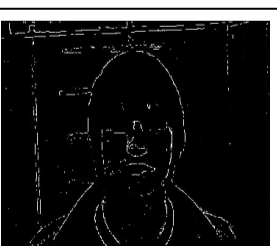
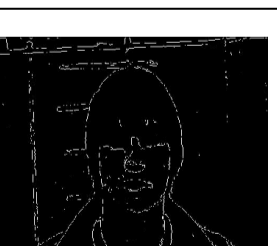
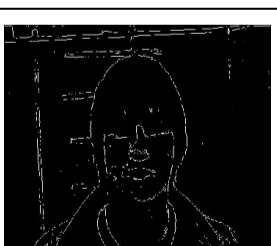
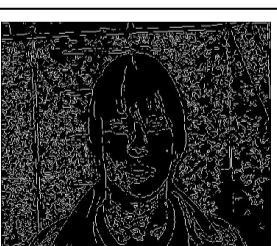
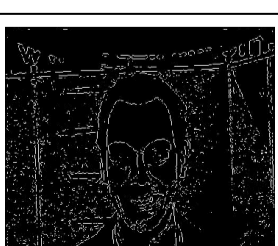

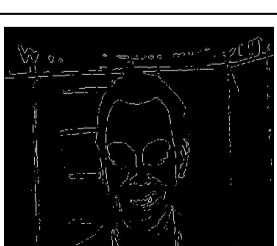
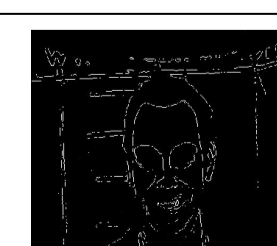
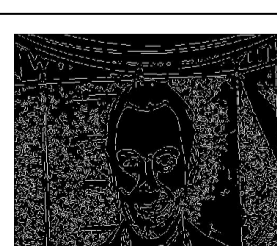
18					
19					
20					
21					
22					
23					
24					
25					
26					


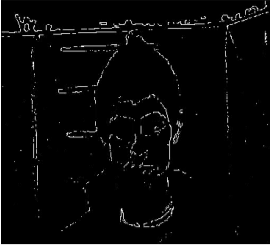









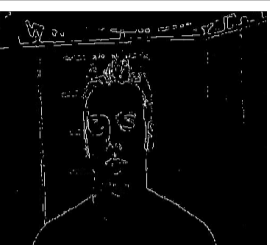
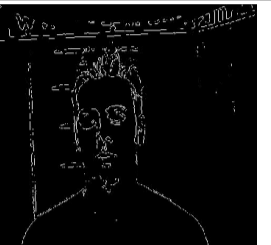
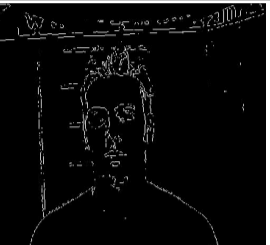



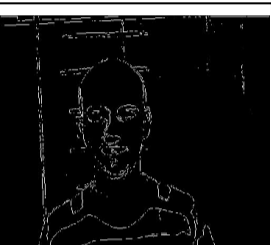



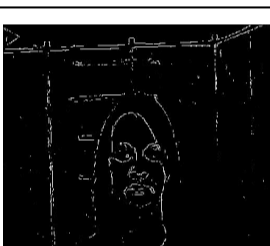

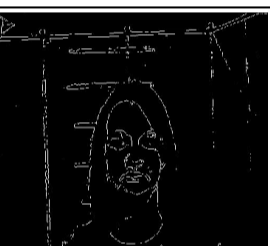
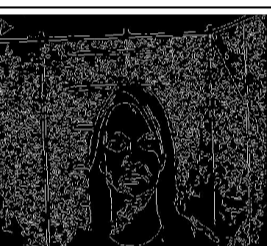









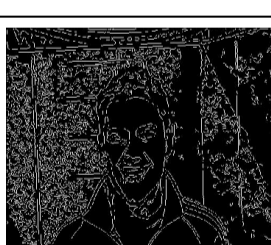


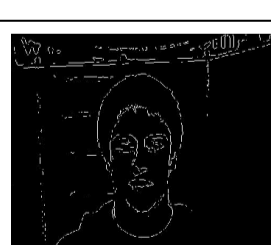
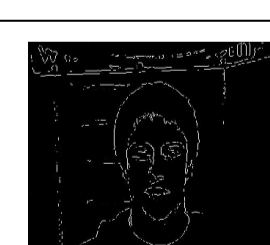





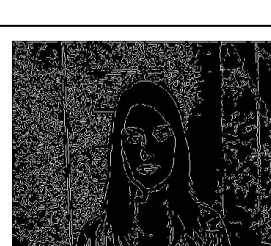
27					
28					
29					
30					
31					
32					
33					
34					
35					


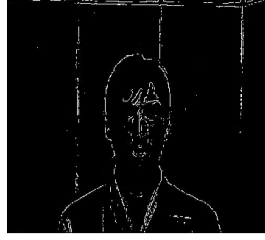

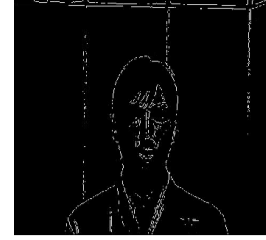
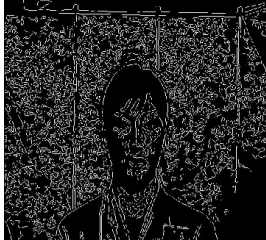

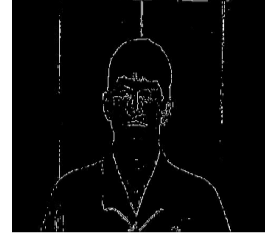
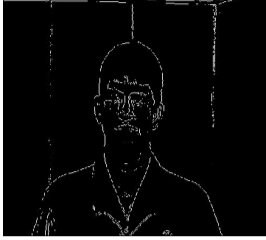
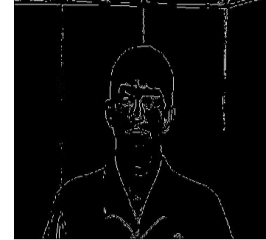
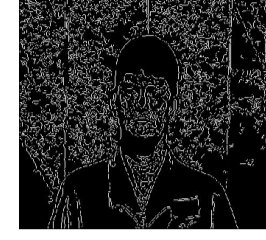




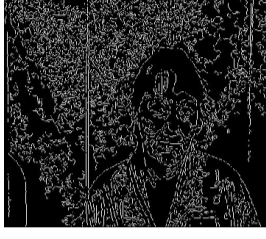









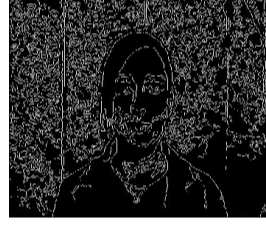





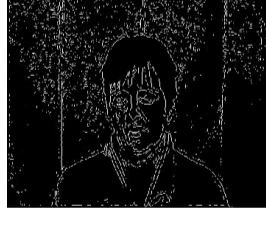








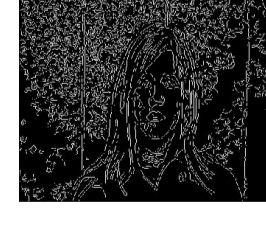





36					
37					
38					
39					
40					
41					
42					
43					
44					






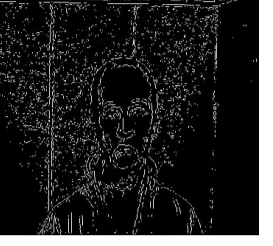


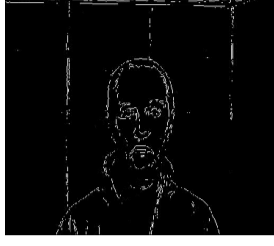




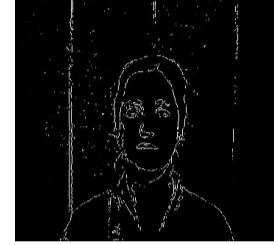

















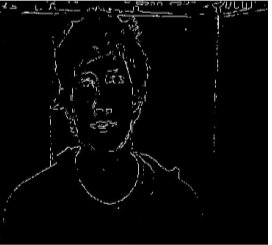













45					
46					
47					
48					
49					
50					
51					
52					
53					










54					
55					
56					
57					
58					
59					
60					
61					
62					

63					
64					
65					
66					
67					
68					
69					
70					
71					

72					
73					
74					
75					
76					
77					
78					
79					
80					

81					
82					
83					
84					
85					
86					
87					
88					
89					

90					
91					
92					
93					
94					
95					
96					
97					
98					

99					
100					

CONCLUSION

8. Conclusion

This project was aimed to Pre-Processing mechanism for Face detection system, which not only be efficient for face detection but also be useful in extending the face analysis for further research such as face expression analysis. For the same, 200 sample data from different ethnic background, different genders and different age groups was tested and analyzed leading to the following solutions

Noise Reduction: In this project, maximum distorted image (in consideration of lose of feature details) was created by adding Salt & Pepper noise to images. These noisy images were filtered using 5 x 5 median filter. It was seen that the distortion is removed and the loss of image details is less.

Reduction of Ambiguity due to poor Lighting Conditions: The ambiguity created by lighting conditions can be reduced by using the histogram equalization method; it equalizes the grey levels such that the important features aren't ignored due to poor exposure. It was seen that edge detected from an equalized image gave more clear edges.

Use of Canny Edge Detector: The Canny Edge detector was considered so that the detailed features of the face aren't left out during the process of the edge detection. Considering any other detector, only the maximum intensity value is taken into consideration. Whereas Canny takes into consideration, so both the background and features are retained in the process.

REFERENCES

Appendix 1: References

1. C. Rama and K. Z. Shaohua, "Face Tracking and Recognition from Video," In *Handbook of Face Recognition*, Springer, 2011, Pp. 323-348.
2. T. Mathew and P. Alex, "Eigen faces For Recognition," *Journal of Cognitive Neuroscience*, Pp. 71-86, 1991.
3. Zhao, W., Krishnaswamy, A., Chellappa, R., Swets, D. L., & Weng, J. (1998). Discriminant Analysis of Principal Components for Face Recognition. In *Face Recognition* (Pp. 73-85). Springer Berlin Heidelberg.
4. L. Kwan-Ho, L. Kin-Man And S. Wan-Chi, "Spatially Eigen-Weighted Hausdroff Distances For Human Recognition," *The Journal Of Pattern Recognition Society*, Vol. 36, Pp. 1827-1834, 2002.
5. J. K. Klaus, J. Oliver And W. F. Robert, "Genetic Model Optimization For Hausdroff Distance-Based Face Localization," *International ECCV 2002 Workshop On Biometric Authentication, Springer, Lecture Notes In Computer Science*, Vol. 2359, Pp. 103-111, 2002.
6. H. Yunakui and W. Zengfu, "A Similarity Measure Based N Hausdroff Distance for Human Recognition," *IEEE*, 2006.
7. W. Kwok-Wai, L. Kin-Man and S. Wan-Chi, "An Efficient Algorithm for Human Face Detection and Face Feature Extraction under Different

- Condition," *The Journal of the Pattern Recognition Society*, Vol. 34, Pp. 1993-2004, 2001.
8. Ge, S. S., Yang, Y., & Lee, T. H. (2008). Hand Gesture Recognition and Tracking Based On Distributed Locally Linear Embedding. *Image and Vision Computing*, 26(12), 1607-1620.
 9. Huttenlocher, D. P., Klanderman, G. A., & Rucklidge, W. J. (1993). Comparing Images Using the Hausdroff Distance. *Pattern Analysis and Machine Intelligence, IEEE Transactions On*, 15(9), 850-863.
 10. Srisuk, S., & Kuratach, W. (2001). New Robust Hausdroff Distance-Based Face Detection. In *Image Processing, 2001. Proceedings. 2001 International Conference on (Vol. 1, Pp. 1022-1025)*. IEEE.
 11. Nigam, A., & Gupta, P. (2009, September). A New Distance Measure for Face Recognition System. In *Image and Graphics, 2009. Icg'09. Fifth International Conference on (Pp. 696-701)*. IEEE.
 12. Alajel, K. M., Xiang, W., & Leis, J. (2011, January). Face Detection Based On Skin Color Modeling And Modified Hausdroff Distance. In *Consumer Communications and Networking Conference (CCNC), 2011 IEEE (Pp. 399-404)*. IEEE.
 13. Tan, H., Zhang, Y. J., Wang, W., Feng, G., Xiong, H., Zhang, J., & Li, Y. (2011). Edge Eigen faces Weighted Hausdroff Distance for Face

- Recognition. *International Journal Of Computational Intelligence Systems*, 4(6), 1422-1429.
14. Butko, N. J., Theocharous, G., Philipose, M., & Movellan, J. R. (2011, March). Automated Facial Affect Analysis For One-On-One Tutoring Applications. In *Automatic Face & Gesture Recognition And Workshops (FG 2011)*, 2011 IEEE International Conference On (Pp. 382-387). IEEE.
 15. Silapachote, P., Karuppiah, D. R., & Hanson, A. R. (2005). Feature Selection Using Adaboost for Face Expression Recognition. Massachusetts University Amherst Department of Computer Science.
 16. Phillips, P. J. (1996). FERET (Face Recognition Technology) Recognition Algorithm Development and Test Results. Adelphi, Md: Army Research Laboratory.
 17. Ryan, A., Cohn, J. F., Lucey, S., Saragih, J., Lucey, P., De La Torre, F., & Rossi, A. (2009, October). Automated Facial Expression Recognition System. In *Security Technology, 2009. 43rd Annual 2009 International Carnahan Conference on* (Pp. 172-177). IEEE.
 18. Grafsgaard, J. F., Wiggins, J. B., Boyer, K. E., Wiebe, E. N., & Lester, J. C. (2013). Automatically Recognizing Facial Expression: Predicting Engagement and Frustration. In *Proceedings of the 6th International Conference on Educational Data Mining*.

19. Deriso, D. M., Susskind, J., Tanaka, J., Winkielman, P., Herrington, J., Schultz, R., & Bartlett, M. (2012, January). Exploring the Facial Expression Perception-Production Link Using Real-Time Automated Facial Expression Recognition. In *Computer Vision–ECCV 2012. Workshops and Demonstrations* (Pp. 270-279). Springer Berlin Heidelberg.
20. Littlewort, G., Bartlett, M. S., Fasel, I., Susskind, J., & Movellan, J. (2006). Dynamics Of Facial Expression Extracted Automatically From Video. *Image And Vision Computing*, 24(6), 615-625.
21. Lucey, P., Cohn, J. F., Kanade, T., Saragih, J., Ambadar, Z., & Matthews, I. (2010, June). The Extended Cohn-Kanade Dataset (Ck+): A Complete Dataset for Action Unit and Emotion-Specified Expression. In *Computer Vision and Pattern Recognition Workshops (CVPRW), 2010 IEEE Computer Society Conference on* (Pp. 94-101). IEEE.
22. Jesorsky, O., Kirchberg, K. J., & Frischholz, R. W. (2001, January). Robust Face Detection Using the Hausdroff Distance. In *Audio-And Video-Based Biometric Person Authentication* (Pp. 90-95). Springer Berlin Heidelberg.
23. Yuen, C. T., Rizon, M., San, W. S., & Sugisaka, M. (2008). Automatic Detection of Face and Facial Features. *ISPRA*, 8, 230-234.
24. Boskovitz, V., & Guterman, H. (2002). An Adaptive Neuro-Fuzzy System for Automatic Image Segmentation and Edge Detection. *Fuzzy Systems, IEEE Transactions On*, 10(2), 247-262.

25. Rani, A. A., Rajagopal, G., & Jagadeeswaran, A. Bi-Histogram Equalization with Brightness Preservation Using Contrast Enhancement.
26. Ko, S. J., & Lee, Y. H. (1991). Center Weighted Median Filters And Their Applications To Image Enhancement. *Circuits and Systems, IEEE Transactions On*, 38(9), 984-993.
27. Roushdy, M. (2006). Comparative Study of Edge Detection Algorithms Applying On the Grayscale Noisy Image Using Morphological Filter. *GVIP Journal*, 6(4), 17-23.
28. Tan, X., & Triggs, B. (2007). Preprocessing And Feature Sets For Robust Face Recognition. In *IEEE Conference on Computer Vision and Pattern Recognition, CVPR (Vol. 7, Pp. 1-8)*.
29. Al-Amri, S. S., Kalyankar, N. V., & Khamitkar, S. D. (2010). A Comparative Study of Removal Noise from Remote Sensing Image. *International Journal of Computer Science Issues (IJCSI)*, 7(1).
30. Pezeshki, M., Gholami, S., & Nickabadi, A. (2013). Distinction Between Features Extracted Using Deep Belief Networks. *Arxiv Preprint Arxiv: 1312.6157*.
31. Vasudha, S., Patil, N. K. , & Lokesh , R. , Face Recognition System: Performance Improvement Using A Novel Method For Illumination Normalization. *International Journal Of Computers And Distributed*

Systems, Vol. No.4, Issue I, Oct-Nov 2013.

32. Kandeel, A. A., Abbas, A. M., Hadhoud, M. M., & El-Saghir, Z. A Study of A modified Histogram Based Fast Enhancement Algorithm (MHBFE). *Signal & Image Processing : An International Journal (SIPIJ)* Vol.5, No.1, February 2014
33. Sartin, M. A., & Da Silva, A. C. Evaluation of Image Segmentation and Filtering With Ann in the Papaya Leaf. *International Journal Of Computer Science & Information Technology (IJCSIT)* Vol. 6, No 1, February 2014
34. Sahnoun, K., & Benabadji, N. Satellite Image Compression Algorithm Based On the FFT. *The International Journal Of Multimedia & Its Applications (IJMA)* Vol.6, No.1, February 2014
35. Pisano, E. D., Zong, S., Hemminger, B. M., Deluca, M., Johnston, R. E., Muller, K., & Pizer, S. M. (1998). Contrast Limited Adaptive Histogram Equalization Image Processing To Improve the Detection of Simulated Speculations in Dense Mammograms. *Journal Of Digital Imaging*, 11(4), 193-200.
36. Sharifi, M., Fathy, M., & Tayefeh Mahmoudi, M. (2002, April). A Classified And Comparative Study Of Edge Detection Algorithms. In *Information Technology: Coding and Computing, 2002. Proceedings.*

International Conference on (Pp. 117-120). IEEE.

37. Peli, T., & Malah, D. (1982). A Study of Edge Detection Algorithms. *Computer Graphics and Image Processing*, 20(1), 1-21.
38. Agrawal, P., Shriwastava, S. K., & Limaye, S. S. (2010, July). MATLAB Implementation of Image Segmentation Algorithms. In *Computer Science and Information Technology (ICCSIT)*, 2010 3rd IEEE International Conference on (Vol. 3, Pp. 427-431). IEEE.
39. Li, Y., Sun, J., & Luo, H. (2014). A Neuro-Fuzzy Network Based Impulse Noise Filtering For Gray Scale Images. *Neuro-computing*, 127, 190-199.
40. Kundur, D., & Hatzinakos, D. (1998). A Novel Blind Deconvolution Scheme for Image Restoration Using Recursive Filtering. *Signal Processing, IEEE Transactions On*, 46(2), 375-390.
41. Peng, B., Zhang, L., & Zhang, D. (2013). A Survey of Graph Theoretical Approaches to Image Segmentation. *Pattern Recognition*, 46(3), 1020-1038.
42. Hedberg, H. (2010). A Survey of Various Image Segmentation Techniques. Dept. Of Electrosience, Box, 118.
43. Lu, J., Plataniotis, K. N., & Venetsanopoulos, A. N. (2003). Face Recognition Using LDA-Based Algorithms. *Neural Networks, IEEE*

Transactions On, 14(1), 195-200.

44. Beymer, D. J. (1994, June). Face Recognition under Varying Pose. In Computer Vision and Pattern Recognition, 1994. Proceedings CVPR'94. 1994 IEEE Computer Society Conference on (Pp. 756-761). IEEE.
45. Dutt, A., & Rokhlin, V. (1993). Fast Fourier Transforms for Non-equispaced Data. *Siam Journal on Scientific Computing*, 14(6), 1368-1393.
46. Heisele, B., Ho, P., & Poggio, T. (2001). Face Recognition with Support Vector Machines: Global Versus Component-Based Approach. In Computer Vision, 2001. ICCV 2001. Proceedings. Eighth IEEE International Conference on (Vol. 2, Pp. 688-694). IEEE.
47. Pizer, S. M., Amburn, E. P., Austin, J. D., Cromartie, R., Geselowitz, A., Greer, T., & Zuiderveld, K. (1987). Adaptive Histogram Equalization and Its Variations. *Computer Vision, Graphics, and Image Processing*, 39(3), 355-368.
48. Stark, J. A. (2000). Adaptive Image Contrast Enhancement Using Generalizations of Histogram Equalization. *Image Processing, IEEE Transactions On*, 9(5), 889-896.
49. Valenciano, A., & Biondi, B. (2003, January). 2-D Deconvolution Imaging Condition for Shot-Profile Migration. In 73rd Ann. International Mtg., Soc.

Of Expl. Geophys. , Expanded Abstracts (Pp. 1059-1062).

50. Alvarez, L., Lions, P. L., & Morel, J. M. (1992). Image Selective Smoothing and Edge Detection by Nonlinear Diffusion. Ii. Siam Journal on Numerical Analysis, 29(3), 845-866.
51. Ferzli, R., & Karam, L. J. (2005, September). No-Reference Objective Wavelet Based Noise Immune Image Sharpness Metric. In Image Processing, 2005. ICIP 2005. IEEE International Conference on (Vol. 1, Pp. I-405). IEEE.
52. Wang, Z., & Zhang, D. (1999). Progressive Switching Median Filter for the Removal of Impulse Noise from Highly Corrupted Images. Circuits And Systems Ii: Analog And Digital Signal Processing, IEEE Transactions On, 46(1), 78-80.
53. Senthilkumaran, N., & Rajesh, R. (2009). Edge Detection Techniques for Image Segmentation—A Survey of Soft Computing Approaches. International Journal of Recent Trends in Engineering, 1(2), 250-254.
54. Di Zenzo, S. (1986). A Note on the Gradient of a Multi-Image. Computer Vision, Graphics, and Image Processing, 33(1), 116-125.
55. Dai, D. Q., & Yan, H. (2007). Wavelets and Face Recognition. Face Recognition, 59-74.

56. Pentland, A., Moghaddam, B., & Starner, T. (1994, June). View-Based and Modular Eigen spaces For Face Recognition. In *Computer Vision and Pattern Recognition, 1994. Proceedings Cvpr'94. 1994 IEEE Computer Society Conference on* (Pp. 84-91). IEEE.
57. Kim, J. Y., Kim, L. S., & Hwang, S. H. (2001). An Advanced Contrast Enhancement Using Partially Overlapped Sub-Block Histogram Equalization. *Circuits and Systems for Video Technology, IEEE Transactions On*, 11(4), 475-484.
58. Cumani, A. (1991). Edge Detection in Multispectral Images. *CVGIP: Graphical Models and Image Processing*, 53(1), 40-51.
59. Paris, S. (2008). Edge-Preserving Smoothing and Mean-Shift Segmentation of Video Streams. In *Computer Vision–ECCV 2008* (Pp. 460-473). Springer Berlin Heidelberg.
60. Shan, Q., Jia, J., & Agarwala, A. (2008, August). High-Quality Motion Deblurring From a Single Image. In *ACM Transactions on Graphics (Tog)* (Vol. 27, No. 3, P. 73). ACM.
61. Zhu, S. C., & Yuille, A. (1996). Region Competition: Unifying Snakes, Region Growing, and Bayes/Mdl for Multiband Image Segmentation. *Pattern Analysis and Machine Intelligence, IEEE Transactions On*, 18(9), 884-900.

62. Yuan, L., Sun, J., Quan, L., & Shum, H. Y. (2007, August). Image Deblurring With Blurred/Noisy Image Pairs. In *ACM Transactions on Graphics (Tog)* (Vol. 26, No. 3, P. 1). ACM.
63. Duhamel, P., & Vetterli, M. (1990). Fast Fourier Transforms: A Tutorial Review and a State Of The Art. *Signal Processing*, 19(4), 259-299.
64. Zhang, Y. J. (1996). A Survey on Evaluation Methods for Image Segmentation. *Pattern Recognition*, 29(8), 1335-1346.
65. Hall, P., & Titterton, D. M. (1992). Edge-Preserving and Peak-Preserving Smoothing. *Technometrics*, 34(4), 429-440.
66. Sharif, M., Shah, J. H., Mohsin, S., & Raza, M. (2013). Sub-Holistic Hidden Markov Model for Face Recognition. *Research Journal Of Recent Sciences*
67. Yang, Q., Ji, P., Li, D., Yao, S., & Zhang, M. (2014). Fast Stereo Matching Using Adaptive Guided Filtering. *Image and Vision Computing*.
68. Charbonnier, P., Blanc-Féraud, L., Aubert, G., & Barlaud, M. (1997). Deterministic Edge-Preserving Regularization in Computed Imaging. *Image Processing, IEEE Transactions On*, 6(2), 298-311.
69. Ismaeel, A. D., & Ahmad, G. (2013). Eye Localization in a Full Frontal Still Image. *Al-Rafadain Engineering Journal*, 21(4).

70. Brunelli, R., & Poggio, T. (1993). Face Recognition: Features versus Templates. *IEEE Transactions on Pattern Analysis and Machine Intelligence*, 15(10), 1042-1052.
71. Shi, J., & Malik, J. (2000). Normalized Cuts and Image Segmentation. *Pattern Analysis and Machine Intelligence, IEEE Transactions On*, 22(8), 888-905.
72. Fatima, A. Designing And Simulation Of 32 Point FFT Using Radix-2 Algorithm For FPGA. *IOSR Journal Of Electrical And Electronics Engineering (IOSR-JEEE) Volume 9, Issue 1 Ver. Iii (Jan. 2014), Pp 42-50*
73. Greengard, L., & Lee, J. Y. (2004). Accelerating the Non-uniform Fast Fourier Transform. *Siam Review*, 46(3), 443-454.
74. Eng, H. L., & Ma, K. K. (2001). Noise Adaptive Soft-Switching Median Filter. *Image Processing, IEEE Transactions On*, 10(2), 242-251.
75. Huang, T., Yang, G., & Tang, G. (1979). A Fast Two-Dimensional Median Filtering Algorithm. *Acoustics, Speech And Signal Processing, IEEE Transactions On*, 27(1), 13-18.
76. Bao, P., Zhang, D., & Wu, X. (2005). Canny Edge Detection Enhancement by Scale Multiplication. *Pattern Analysis and Machine Intelligence, IEEE Transactions On*, 27(9), 1485-1490.

77. Mignotte, M. (2007). A Post-Processing Deconvolution Step for Wavelet-Based Image Denoising Methods. *Signal Processing Letters, IEEE*, 14(9), 621-624.
78. Kaur Seerha, G. (2013). Review On Recent Image Segmentation Techniques. *International Journal On Computer Science And Engineering (IJCSE)* Vol. 5 No. 02 Feb 2013 (109-112)
79. Felzenszwalb, P. F., & Huttenlocher, D. P. (2004). Efficient Graph-Based Image Segmentation. *International Journal of Computer Vision*, 59(2), 167-181.
80. Naik, J., & Patel, S. Tumor Detection And Classification Using Decision Tree In Brain MRI. *International Journal Of Engineering Development And Research (IJEDR)*
81. Uemura, T., Koutaki, G., & Uchimura, K. (2011). Image Segmentation Based On Edge Detection Using Boundary Code. *Int. J. Innovative Computing*, 7(10), 765-778.
82. Zhang, W. (2013). Image Denoising Algorithm of Refuge Chamber by Combining Wavelet Transform and Bilateral Filtering. *International Journal of Mining Science and Technology*, 23(2), 221-225.
83. Verma, S., Khare, D., Gupta, R., & Chandel, G. S. (2013, January). Analysis of Image Segmentation Algorithms Using MATLAB. In

- Proceedings of the Third International Conference on Trends in Information, Telecommunication and Computing (Pp. 163-172). Springer New York.
84. Pavlidis, T., & Liow, Y. T. (1990). Integrating Region Growing and Edge Detection. *Pattern Analysis and Machine Intelligence, IEEE Transactions On*, 12(3), 225-233.
85. Nanni, L., Lumini, A., Brahnam, S., & Migliardi, M. Ensemble of Patterns of Oriented Edge Magnitudes Descriptors for Face Recognition. *Proceedings The 17th International Conference On Image Processing, Computer Vision, And Pattern Recognition (Ipcv13)*, Las Vegas, USA, July 2013
86. Marsh, M. A Literature Review of Image Segmentation Techniques and Matting For The Purpose Of Implementing “Grab-Cut”. Department Of Computer Science at Rhodes University, South Africa.
87. Patil, M. M., & Thakare, S. Y. Histogram Equalization for Standard Images. *International Journal of Science and Research (IJSR)*. Volume 3 Issue 2, February 2014
88. Levin, A., Weiss, Y., Durand, F., & Freeman, W. T. (2009, June). Understanding and Evaluating Blind Deconvolution Algorithms. In *Computer Vision and Pattern Recognition, 2009. CVPR 2009. IEEE Conference on* (Pp. 1964-1971). IEEE.

89. Rowley, H. A., Baluja, S., & Kanade, T. (1998). Neural Network-Based Face Detection. *Pattern Analysis and Machine Intelligence, IEEE Transactions On*, 20(1), 23-38.
90. Ahmed, N., Natarajan, T., & Rao, K. R. (1974). Discrete Cosine Transform. *Computers, IEEE Transactions On*, 100(1), 90-93.
91. Kakadiaris, I. A., Passalis, G., Toderici, G., Murtuza, M. N., Lu, Y., Karampatziakis, N., & Theoharis, T. (2007). Three-Dimensional Face Recognition In The Presence Of Facial Expressions: An Annotated Deformable Model Approach. *Pattern Analysis and Machine Intelligence, IEEE Transactions On*, 29(4), 640-649.
92. Gross, R., & Brajovic, V. (2003, January). An Image Preprocessing Algorithm for Illumination Invariant Face Recognition. In *Audio-And Video-Based Biometric Person Authentication* (Pp. 10-18). Springer Berlin Heidelberg.
93. Tripathi, S., Kumar, K., Singh, B. K., & Singh, R. P. (2012). Image Segmentation: A Review. *International Journal of Computer Science and Management Research*, 1(4).
94. Perona, P., & Malik, J. (1990). Scale-Space and Edge Detection Using Anisotropic Diffusion. *Pattern Analysis and Machine Intelligence, IEEE Transactions On*, 12(7), 629-639.

95. Reddy, B. S., & Chatterji, B. N. (1996). An FFT-Based Technique for Translation, Rotation, and Scale-Invariant Image Registration. *IEEE Transactions on Image Processing*, 5(8), 1266-1271.
96. Pal, N. R., & Pal, S. K. (1993). A Review on Image Segmentation Techniques. *Pattern Recognition*, 26(9), 1277-1294.
97. Holappa, J., Ahonen, T., & Pietikainen, M. (2008, September). An Optimized Illumination Normalization Method for Face Recognition. In *Biometrics: Theory, Applications And Systems, 2008. BTAS 2008. 2nd IEEE International Conference on* (Pp. 1-6). IEEE.
98. Qiu, G. (1996). An Improved Recursive Median Filtering Scheme for Image Processing. *Image Processing, IEEE Transactions On*, 5(4), 646-648.
99. Dass, R., & Devi, S. (2012). Image Segmentation Techniques *IJECT Vo L. 3, Issue 1, Jan. - March 2012*
100. Tan, X., & Triggs, B. (2010). Enhanced Local Texture Feature Sets For Face Recognition Under Difficult Lighting Conditions. *Image Processing, IEEE Transactions On*, 19(6), 1635-1650.
101. Tomasi, C., & Manduchi, R. (1998, January). Bilateral Filtering For Gray and Color Images. In *Computer Vision, 1998. Sixth International Conference on* (Pp. 839-846). IEEE.

102. Unnikrishnan, R., & Hebert, M. (2005, January). Measures of Similarity. In *Application of Computer Vision, 2005. WACV/Motions'05 Volume 1. Seventh IEEE Workshops on (Vol. 1, Pp. 394-394)*. IEEE.
103. Ziou, D., & Tabbone, S. (1998). Edge Detection Techniques-An Overview. *Pattern Recognition And Image Analysis C/C Of Raspoznavaniye Obrazov I Analiz Izobrazhenii*, 8, 537-559.
104. Bishop, T. E., Babacan, S. D., Amizic, B., Katsaggelos, A. K., Chan, T., & Molina, R. (2007). Blind Image Deconvolution: Problem Formulation and Existing Approaches. *Blind Image Deconvolution: Theory and Applications*, 1-41.
105. Wen-Hsiung, C., Harrison, S.C. & Fralick, S.C., *Discrete Cosine Transform*, (1977). *IEEE Transactions on Communications*, 25(9).
106. Burton, A.M., White, D., & McNeill, A. (2010). The Glasgow Face Matching Test. *Behavior Research Methods*, 42(1), 286–291.
107. [BOOK] Gonzalez, R. C., Woods, R. E., & Eddins, S. L. (2004). *Digital image processing using MATLAB*. Pearson Education India.
108. [BOOK] Jayaraman, S., Esakkirajan, S., Veerakumar, T. (2009). *Digital image processing*. McGraw Hill Education (India) Pvt. Ltd.